

The *IGF2* mRNA binding protein p62 as a regulator of IGF2 and *H19* expression – potential implications in tumorigenesis

Dissertation

zur Erlangung des Grades

des Doktors der Naturwissenschaften

der Naturwissenschaftlich-Technischen Fakultät III

Chemie, Pharmazie, Bio- und Werkstoffwissenschaften

der Universität des Saarlandes

von

Sonja M. Keßler

Saarbrücken

2011

1. Berichterstatter: Prof. Dr. Alexandra K. Kiemer
2. Berichterstatter: Prof. Dr. Rolf W. Hartmann

Erklärung

Hiermit versichere ich an Eides statt, dass ich die vorliegende Arbeit selbständig und ohne Benutzung anderer als der angegebenen Hilfsmittel angefertigt habe. Die aus anderen Quellen oder indirekt übernommenen Daten und Konzepte sind unter Angabe der Quelle gekennzeichnet.

Die Arbeit wurde bisher weder im In- noch im Ausland in gleicher oder ähnlicher Form in einem Verfahren zur Erlangung eines akademischen Grades vorgelegt.

Saarbrücken, März 2011

.....

(Sonja M. Keßler)

Contents

Abbreviations.....	V
Abstract	1
1 Introduction	3
1.1 Hepatocellular carcinoma.....	4
1.1.1 HCC as a complication of non-alcoholic steatohepatitis (NASH)	4
1.2 Insulin-like growth factor 2-mRNA binding protein p62	7
1.3 Imprinted genes	9
1.3.1 Insulin-like growth factor (IGF) 2.....	10
1.3.2 The non-coding RNA H19.....	11
1.4 The phosphatase and tensin homolog deleted from chromosome 10.....	12
1.5 Extracellular-activated kinases (ERKs)	13
2 Materials and Methods	17
2.1 Materials.....	18
2.2 Mice.....	19
2.2.1 Animal welfare	19
2.2.2 Generation of p62 transgenic animals	19
2.2.3 Genotyping.....	19
2.2.4 Treatment.....	21
2.2.5 Serum parameters	21
2.3 Cell culture	21
2.3.1 Cell lines	21
2.3.2 Determination of cell viability.....	22
2.3.3 Detection of mycoplasma.....	22
2.4 Bacterial culture	23
2.4.1 Generation of competent E.coli.....	23
2.4.2 Transformation.....	23

2.5	Plasmid generation	24
2.5.1	Vectors for mammalian cell transfections	24
2.5.2	siRNA.....	24
2.5.3	Real-Time RT-PCR standard plasmids.....	24
2.6	Isolation of bacterial DNA.....	25
2.6.1	Plasmid purification.....	25
2.6.2	Determination of DNA concentrations.....	25
2.7	Agarose gel electrophoresis.....	25
2.7.1	Detection of DNA	25
2.7.2	Detection of RNA	25
2.8	RNA isolation and reverse transcription	26
2.8.1	RNA isolation	26
2.8.2	DNase digestion.....	26
2.8.3	Measurement of RNA concentrations	26
2.8.4	Alu PCR.....	27
2.8.5	Reverse transcription	28
2.9	Restriction fragment length polymorphism	28
2.9.1	Genomic DNA Isolation and screening	28
2.9.2	Digestion with restriction enzymes.....	30
2.10	SNuPE analysis	30
2.11	Real-time RT-PCR	32
2.11.1	Primer and probe sequences.....	32
2.11.2	Standard dilution series	33
2.11.3	Experimental procedure.....	33
2.12	Western Blot analysis.....	36
2.12.1	Preparation of protein samples	36
2.12.2	SDS-polyacrylamide gel electrophoresis (SDS-PAGE).....	36
2.12.3	Blotting.....	37

2.12.4	Immunodetection	37
2.13	Transfection of HepG2 cells	38
2.13.1	Plasmid transfection.....	38
2.13.2	siRNA transfection	38
2.14	Determination of mRNA stability	39
2.15	Caspase-3-activity assay	39
2.16	ELISA.....	39
2.17	Fatty acid measurement.....	40
2.18	Human HCC samples.....	41
2.19	Statistics.....	42
3	Results.....	43
3.1	Effects of p62 on hepatic metabolism	44
3.1.1	p62 expression in DEN-treated mice	44
3.1.2	Effect of p62 on the metabolism of fatty acids.....	44
3.1.3	p62 downregulates PTEN expression.....	47
3.1.4	Expression of glucocorticoid-induced leucine zipper (GILZ)	48
3.1.5	p62 induces inflammatory cytokines	49
3.2	Antiapoptotic effect of p62.....	52
3.2.1	p62 expression results in high expression of Igf2	52
3.2.2	Role of p62 and IGF2 in human HCC	54
3.2.3	Role of IGF2 in anti-apoptotic action of p62.....	56
3.2.4	The antiapoptotic effect of p62 is facilitated <i>via</i> ERK phosphorylation ..	60
3.3	Role of <i>H19</i> in HCC.....	62
3.3.1	<i>H19</i> expression in DEN-treated mice.....	62
3.3.2	<i>H19</i> expression in human HCC.....	64
3.3.3	<i>H19</i> expression in hepatoma cells	65
4	Discussion	67
4.1	Effects of p62 on metabolism and inflammation.....	68

Contents

4.1.1	Effects of p62 on fatty acid metabolism	68
4.1.2	p62 downregulates PTEN	70
4.1.3	Interaction of p62 and GILZ	71
4.1.4	p62 induces inflammatory cytokines	72
4.2	Antiapoptotic effect of p62.....	74
4.2.1	p62 expression in human HCC	74
4.2.2	Mechanism of the anti-apoptotic action of p62.....	75
4.3	Role of <i>H19</i> in HCC.....	79
5	Summary	81
6	References	85
	Publications	105
	Acknowledgements	107

Abbreviations

A	ampere
amp	ampicilline
AP-1	activator protein 1
APS	ammonium persulfate
BHQ1	black hole quencher 1
bp	base pair
BSA	bovine serum albumin
CCD	centrally conserved domain
cDNA	complementary DNA
co	control
CpG	undermethylated 5'-CG-3' sequences
CREB	cAMP response element-binding protein
DEPC	diethyl dicarbonate
DMR	differential methylated region
DMSO	dimethyl sulfoxide
DNA	desoxyribonucleic acid
DNase	desoxyribonuclease
dNTP	desoxyribonucleosidtriphosphate
DTT	dithiothreitol
<i>E. coli</i>	<i>Escherichia coli</i>
EDTA	ethylenediamine-N,N,N,N'-tetra acid
EGTA	ethylene glycol tetraacetic acid
ERK	extracellular-activated kinase
f	femto (10^{-15})
FAM	6-carboxy-fluorescein
FCS	fetal calf serum

Abbreviations

g	gram
gDNA	genomic DNA
GILZ	glucocorticoid-induced leucine zipper
GSK-3	glycogen synthase kinase-3
h	hour
HBV	hepatitis B virus
HCC	hepatocellular carcinoma
HCV	hepatitis C virus
HDL	high density lipoprotein
ICR	imprinting control region
IGF	insulin-like growth factor
I κ B	inhibitory protein kappa B
IMP	IGF2 mRNA binding protein
IL6	interleukin 6
kb	kilo bases
kDa	kilo Dalton
KH	hnRNP K homology domain
l	litre
LB	Luria-Bertani
LDL	low density protein
LOI	loss of imprinting
m	milli (10^{-3})
M	molar
MAPK	mitogen-activated protein kinase
MEK	mitogen extracellular protein kinase
min	minute
mRNA	messenger ribonucleic acid
μ	micro (10^{-6})

Abbreviations

n	nano (10^{-9})
NAFLD	non-alcoholic fatty liver disease
NASH	non-alcoholic steatohepatitis
NF- κ B	nuclear factor kappa B
PAGE	polyacrylamide gel electrophoresis
PBS	phosphate buffered saline
PBST	phosphate buffered saline with Tween 20
PCR	polymerase chain reaction
PI3-K	phosphatidylinositol 3-kinase
PMSF	phenylmethylsulfonyl fluoride
PTEN	phosphatase and tensin homolog deleted from chromosome 10
RAF	v-raf murine leukemia viral oncogene homolog
RAS	rat sarcoma
RNA	ribonucleic acid
RNAse	ribonuclease
rpm	rounds per minute
RRM	RNA recognition motif
RT	reverse transcriptase
SDS	sodium dodecyl sulfate
s	second
SEM	standard error of mean
siRNA	short interfering RNA
SREBP	trans-unsaturated fatty acids activate sterol regulatory binding protein
STAT	signal transducer and activator of transcription
TBE	tris-boric acid-EDTA buffer
TE	tris-EDTA buffer
tg	transgenic
TGF- β	Transforming growth factor beta

Abbreviations

TNF- α	tumor necrosis factor alpha
Tris	α,α,α -tris-(hydroxymethyl)-methylamine
U	unit
UV	ultra violet
V	volt
[v/v]	volume per volume
[w/v]	weight per volume
xg	fold gravitational force

Abstract

Hepatocellular carcinoma (HCC) represents the fifth most common cancer worldwide. The overall survival of patients with HCC is low due to both late diagnosis and the lack of efficient systemic treatment options. Autoantigens are considered as possible diagnostic markers for several types of cancer. Aim of this work was to characterize functional implications of p62/IMP2-2, an insulin-like growth factor 2 (IGF2) mRNA binding protein and autoantigen in HCC, in liver pathogenesis. In transgenic mice expressing p62 only in the liver, levels of both *Igf2* mRNA and *H19*, a non-coding RNA with which it shares an imprinting control region, were strongly elevated. Interestingly, although elevated p62 levels in human HCC tissues correlated with *Igf2* expression, the observed antiapoptotic effect of p62 was IGF2-independent, but rather facilitated *via* extracellular regulated kinase (ERK) activation. p62 attenuated the expression of the tumor suppressor phosphatase and tensin homolog (PTEN), increased the levels of inflammatory cytokines, and altered hepatic fatty acid composition. Taken together, this work provides evidence for p62 being a new interesting target for both diagnostic and therapeutic options in HCC.

Zusammenfassung

Das hepatozelluläre Karzinom (HCC) stellt die fünfthäufigste Krebsart weltweit dar. Die Überlebensrate der HCC-Patienten ist gering, da oft erst eine späte Diagnose erfolgt und effiziente Behandlungsmöglichkeiten fehlen. Autoantigene werden als mögliche diagnostische Marker bei verschiedenen Krebsarten diskutiert. Ziel dieser Arbeit war daher die Charakterisierung der funktionellen Wirkungen des Autoantigens p62 in der Pathogenese der Leber. Bei p62 handelt es sich um ein Insulinähnlicher Wachstumsfaktor 2 (IGF2) mRNA bindendes Protein. Wie erwartet, wurde eine Beeinflussung der Expression von *Igf2*-mRNA und *H19*, einer nicht-codierenden RNA, durch p62 in transgenen Mäusen beobachtet. Interessanterweise war der festgestellte antiapoptotische Effekt von p62 IGF2-unabhängig und vielmehr ermöglicht durch Phosphorylierung der extrazellulär regulierten Kinase ERK. Außerdem veränderte die p62-Expression die Expression des Tumorsuppressors Phosphatase und Tensin Homolog (PTEN), die Ausschüttung an inflammatorischen Zytokinen sowie die hepatische Fettsäurezusammensetzung. Zusammenfassend stellt diese Arbeit p62 als neuen interessanten Angriffspunkt für diagnostische und therapeutische Ansätze bei der Behandlung des hepatozellulären Karzinoms heraus.

1 Introduction

1.1 Hepatocellular carcinoma

The incidence of primary liver cancers including hepatocellular carcinoma (HCC) has dramatically increased in the last years. HCC is one of the most lethal types of cancer and represents the fifth most common solid tumor in the world (Sherman, 2005). Although most HCC cases occur in Asian and African countries (Duvoux, 1998) due to a higher prevalence of hepatitis C virus (HCV) and hepatitis B virus (HBV) (Bosch et al., 2004; McGlynn et al., 2001), incidence of and mortality from HCC are rising also in most industrialized countries including Germany (figure 1).

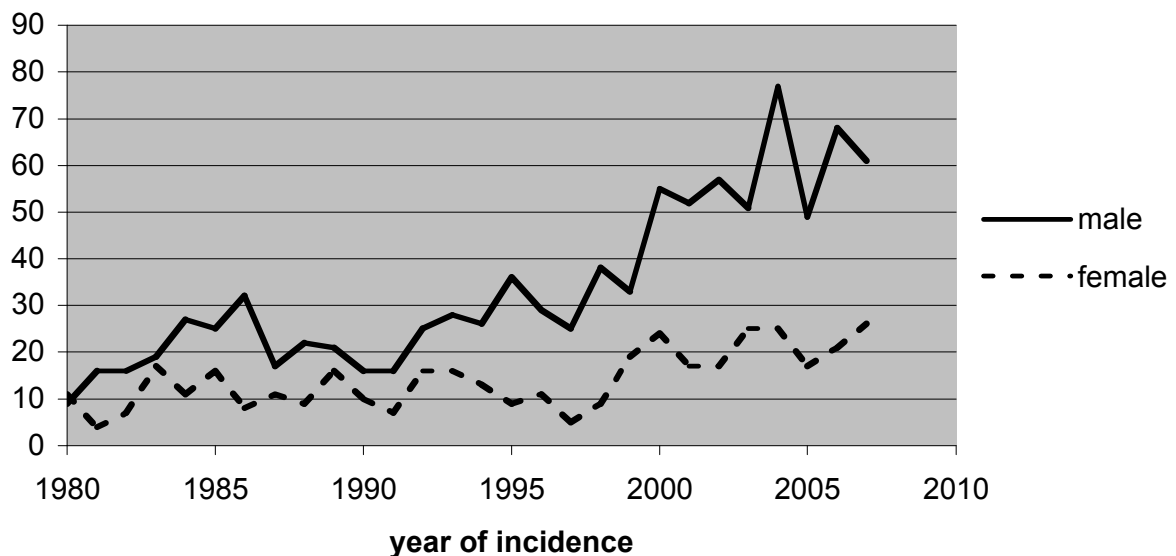


Figure 1: Incidence of liver cancer in Germany (Krebsregister Saarland)

1.1.1 HCC as a complication of non-alcoholic steatohepatitis (NASH)

Alcohol intake induces a fatty liver by various mechanisms, which alter the balance between delivery and removal of fatty acids: enhanced esterification of fatty acids due to higher hepatic levels of glycerol 3-phosphate, increased levels of free fatty acids, enhanced lipolysis because of a direct stimulatory effect on the adrenal and pituitary axis, inhibition of fatty acid oxidation in the liver, and the release of very low-density lipoprotein (VLDL) (Purohit et al., 2009). Nonalcoholic fatty liver disease (NAFLD) was first identified in patients after long-term treatment with glucocorticoids (Itoh et al., 1977). NAFLD is a chronic liver disease characterized by the histological features of steatohepatitis in the absence of alcohol consumption. Simple steatosis generally follows a benign course (Page and Harrison, 2009). NAFLD, commonly occurring in obese patients, can result in cirrhosis and HCC when associated with

necrosis and inflammation. The disease is then referred to as NASH (Matteoni et al., 1999). The prevalence of NAFLD is 10-25% in western countries (Farrell and Larter, 2006) and more than one third of the adult population of the United States of America suffers from a fatty liver (Browning et al., 2004). Approximately 70% of obese patients, i.e. patients with a body mass index $> 30 \text{ kg/m}^2$, develop some kind of a fatty liver disease (Neuschwander-Tetri and Caldwell, 2003).

The progression from NAFLD to NASH might be explained by the 'two hit' hypothesis, which proposes that steatosis is the first hit resulting in a higher susceptibility of the liver to subsequent hits, such as inflammation, lipid peroxidation, and the generation of reactive oxygen species (McAvoy et al., 2006).

Development of NASH

Several different factors, including environmental as well as genetic conditions associated with obesity and type 2 diabetes, have been reported to promote fat accumulation in the human liver (Koutsari and Lazaridis). Hepatic steatosis is defined as liver fat in more than 5% of hepatocytes (Tsochatzis et al., 2009), the mechanisms involved influence fatty acid metabolism. There are different sources of fatty acids in the liver, which contribute to the pathophysiology of NAFLD (Donnelly et al., 2005). Interestingly, the fatty acid pattern may be more important than the total amount (Cortez-Pinto et al., 2006). Saturated and trans-unsaturated fatty acids activate sterol regulatory binding protein (SREBP)-1c, which is involved in lipogenesis and triglyceride synthesis (Biddinger et al., 2005). In fact, overexpression of a dominant-positive SREBP-1 in transgenic mice is associated with severe hepatic steatosis (Shimano et al., 1996), whereas SREBP-1 knockout mice are resistant to fatty liver development (Yahagi et al., 2002).

Accumulation of free fatty acids in the liver can result in inflammation by activating nuclear factor kappa B (NF- κ B), which subsequently increases cytokine levels, e.g. of tumor necrosis factor alpha (TNF- α) and interleukin 6 (IL6) (Arkan et al., 2005; Cai et al., 2005; Feldstein et al., 2004). Studies with patients suffering from NASH have shown increased cytokine gene expression in hepatic tissue as well as in peripheral fat (Crespo et al., 2001). Additionally, lipids in hepatocytes are able to activate c-Jun N-terminal kinase (JNK)/activator protein-1 (Malhi et al., 2006), which also play an

important role in inflammation (Shoelson et al., 2006). Therefore, steatosis can lead to the development of NASH *via* an establishment of chronic inflammation (figure 2).

Progression to HCC

Patients with a chronic HCV infection combined with a fatty liver carry a higher risk for the development of HCC than those suffering from only one of these diseases (Pekow et al., 2007). In fact, also a rodent model recently gave evidence for the progression from NASH to cirrhosis and HCC (de Lima et al., 2008). The NF- κ B pathway, which is already activated in NASH, also plays an important role in carcinogenesis (Pikarsky et al., 2004). Furthermore, the accumulation of free fatty acids leads to an excess of reactive oxygen species (ROS), which can cause DNA damage and therefore malignancy (Stickel and Hellerbrand, 2010). Activated lipogenic pathways correlate with poor prognosis in HCC (Yamashita et al., 2009). Moreover, insulin resistance and subsequent hyperinsulinemia activate the PI3-K/AKT pathway often altered in HCC (Stickel and Hellerbrand, 2010). Other gene alterations and signaling pathways implicated in HCC, such as p53, Wnt, TGF- β , MAPK, can also trigger the progression from NASH to cirrhosis and HCC (figure 2).

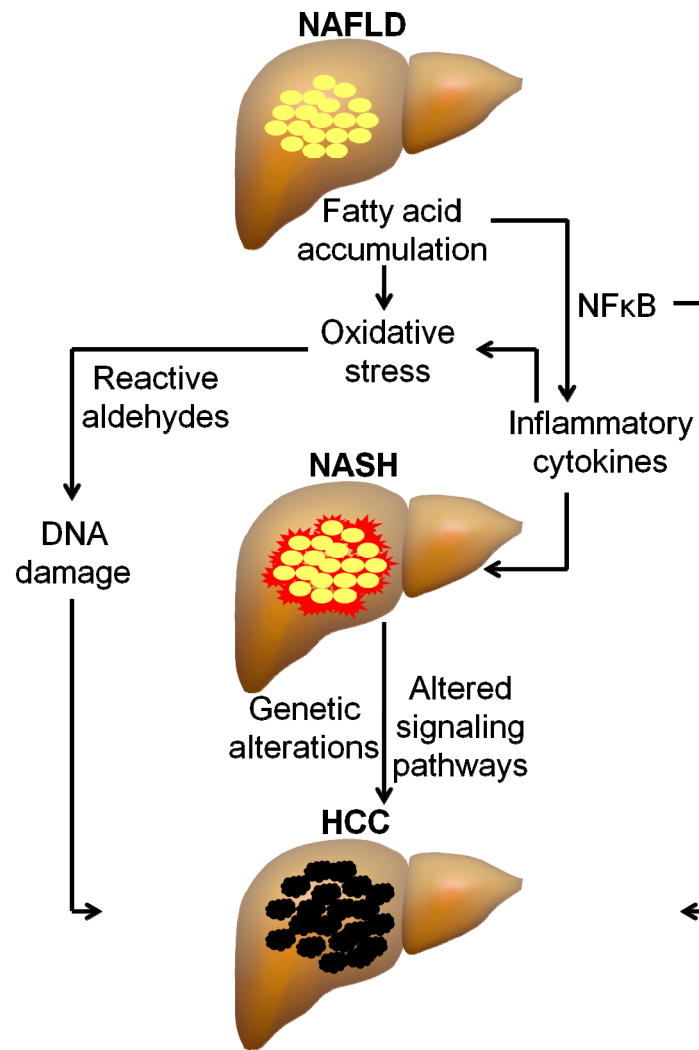


Figure 2: From NAFL to HCC (Day, 2006; Stickel and Hellerbrand, 2010)

1.2 Insulin-like growth factor 2-mRNA binding protein p62

p62 is a member of the family of insulin-like growth factor II (IGF2)-mRNA binding proteins (IMPs). It represents a splice variant of IMP2 lacking exon 10 of the IMP2 gene. p62/IMP2-2 was originally identified in 1999 as an autoantigen in an HCC patient (Zhang et al., 1999). In the following years, p62 was demonstrated to be overexpressed in HCC in about one third to two thirds of patients with HCC (Lu et al., 2001; Qian et al., 2005; Zhang et al., 1999). Interestingly, p62 was shown to be also expressed in α -fetoprotein negative HCC as well as in cirrhotic nodules (Lu et al., 2001).

IMPs are mRNA binding proteins, whose functions are only marginally described. Known IMP functions include effects on mRNA stability, translatability, localization,

and transport (Hansen et al., 2004; Nielsen et al., 1999; Runge et al., 2000). IMPs have been regarded as oncofetal, but some reports also suggest postnatal expression (Hansen et al., 2004; Mori et al., 2001; Wang et al., 2003), especially for IMP2 (Hammer et al., 2005).

The IMP2 gene is located on chromosome 3 q27.2 and is encoded by 16 exons. RNA binding proteins contain one or more RNA-binding motifs. IMPs show a characteristic pattern of two RNA recognition motifs (RRM-1 and -2) and four hnRNP K homology domains (KH1-4) (figure 3), which might bind to a putative 5'UTR binding motif of the IGFII-leader 3 mRNA (Nielsen et al., 1999). Compared to IMP2 p62 lacks 43 amino acids between KH2 and KH3 (figure 3), but as IMP2 p62 is able to form homodimers (Nielsen et al., 2004). Interestingly, the KH4 domain of IMP1 and -2 was demonstrated to be important for modulating human immunodeficiency virus type 1-RNA expression (Zhou et al., 2009). Although the structures of the KH domains and the two RRM s are conserved within in the IMP family, they may have different RNA sequence preference and binding affinity (Chao et al., 2010).

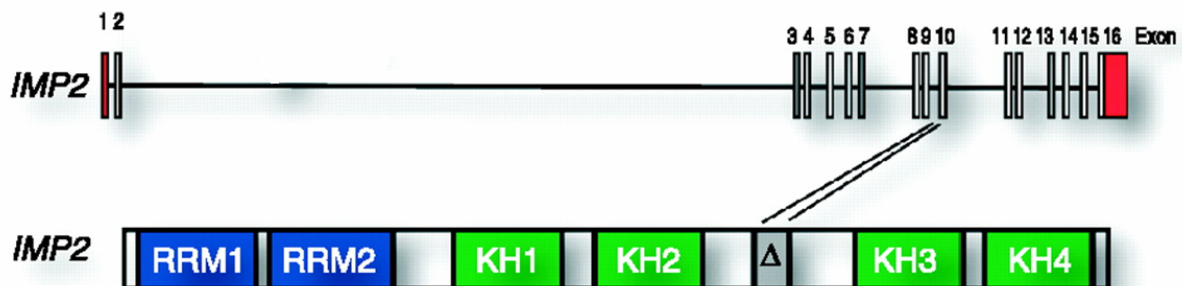


Figure 3: Structure of the IMP2 protein (Christiansen et al., 2009) The splice variant p62 lacks exon 10 between KH2 and KH3 of IMP2 gene.

Recent reports suggest the family member IMP3 as a prognostic marker for malignancy and poor prognosis in several tumors (Hutchinson, 2010) including HCC (Jeng et al., 2008a; Jeng et al., 2008b). p62 has been shown to be overexpressed not only in HCC but also in other digestive tumorous and surrounding tissues (Su et al., 2005). In a mouse model with p62 transgenic animals expressing the transgene exclusively in the liver, 66% of female and 44% of male mice develop a fatty liver phenotype (Tybl et al., 2011), suggesting a critical role for p62 in liver disease.

1.3 Imprinted genes

The human chromosome 11p15.5 contains a cluster of imprinted genes including the insulin-like growth factor 2 (*IGF2*) and the non-translated *H19* RNA. The *IGF2* gene is localized only 90 kb upstream of the *H19* gene and both genes are reciprocally expressed: *IGF2* is encoded by the paternal (Giannoukakis et al., 1993) and *H19* by the maternal allele (Rachmilewitz et al., 1992). In mice the *Igf2/H19* locus is located on chromosome 7 and similarly imprinted. The promoters of both genes use the same enhancers (Leighton et al., 1995). In a small subset of tissues of mesodermal and neural crest origin an additional enhancer region at the centrally conserved domain (CCD) was observed to drive expression of *Igf2* (Charalambous et al., 2004). Imprinting of *Igf2* on the maternal allele is achieved by the insulator factor CTCF, which can bind to the unmethylated imprinting control region (ICR) and therefore block enhancer access to the *Igf2* promoter (figure 4). The ICR displays a 42 bp sequence that is highly homologous between human and mouse (Frevel et al., 1999). In order to block the enhancer access, the ICR interacts with a matrix attachment region and the DMR1 or DMR2 at the *Igf2* locus to generate a tight loop around the *Igf2* gene, cutting off *Igf2* expression (Kurukuti et al., 2006). On the paternal allele methylation of CpGs within the CTCF-binding sites eliminates binding of the insulator, thereby allowing *Igf2* gene transcription (Bell and Felsenfeld, 2000) (figure 4). Deletion of a *cis*-acting silencing element in the ICR results in the relaxation of *H19* silencing after paternal inheritance, without disrupting expression of *Igf2* (Drewell et al., 2000) (figure 4).

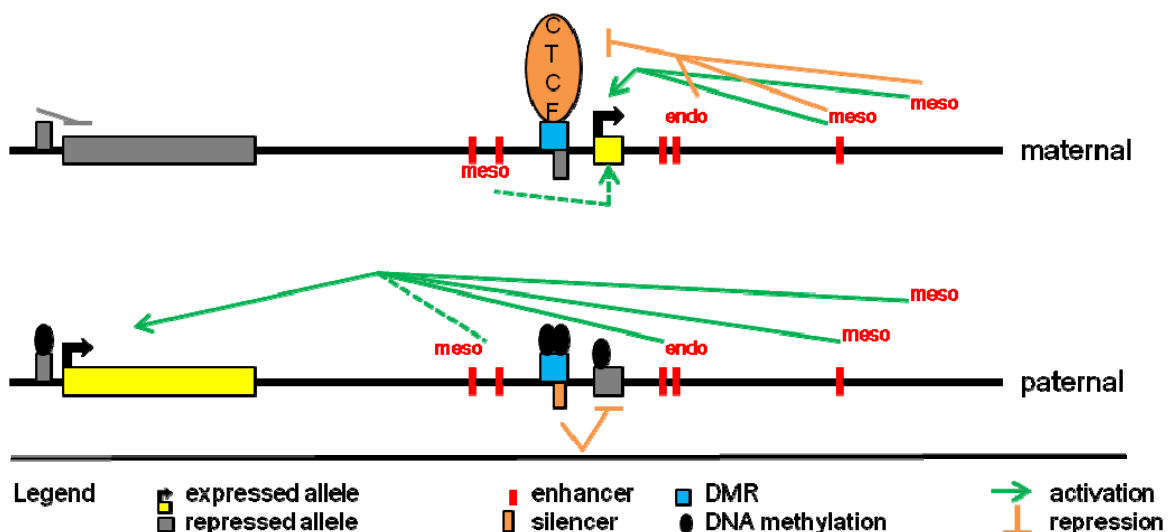


Figure 4: Imprinting mechanisms at the *H19/Igf2* locus (Gabory et al., 2006b)

Loss of imprinting (LOI) is believed to be caused by *de novo* methylation of the differential methylated region (DMR), which controls the expression of *Igf2* and *H19* (Xu et al., 2006). Deletion of the DMD/ICR can be regarded as an epigenetic alteration, which leads to biallelic expression of *Igf2* and silencing of the *H19* gene (Thorvaldsen et al., 1998).

Interestingly, both *H19* and *IGF2* have been shown to encode microRNAs of as yet largely unknown function (Cai and Cullen, 2007; Landgraf et al., 2007).

1.3.1 Insulin-like growth factor (IGF) 2

IGF2 is an autocrine/paracrine growth factor which is only expressed in the embryonic and neonate state in most tissues. IGF2 expression dramatically decreases after birth (Takeda et al., 1996). The 67 amino acid peptide belongs to the insulin-like growth factor family and is encoded by nine exons (Schofield et al., 1991). *Igf2* was shown to be tumorigenic in mice and is highly overexpressed in subsets of different human tumors including HCC (Cariani et al., 1988a; Lu et al., 2005; Thorgeirsson and Grisham, 2002). In addition, a loss of imprinting (LOI) was demonstrated in several tumors (Cruz-Correa et al., 2004; Cui et al., 2003; Nonomura et al., 1997b; Rainier et al., 1993; Steenman et al., 1994) including hepatoblastoma (Rainier et al., 1995). Overexpression of IGF2 in HCC is associated with re-expression of the fetal pattern of IGF2 transcripts in HCC, i.e. through activation of the fetal promoters P2–P4 (Uchida et al., 1997) and loss of activity of the adult promoter P1 (Li et al., 1997). Hypomethylation at the IGF2 locus in the liver might be predictive for HCC occurrence in HCV cirrhosis (Couvert et al., 2008). Overexpression of the DNA methyltransferases (DNMT) DNMT1 and DNMT3a, DNA hypermethylation on CpG islands, and DNA hypomethylation on pericentromeric satellite regions are early events during hepatocarcinogenesis (Lin et al., 2001; Saito et al., 2001). In contrast to the data mentioned above, it was also demonstrated that LOI of *Igf2* in mouse hepatic tumor cells is not necessarily linked to abnormal methylation in the *Igf2* locus (Ishizaki et al., 2003).

Circulating IGF2 protein and mRNA might be utilized as molecular markers for HCC differential diagnosis and metastasis (Qian et al.). IGF2 binds to the IGF-1 receptor, which activates mitogen-activated protein kinase (MAPK) and phosphatidylinositol 3-kinase (PI3-K) signalling (Sepp-Lorenzino, 1998; Zhang et al., 2000), two pathways

often altered in tumorigenesis. The mechanism by which PI3-K protects cells from apoptosis involves a downstream activation of the protein kinase AKT. AKT in turn has several downstream targets, which mediate cell survival, such as the Bcl-2 family member BAD leading to the release of anti-apoptotic Bcl-2 (Datta et al., 1997). AKT also phosphorylates and thereby inactivates the death protease caspase-9 (Cardone et al., 1998). Increased proliferation after AKT activation is mediated by phosphorylation of glycogen synthase kinase-3 (GSK-3), which is involved in cell cycle regulation (Diehl et al., 1998).

1.3.2 The non-coding RNA H19

The *H19* gene encodes a 2.3-kb non-coding mRNA which is only expressed during embryogenesis and in cancerous tissue (Brannan et al., 1990; Gabory et al., 2006b). After birth *H19*, like IGF2, is strongly down-regulated in all tissues with the exception of skeletal muscle, in which H19 continues to be expressed (Weber et al., 2001).

Presently the biological functions of *H19* remain elusive. H19 has been described to influence growth by means of a *cis* control on *Igf2* expression, which is suggested to interfere with post-transcriptional regulation or translation of the *Igf2* mRNA (Gabory et al., 2006b; Vernucci et al., 2000). Several studies imply *H19* being a tumor suppressor gene (Hao et al., 1993; Juan et al., 2000), whereas expression of *H19* has also been reported to be increased in different tumors and during hepatocarcinogenesis (Yvonne P. Dragan, 2004). Furthermore, biallelic expression of *H19* has been shown for several tumors (Nonomura et al., 1997a; Rachmilewitz et al., 1992), especially HCC (Kim and Lee, 1997; Matouk et al., 2007). It is as yet unknown, however, whether *H19* plays an active role in tumorigenesis or whether its expression is induced secondary to tumorigenesis. In fact, *H19* might even antagonize tumor development (Gabory et al., 2006a). Taken together, the role of the *H19* RNA in tumorigenesis still remains unclear.

1.4 The phosphatase and tensin homolog deleted from chromosome 10

The phosphatase and tensin homolog deleted from chromosome 10 (PTEN) is located on human chromosome 10q23, a genomic region that suffers from loss of heterozygosity (LOH) in many human cancers (Cantley and Neel, 1999). PTEN is a lipid phosphatase that removes the phosphate from the D3 position of phosphatidylinositol 3,4,5-triphosphate (PIP3) (Maehama and Dixon, 1998). Phosphatidylinositol (PI) is a membrane phospholipid that can be phosphorylated at the 3, 4 and 5 position of the inositol ring to produce PI-3/4/5-phosphate, PI-3,4/3,5-biphosphate, PI-4,5-biphosphate (PIP2), and PI-3,4,5-triphosphate (PIP3) (Bunney and Katan). PIP3 recruits the serine/threonine kinase AKT to the plasma membrane, where it is phosphorylated by a variety of activators, such as the mammalian target of rapamycin, integrin-linked kinase, and 3-phosphoinositide-dependent protein kinase 1 (Persad et al., 2000). By dephosphorylating PIP3 to PIP2 PTEN directly antagonizes the action of the phosphatidylinositol 3-kinases (PI3-K) (Stambolic et al., 1998). This accentuates PTEN as a critical negative regulator of the ubiquitous PI3-K/AKT pathway that transduces signals regulating growth, proliferation and survival (Vivanco and Sawyers, 2002). Therefore, PTEN represents a tumor suppressor gene.

PTEN can also act independent of PI3-K/AKT: PTEN was reported to differentially block cell cycle progression through down-regulation of the positive cell cycle regulator cyclin D1 by its protein phosphatase activity, and up-regulating the negative cell cycle regulator p27 by its lipid phosphatase activity (Weng et al., 2001). Interestingly, PTEN also improves protein stability of another tumor suppressor gene, p53, and regulates the transcriptional activity of p53 by modulating its DNA binding (Freeman et al., 2003).

Epigenetic PTEN silencing by hypermethylation of its promoter has been suggested as a potential mechanism contributing to PTEN downregulation in several forms of cancer, including HCC (Tamguney and Stokoe, 2007). Weak expression or mutations/deletions of PTEN, as well as upregulation of microRNAs specifically targeting PTEN for degradation, are frequently observed in human HCC (Dong-Dong et al., 2003; Meng et al., 2007; Yao et al., 1999). Genetic inhibition of PTEN expression, specifically in the liver of rodents, was shown to trigger liver steatosis and steatohepatitis at early stages of development, as well as hepatomegaly and HCC in

later life (Di Cristofano et al., 1998; Horie et al., 2004; Stiles et al., 2004). Loss of a PTEN allele was identified in 20-30% of patients with HCC (Fujiwara et al., 2000; Kawamura et al., 1999).

Reactive oxygen species and carbonyl species can inhibit PTEN protein function *via* alkylation, which represents a link between persistent inflammation and cancer (Covey et al.).

1.5 Extracellular-activated kinases (ERKs)

The RAF/mitogen extracellular protein kinase (MEK)/ERK pathway regulates cellular processes, including proliferation, differentiation, angiogenesis, and survival (Gollob et al., 2006). Importantly, the activation of components of this pathway is believed to contribute to tumorigenesis, tumor progression, and metastasis in a variety of solid tumors (Leicht et al., 2007).

Activation of the RAF/MEK/ERK pathway triggers a cascade of specific phosphorylation events (Avila et al., 2006). Within this cascade, the small GTPase RAS and the serine/threonine kinase RAF are the key signal regulators (Avila et al., 2006). RAS, stimulated by growth factors or cytokines, binds to RAF and conveys it to the plasma membrane (Jelinek et al., 1996; Morrison and Cutler, 1997), where MEK1 and MEK2 get phosphorylated (Seeger et al., 1992) (figure 5). MEK1/2 consist of an amino-terminal negative regulatory domain and a carboxy-terminal mitogen-activated protein kinase (MAPK)-binding domain, which are necessary for binding and activation of ERKs due to phosphorylation (Crews and Erikson, 1992) (figure 5). These 44 and 42 kDa proteins (ERK1/2) were originally isolated due to their ability to phosphorylate microtubule-associated protein 2 (Sturgill and Ray, 1986). Phosphorylated ERK translocates into the nucleus and interacts with various transcription factors, such as CREB, AP-1, Ets, and c-Myc (Chang et al., 2003). ERK1/2 also regulate cytoskeletal proteins, other kinases, and phosphatases (Kolch et al., 2002).

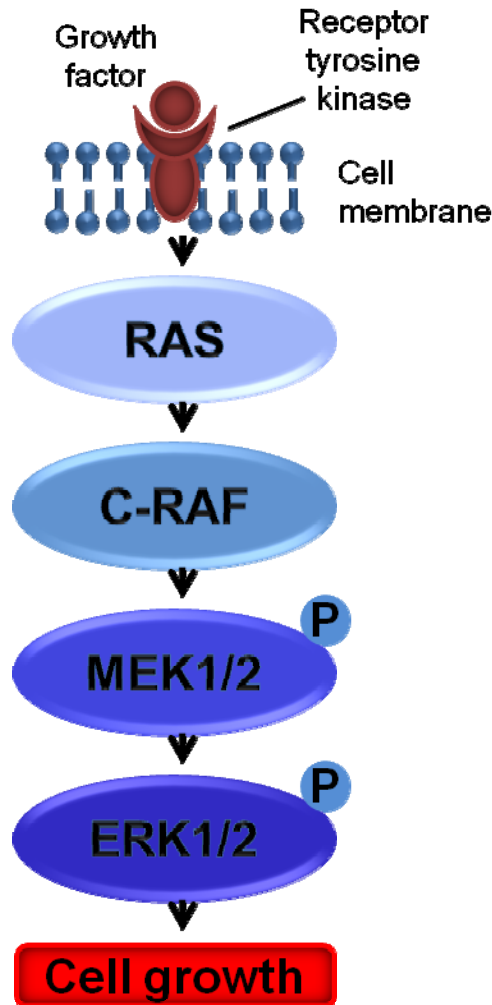


Figure 5: The RAF/MEK/ERK pathway (Roberts and Gores, 2005)

It has been shown that the RAF/MEK/ERK pathway is activated in many malignant tumors, including HCC (Hoshino et al., 1999; Schmidt et al., 1997; Schmitz et al., 2008). Activation of this pathway is often established due to mutations in one of the three isoforms of the RAF gene: A-RAF, B-RAF and C-RAF. B-RAF mutations have been detected in 70% of melanomas, 30% of thyroid cancers, 15% of colon cancers, and in several other cancer types (Emuss et al., 2005; Mercer et al., 2005; Wellbrock et al., 2004). Thereby, a single amino acid substitution accounts for up to 90% of the mutations. This mutation results *in vivo* in a constitutive activation of RAF downstream targets MEK and ERK (Davies et al., 2002; Wellbrock et al., 2004). In HCC, mutations within the B-RAF gene are extremely rare (Tannapfel et al., 2003). As a second mechanism C-RAF has been found to be overexpressed in a variety of primary human cancers, such as lung, liver, prostate, primitive neuroectodermal tumors, myeloid leukemia and head and neck squamous cell carcinoma (Hwang et

al., 2004) due to dysregulated overexpression of growth factors and their receptors (Gollob et al., 2006).

Hwang et al. observed an up-regulation of C-RAF-1, MEK, and MAPK in 40%, 80%, and 86.7% of 45 cirrhosis specimens, respectively. In 22 HCC samples, 50%, 63.6%, and 59.1% showed an up-regulation of C-RAF-1, MEK, and MAPK, respectively. Western blot analysis showed that activated RAF-1 was overexpressed in 91.2% (52/57) of cirrhosis and in 100% (30/30) of hepatocellular carcinoma tissues (Hwang et al., 2004). Furthermore, an immunohistochemical evaluation of tissue samples revealed an approximately seven-fold increase in MEK1/2 phosphorylation in HCC tissues compared to adjacent benign liver tissues (Huynh et al., 2003). Other studies have shown an increase in ERK phosphorylation compared to surrounding liver tissue (Feng et al., 2001; Ito et al., 1998; McKillop et al., 1997).

Additionally, the phosphatidylethanolamine binding protein 1 (RKIP) and the Sprouty/Spred proteins, both negative regulators of MAPK, are downregulated in HCC, resulting in an excessive activation of the MAPK pathway (Schuierer et al., 2006; Yoshida et al., 2006). RKIP expression alters cell proliferation and cell migration in HCC cell lines (Lee et al., 2006).

MAPK/ERK activity was also shown to correlate positively with tumor size in human HCC tissue samples (Ito et al., 1998). A more recent study of 208 HCC samples reports ERK1/2 activation to be associated with poor prognosis (Schmitz et al., 2008). Moreover, activation of the RAF/MEK/ERK pathway confers a chemoresistant phenotype and induces rapid tumor cell proliferation. Interruption of this cascade may increase drug sensitivity and promote apoptosis (Dent and Grant, 2001; Weinstein-Oppenheim et al., 2001).

Importantly, RAS also has a regulatory role in other signaling pathways, e.g. the PI3-K/AKT pathway and the phospholipase C/protein kinase C pathway (Harden and Sondek, 2006; To et al., 2005). Furthermore, ERK mediates STAT activity, indicating a point of interaction between the RAF/MEK/ERK and JAK/STAT pathways (Winston and Hunter, 1995).

1.6 Aim of the present work

IMPs have been reported to be overexpressed in various types of cancer. Still, very few is known about cellular mechanisms of action of IMPs, especially p62.

p62 has been identified as an autoantigen in HCC. The potential involvement in hepatocarcinogenesis and molecular mechanisms involved, however, are as yet poorly understood.

Aim of the present work was to elucidate the role of p62 in liver disease, especially HCC.

Concerning the characterization of p62 and its role in HCC the following aspects were investigated:

- 1) Effects of p62 on metabolism and inflammation
- 2) Anti-apoptotic action of p62
- 3) Role of *H19* in HCC

2 Materials and Methods

2.1 Materials

Cell media, fetal calf serum (FCS), penicillin, streptomycin and glutamine were purchased from PAA (Cölbe, Germany). Doxorubicin, PI3K-inhibitors (Ly294002, wortmannin) and ERK-inhibitors (PD98059, U126) were obtained from Sigma-Aldrich (Taufkirchen, Germany), dissolved in DMSO under sterile conditions at a stock concentration of 50 mg/ml and 1 mg/ml, respectively, aliquoted and stored according to the manufacturer's guidelines. IGF2-antibody was purchased from Abcam (Cambridge, United Kingdom), aliquoted and stored at -20°C. siRNA targeting p62 mRNA (Hs-IMP-2_2_HP siRNA) was purchased from Qiagen (Hilden, Germany), control siRNA (siGENOME) was from Dharmacon (Nidderau, Germany). Both siRNAs were diluted in siRNA buffer as recommended by the supplier. INTERFERINTM and jetPEITM-Hepatocyte were obtained from peqlab (Erlangen, Germany). Real-Time RT-PCR primers, standard PCR primers and dual-labelled probes were obtained from Eurofins MWG Operon (Ebersberg, Germany). *Taq*-Polymerase (5 U/μl), 10 x *Taq* buffer and the dNTP mix (containing dATP, dCTP, dGTP and dTTP at a concentration of 10 mM, each) were from Genscript (Piscataway, NJ, USA). Restriction enzymes Apal (ER1411) and AluI (ER0011) were purchased from Fermentas (St. Leon-Rot, Germany). Rabbit anti-phosphoAKT antibody (#9271), anti-phosphoERK1/2 (#4376), anti-ERK1/2 (#4696), anti-PTEN (#9552) were obtained from Cell Signaling Technology (Danvers, MA, USA), anti-IkBα (sc-371) was from Santa Cruz Biotechnology (Heidelberg, Germany). Mouse anti-tubulin (T9026) was purchased from Sigma-Aldrich (Taufkirchen, Germany). IRDye 680 or IRDye 800 conjugated antibodies (anti-mouse #926-32220, anti-rabbit #926-32221) were obtained from Licor Biosciences (Bad Homburg, Germany). 7-Amino-4-trifluoro-methylcoumarin (AFC) was purchased from Sigma-Aldrich (Taufkirchen, Germany), Ac-Asp-Glu-Val-Asp-AFC (Ac-DEVD-AFC) was from Alexis Biochemicals (Lörrach, Germany).

All other chemicals were purchased either from Sigma-Aldrich or Roth unless marked otherwise.

2.2 Mice

2.2.1 Animal welfare

Mice were kept under controlled conditions in terms of temperature, humidity, 12 h day/night rhythm and food delivery. Animals were 2.5 and 5 weeks of age when experiments were performed. All animal procedures were performed in accordance with the local animal welfare committee.

2.2.2 Generation of p62 transgenic animals

In the DBA2J *p62* transgenic mice the *p62* expression is repressed by the TRE-CMV promoter. For experiments animals were crossed with C57BL/6 LT2 mice, which carry a transactivator (Kistner et al., 1996), leading to a depression of the promoter, thereby allowing *p62* expression in the $p62^+/LT2^+$ offspring (Tybl et al., 2011).

For SNuPE analysis, homozygous SD7 mice carrying the *Mus spretus* allele on chromosome 7 (courtesy provided by Prof. Dr. Jörn Walter, Institute of Genetics, Saarland University), were crossed with LT2 mice to produce reciprocal progeny (LT2 x *Mus spretus*) (Lewis et al., 2004). F1 hybrids were mated to homozygous SD7 to produce heterozygous F2 offspring. For imprinting studies, *p62* transgenic mice were mated with F2 hybrids. Mice carrying no *p62* transgene but the heterozygous LT2/SD7 background served as control.

The offspring carried single nucleotide primer polymorphisms (SNPs) for IGF2 and H19 on chromosome 7.

2.2.3 Genotyping

For genotyping of mice, an ear biopsy was taken and incubated in 89 μ l water premixed with 10 μ l 10x *Taq* buffer and 1 μ l Proteinase K (20 mg/ml) at 55°C for several hours while shaking. After total lysis of the tissue Proteinase K was heat-inactivated at 95°C for 15 min. 1 μ l of the supernatant was used in the PCR reaction.

Table 1: Primer sequences as used for genotyping PCR.

mRNA	primer sense, 5'→ 3'	primer antisense, 5'→ 3'
p62	CATCAAACAGCTGGCGAGAT	GTGCCCGATAATTCTGACGA
LT2	CTTAATGAGGTCGGAATCGA	GCTTGTCGTAATAATGGCGGCATA
D7Mit140	GGAAGTTGTGGGACCTTTAGG	CCTCTTCTGGCCTGTGAGGG
D7Mit12	GCTGGGTTTATTCATTGAAA	TCCAGCTCATGGGTAGAAGA

Reaction mixture

<i>Taq</i> -Polymerase	2.5 U
dNTPs	125 µM
10 x <i>Taq</i> -buffer	2.0 µl
primers (10 µM, each)	400 nM
template	1 µl
H ₂ O	ad 20 µl

Conditions

denaturation	5 min 95°C	} 35 cycles
denaturation	30 s 95°C	
annealing	30 s 56°C	
elongation	30 s 72°C	
final elongation	5 min 72°C	

2.2.4 Treatment

Mice were injected intraperitoneally with 100 µg diethylnitrosamine (DEN) diluted in saline. 48 h after injection, mice were sacrificed and serum and livers were removed for experiments.

2.2.5 Serum parameters

Mice were killed by cervical dislocation at the age of 48 h after treatment for blood sampling. To obtain serum, whole blood was centrifuged for 10 min at 4,000 rpm before the supernatant was transferred into a fresh tube, diluted with 0.9% NaCl, stored at -20°C and transported at 4°C until measurement.

All samples were measured in a PPE Modular analyser using Roche® reagents at a constant temperature of 37°C (Roche Diagnostics, Mannheim, Germany). Measurement was performed at the “Zentrallabor des Universitätsklinikums des Saarlandes” (Homburg, Germany).

2.3 Cell culture

2.3.1 Cell lines

HepG2, HUH-7 and PLC/PRF/5 ‘Alexander’ cells

Cells were cultivated in RPMI-1640 supplemented with 10% [v/v] FCS, 1% [v/v] glutamine and 1% [v/v] penicillin/streptomycin at 37°C and 5% CO₂ in a cell incubator (Hepa Class 100, Thermo Electron Corporation, Germany). Upon reaching confluence, cells were washed with PBS and detached from culture flasks by treatment with trypsin/EDTA solution (PAA). After 2-3 min, digestion was stopped with RPMI-1640 containing 10% FCS [v/v], penicillin (100 U/ml), and streptomycin (100 µg/ml). The suspension was centrifuged and resuspended in RPMI 1640 medium with 10% FCS, 1% glutamine [v/v] and 1% penicillin/streptomycin [v/v] and appropriate aliquots of the cell suspension were added to new culture vessels.

Freezing and thawing of cells

For freezing, cell suspensions were washed with PBS and cells were resuspended in ice cold freezing medium (70% [v/v] RPMI 1640, 20% [v/v] FCS, 10% [v/v] DMSO). After cells were transferred into cryovials, they were stored at -80°C for 1 d and afterwards in liquid nitrogen.

To minimize the cytotoxic effects of DMSO, cells were rapidly thawed for 2 or 3 min at 37°C and instantly transferred into the respective pre-warmed cell growth medium.

2.3.2 Determination of cell viability

Viable cell counts were assessed using a hemocytometer and trypan blue (0.5% [v/v] in PBS) exclusion.

Additionally, MTT assays were performed in order to determine potential cytotoxic effects of cell treatment. Cells were seeded at a density of 1×10^4 cells per well in a 96-well plate and treated as indicated. Afterwards, cells were washed and 200 μ l medium containing MTT (0.5 μ g/ml) were added for 2 h. After medium was removed, cells were lysed and the water-insoluble purple formazan was solubilized by the addition of 80 μ l DMSO. Absorbance was detected at a wavelength of 550 nm using a Sunrise absorbance reader (Tecan).

2.3.3 Detection of mycoplasma

To exclude contamination with mycoplasma, cell lines were tested using the Venor[®]GeM-Mycoplasma Detection Kit (#11-1025, Minerva Biolabs, Berlin), a PCR-based test with a detection limit of 1-5 fg mycoplasma DNA. The test was performed according to the manufacturer's instructions.

2.4 Bacterial culture

The following *Escherichia coli* (*E. coli*) strains were used as host organisms for plasmid amplification:

- XL1 Blue (Stratagene), genotype *endA1 gyrA96(nal^R) thi-1 recA1 relA1 lac glnV44 F'[::Tn10 proAB⁺ lacI^q Δ(lacZ)M15] hsdR17(rK mK⁺)*
- TOP10 (Invitrogen), genotype F- *mcrA Δ(mrr-hsdRMS-mcrBC) φ80lacZΔM15 ΔlacX74 nupG recA1 araD139 Δ(ara-leu)7697 galE15 galK16 rpsL(Str^R) endA1 λ⁻*

Bacteria were grown in Luria-Bertani (LB; 10% tryptone [w/v], 5% yeast extract [w/v], 5% [w/v] NaCl, diluted in H₂O, pH 7.5) medium supplemented with ampicillin (100 µg/ml). For selection of single clones, LB_{amp} agar (30% [w/v] agar in LB containing ampicillin) plates were used.

2.4.1 Generation of competent *E. coli*

Competent *E. coli* were generated using the CaCl₂ method. Briefly, 100 ml of an overnight culture (OD₆₅₀ = 0.4) were incubated on ice for 30 min, centrifuged (2,000 x g, 5 min, 4°C) and resuspended in 2.5 ml ice cold CaCl₂ solution containing 75 mM CaCl₂ and 15% glycerol. Another 20 ml ice cold CaCl₂ were added, and the mixture was incubated on ice for 20 min. Cells were obtained by centrifugation (2,000 x g, 5 min, 4°C), resuspended in 2.5 ml CaCl₂, aliquoted and stored at -80°C.

2.4.2 Transformation

Transformation was carried out by adding 50-150 ng plasmid DNA to 100 µl competent bacteria. After incubation on ice for 20 min, bacteria were heat-shocked for 2 min at 42°C and 900 µl prewarmed LB were added, followed by incubation at 37°C for 1.5 h. 100 µl of the suspension were plated on LB_{amp} plates and incubated at 37°C and 5% CO₂ over night.

2.5 Plasmid generation

2.5.1 Vectors for mammalian cell transfections

GFP Fusion TOPO[®] TA Expression vector

For protein overexpression the open reading frame of the p62 transcript amplified by PCR was cloned into the pcDNA3.1/CT-GFP-TOPO[®] (Invivogen, Toulouse, France) oriented in sense or antisense direction according to the manufacturer's instructions. After cloning, insert sequences were checked using the Eurofins MWG sequencing service.

Table 2: Primer sequences as used for amplification of the open reading frame of the p62 transcript.

mRNA	primer sense, 5'→ 3'	primer antisense, 5'→ 3'
p62_ORF	GATGATGAACAAGCTTTACATCGG	CTTGCTGCGCTGTGAGGC

2.5.2 siRNA

The high-purity, full-length siRNA against p62 used in this work was purchased from Qiagen (Hilden, Germany). As a negative control, the random siRNA siGENOME non-targeting siRNA #2-5, targeting firefly luciferase (Dharmacon, Thermo Fisher Scientific, Karlsruhe, Germany) was used.

p62 siRNA: r(GGG UAG AUA UCC AUA GAA A)dTdT

2.5.3 Real-Time RT-PCR standard plasmids

Standards of the PCR product of the gene of interest were cloned into the pGEM-T Easy vector (Promega) according to the manufacturer's guidelines. Standard plasmids were provided by Prof. Dr. Alexandra K. Kiemer (Saarland University, Pharmaceutical Biology). See 2.9.2 for primer sequences.

2.6 Isolation of bacterial DNA

2.6.1 Plasmid purification

Plasmid DNA was isolated from overnight cultures by using the Mini or Midi plasmid isolation kit (Qiagen, Hilden, Germany) according to the manufacturer's instructions.

2.6.2 Determination of DNA concentrations

DNA concentrations were determined by measuring the extinction of the DNA solutions at 260 nm, whereas an extinction of 1 equates a concentration of 50 µg/ml. The purity of the DNA preparations was checked by absorption measurement at 280 nm, the characteristic absorption maximum of aromatic amino acids. Measurements were done with a BioMate UV-Vis spectrophotometer (ThermoElectron, Schwerte, Germany).

2.7 Agarose gel electrophoresis

2.7.1 Detection of DNA

Depending on the DNA size, 0.5 – 2.5% [w/v] agarose gels containing 0.04% [v/v] ethidium bromide were used for DNA detection. Upon addition of a suitable volume of 6 x loading buffer (18% Ficoll, 0.5 M EDTA, 60 ml 10 x TBE, 0.04% bromphenol blue, 0.04% xylencyanol, H₂O ad 100 ml), DNA was loaded onto a gel and separated in TBE (89.1 mM Tris, 89.1 mM boric acid, 2.21 mM EDTA in H₂O) at 100 V. To determine the size of the DNA, a 50 bp ladder (Fermentas, St. Leon-Rot, Germany) or a 1 kb ladder (Invitrogen, Darmstadt, Germany) was used. Detection of the DNA bands was carried out using a UV transilluminator and the software ArgusX1 (Biostep, Jahnsdorf, Germany).

2.7.2 Detection of RNA

In contrast to DNA gels, RNA gels contained 1% formaldehyde to ensure denaturation of the samples and were prepared with MOPS buffer (0.02 M 3-(N-morpholino)propanesulfonic acid (MOPS), 5 mM sodium acetate, 0.5 mM EDTA in DEPC-treated H₂O, pH 7) instead of TBE with 1% [w/v] agarose. Prior to loading

onto the gels, RNA was denatured at 65°C for 5 min in an appropriate volume of loading buffer (10 ml formamide, 3.5 ml formaldehyde, 1.5 ml 10 x MOPS). Samples were separated in MOPS buffer at 100 V and detected as described in 2.7.1.

2.8 RNA isolation and reverse transcription

2.8.1 RNA isolation

Total RNA was extracted in 500-1,000 µl QIAzol Lysis Reagent (#79306, Qiagen) using a micro grinder (Pellet Pestle[®] Motor, Kontes, Vineland, USA) for the murine liver tissue. After incubation for 5 min at room temperature, 125-250 µl chloroform were added. The mixture was vortexed (15 s), incubated at room temperature (2 min), and centrifuged (12,000 rpm, 15 min, 4°C). Supernatants were transferred to a new reaction tube and RNA was precipitated by addition of 1 volume of ice-cold isopropanol 100% at -20°C over night. For further processing, samples were centrifuged (12,000 rpm, 10 min, 4°C) and the resulting pellets were washed with ice-cold ethanol 70% (v/v), dried and dissolved in DEPC-H₂O. RNA integrity was checked using agarose gel electrophoresis.

From human paraffin embedded tissues RNA was isolated using RNeasy FFPE Kit (Qiagen) was used according to the manufacturers' instructions.

2.8.2 DNase digestion

RNA samples were digested with DNase to exclude contamination of genomic DNA. Therefore DNA free kit (#1906, Ambion) was used according to manufacturers' guidelines.

2.8.3 Measurement of RNA concentrations

Photometric determination of RNA concentrations at 260 nm was carried out using a BioMate UV-Vis spectrophotometer (ThermoElectron). An extinction of 1 equates a concentration of 40 µg/ml.

2.8.4 Alu PCR

To confirm the absence of DNA in our RNA preparations, a PCR for Alu elements, which occur in large numbers throughout the human genome, was performed using the following primer: 5'-TCATGTCGACGCGAGACTCCATCTCAAA-3'.

Reaction mixture

<i>Taq</i> -Polymerase	2.5 U
dNTPs	800 μ M
10 x <i>Taq</i> -buffer	2.5 μ l
MgCl ₂ (50 mM)	5 mM
primer (50 μ M)	100 nM
template	100 ng RNA
H ₂ O	ad 25 μ l

5 ng THP-1 DNA (provided by Jessica Hoppstädter, Saarland University, Pharmaceutical Biology) served as a positive control.

The PCR was carried out in a Thermocycler PX2 (Px2 Thermal Cyclers, Thermo Electron Corporation, Germany) using the following conditions:

denaturation	5 min 94°C	
denaturation	1 min 94°C	} 30 cycles
annealing	1 min 56°C	
elongation	1 min 72°C	
final elongation	10 min 72°C	

Products were detected by agarose gel electrophoresis. RNA was considered to be DNA -free when no product was visible.

2.8.5 Reverse transcription

200 – 1,000 ng of RNA were denatured at 65°C for 5 min, placed on ice, and then reverse transcribed in a total volume of 20 µl using oligo-dT primers (5'-TTT TTT TTT TTT TTT TTT-3') for human samples and random primers for murine samples using the High-Capacity cDNA Reverse Transcription Kit (Applied Biosystems, Darmstadt, Germany) according to the manufacturer's instructions. The resulting cDNA was diluted by addition of 80 µl water (AppliChem, Darmstadt, Germany) and used for real-time RT-PCR.

2.9 Restriction fragment length polymorphism

2.9.1 Genomic DNA Isolation and screening

Genomic DNA (gDNA) was isolated from paraffin-embedded tissues using the QIAamp DNA FFPE Tissue Kit (Qiagen, Hilden, Germany) according to the manufacturer's instructions.

Genomic DNA was amplified to screen liver tissue samples for heterozygosity at a known *Apal* polymorphism at the *Igf2* gene (Tadokoro et al., 1991) and an *AluI* polymorphism at the H19 gene (Zhang and Tycko, 1992). If heterozygous and hence informative, cDNA was amplified to test for biallelic expression.

Table3: Primer sequences as used for IGF2 and H19 PCR.

mRNA	primer sense, 5'→ 3'	primer antisense, 5'→ 3'
IGF2	CTTGGACTTTGAGTCAAATTGG	GGTCGTGCCAATTACATTTCA
H19	TACAACCACTGCACTACCTG	TGGCCATGAAGATGGAGTCG

Reaction mixture for the IGF2 PCR

<i>Taq</i> -polymerase	5 U
10 x <i>Taq</i> -buffer	2.5 µl
primer sense	400 nM
primer antisense	400 nM
dNTPs	125 µM
MgCl ₂	3 mM
template	5 µl
H ₂ O	ad 25 µl

Reaction mixture for the H19 PCR

DyNAmo Flash SYBR [®] Green Master mix	2.5 U
primer sense	400 nM
primer antisense	400 nM
template	5 µl
H ₂ O	ad 25 µl

Conditions

Igf2:

H19:

denaturation	5 min 94°C		denaturation	10 min 95°C	
denaturation	1 min 94°C	} 40 cycles	denaturation	1 min 94°C	} 40 cycles
annealing	1 min 64°C		annealing	1 min 65°C	
elongation	1 min 72°C		elongation	1 min 72°C	
final elongation	5 min 72°C		final elongation	8 min 72°C	

Amplification was performed in a Thermal Cycler (Px2 Thermal Cycler, Thermo Electron Corporation, Schwerte, Germany).

2.9.2 Digestion with restriction enzymes

PCR products were digested for 2 h at 37°C with *Apal* or *Alul*, respectively.

Reaction mixture

PCR product	25 µl
buffer	3 µl
restriction enzyme	1 µl
H ₂ O	3 µl

Detection of existence of polymorphisms and expression status was done by agarose gel electrophoresis as described in 2.7.1.

2.10 SNUPE analysis

Reaction mixture

<i>Taq</i> -Polymerase	2.5 U
10 x <i>Taq</i> -buffer	3.0 µl
primer sense	400 nM
primer antisense	400 nM
dNTPs	800 µM
template cDNA	1.5 µl
H ₂ O	ad 30 µl

Conditions Igf2:

denaturation	5 min 95°C	} 32 cycles
denaturation	30 s 94°C	
annealing	1 min 60°C	
elongation	1 min 72°C	
final elongation	5 min 72°C	

Conditions H19:

denaturation	5 min 95°C		
denaturation	1 min 94°C	}	35 cycles
annealing	1 min 60°C		
elongation	30 s 72°C		
final elongation	5 min 72°C		

Successful PCR was checked by loading 5 µl of the reaction on a 1.5% agarose gel.

The following experimental procedure was kindly performed by Dr. Sascha Tierling, Institute of Genetics, Saarland University (Tierling et al., 2006). SNUPE primers were placed immediately adjacent to the polymorphic sites (Igf2: C/T SNP at position nt 1678 of the mRNA, H19: C/T SNP at position nt 2437 of the mRNA). 5 µl of PCR products were purified using an Exonuclease I/SAP mix (1U/9U, USB) for 30 min at 37°C followed by a 15 min inactivation step at 80°C. 14 µl primer extension mastermix was added and SNUPE reaction was performed.

SNUPE conditions:

denaturation	2 min 96°C	}	35 cycles
annealing	20 s 96°C		
elongation	2 min 60°C		

Obtained products were loaded on a DNASepTM (Transgenomic) column and separated at 50°C applying an acetonitrile gradient. The allele-specific expression index was determined by measuring the peak heights.

2.11 Real-time RT-PCR

2.11.1 Primer and probe sequences

Table 4: Primer sequences as used for real-time RT PCR.

mRNA	primer sense, 5'→ 3'	primer antisense, 5'→ 3'
mu 18S	GCGCTTCTCTTTCCGCCA	AGCTCTCCGACACCTCTCTT
mu cycloph.	GGCCGATGACGAGCCC	TGTCTTTGGAAGTTTGTCTGC
mu H19	CAGAGGTGGATGTGCCTGCC	CGGACCATGTCATGTCTTTCTGTC
mu Igf2	GGAAGTCGATGTTGGTGCTTCTC	CGAACAGACAAACTGAAGCGTGT
mu Gilz	GGGATGTGGTTTCCGTTAAA	ATGGCCTGCTCAATCTTGTT
mu PTEN	GTGAGGATGGTAGGGGAATC	CACCACGCTTCAAAGAGAAA
mu TNF- α	CCAGGAGGGAGAACAGAAAC	CCAGTGAGTGAAAGGGACAGA
mu IL6	CCTCTGGTCTTCTGGAGTAC	CTCTCTGAAGGACTCTGGC
hu β -actin	TGCGTGACATTAAGGAGAAG	GTCAGGCAGCTCGTAGCTCT
hu p62	GTTCCCGCATCATCACTCTTAT	GAATCTCGCCAGCTGTTTGA
hu H19	TTCAAAGCCTCCACGACTCT	CTGAGACTCAAGGCCGTCTC
hu IGF2	GGAAGTGGATCCCTGAACCA	TGAAAATTCCCGTGAGAAGG
hu PTEN	GCTGAAATTGTTCACTAGCTG	GCCTAATCTATTTGCGATCA
hu GILZ	TCCTGTCTGAGCCCTGAAGAG	AGCCACTTACACCGCAGAAC

Table 5: Probe sequences as used for real-time RT-PCR.

mRNA	probe, 5' FAM → 3' BHQ1
mu 18S	CCACGCCAACCCACCGCCCTGTG
mu cyclophilin	TGGGCCGCGTCTCCTTCGA
mu Igf2	CCTTCGCCTTGTGCTGCATCGCTGCT
mu H19	TCACTGAAGGCGAGGATGACAGGT GTG
hu β -actin	CACGGCTGCTTCCAGCTCCTC
hu p62	TGTGAATCTCTTCATCCCAACCCAGGCT
hu GILZ	TCCCGAATCCCCACAAGTGCCCGA

2.11.2 Standard dilution series

In order to determine real-time RT-PCR efficiency and to quantify target mRNAs in a cDNA sample, standards from 10 to 0.0001 attomoles of the PCR product cloned into pGEM-T Easy were run alongside the samples to generate a standard curve. Plasmids were isolated as described in 2.6.1 and diluted in TE-buffer (AppliChem, Darmstadt, Germany). The required amount of plasmid DNA was calculated as follows:

$$c \text{ (target-DNA) } [\mu\text{mol/ml}] = c \text{ (plasmid) } [\mu\text{g/ml}] / \text{MW} * l$$

with MW = molecular weight of the DNA (approx. 660 g/mol) and l = length of plasmid and insert in bp.

2.11.3 Experimental procedure

Real-time RT-PCR using dual-labelled probes

Reaction mixtures were assembled on ice and 20 μl of the mixture were added to 5 μl template cDNA or standard plasmid solution in a 96 well plate. dNTP, probe and MgCl_2 concentrations for each target gene are listed in table 6.

The iCycler iQ5 (Bio-Rad, München, Germany) was used for real-time RT-PCR. Primer and probe sequences are given in table 1 and 2. All samples and standards were analyzed in triplicate. The starting amount of cDNA in each sample was calculated using the iCycler iQ5 software package (Bio-Rad, München, Germany). Absolute mRNA amounts were normalized to mRNA levels of human β -actin or murine 18S or cyclophilin, respectively.

Reaction mixture

<i>Taq</i> -Polymerase	2.5 U
10 x <i>Taq</i> -buffer	2.5 μ l
primer sense	400 nM
primer antisense	400 nM
dNTPs	125, 200 or 800 μ M
dual-labelled probe	1.5 or 2.5 pmole
MgCl ₂	3-5 mM
template	5 μ l
H ₂ O	ad 25 μ l

Conditions

denaturation	8 min 95°C		
denaturation	15 s 95°C	}	40 cycles
annealing	15 s 58-60°C		
elongation	15 s 72°C		
final elongation	25 s 25°C		

Target gene specific annealing temperatures are given in table 6.

Table 6: dNTP-, dual-labelled probe-, MgCl₂- and annealing temperatures as used for real-time RT-PCR.

mRNA	dNTPs	probe	MgCl₂	annealing
mu 18S	125 µM	2.5 pmole	3 mM	60 °C
mu p62	125 µM	2.5 pmole	5 mM	60 °C
mu Igf2	125 µM	1.5 pmole	4 mM	60 °C
mu H19	125 µM	2.5 pmole	3 mM	58 °C
mu cyclophilin	125 µM	1.5 pmole	3 mM	60°C
hu β-actin	800 µM	2.5 pmole	5 mM	58°C
hu p62	125 µM	1.5 pmole	5 mM	60°C
hu GILZ	200 µM	2.5 pmole	4 mM	60°C

Real-time RT-PCR using SYBR Green

For human β-actin, IGF2, H19, PTEN and murine PTEN, GILZ, IL6, TNF-α and 18S PCR, the Dynamo Flash SYBR Green qPCR kit (Finnzymes, Espoo, Finland) was used according to the manufacturer's guidelines. The reaction conditions resembled those described above. An annealing temperature of 60°C was used for the human genes β-actin, IGF2, H19, PTEN and for the murine genes 18S, PTEN, GILZ and TNF-α. The annealing temperature for murine IL6 was set to 64°C. The starting cDNA quantity was calculated using the iCycler iQ5 software (Bio-Rad, München, Germany). Absolute mRNA amounts of the target gene were normalized to β-actin or 18S mRNA levels, respectively.

2.12 Western Blot analysis

2.12.1 Preparation of protein samples

Cells were lysed in lysis buffer (50 mM Tris-HCl, 150 mM NaCl, 1% [v/v] Triton X-100, 0.5% [w/v] sodiumdeoxycholate, 0.1% [m/v] SDS, 1 mM EGTA, 25 mM NaF) supplemented with 1 mM sodiumorthovanadate, 1 mM PMSF and a protease inhibitor mixture (Complete[®], Roche Diagnostics, Mannheim, Germany) according to the manufacturer's instructions. Murine liver tissue was disrupted using a high-performance disperser (T25 digital ULTRATURRAX[®], IKA[®]-Werke, Staufen, Germany) and lysed accordingly. Subsequently, samples were centrifuged (10 min, 20,000 x g, 4°C) and supernatants were removed and stored at -80°C.

2.12.2 SDS-polyacrylamide gel electrophoresis (SDS-PAGE)

Composition of 15% gels:

resolving gel		stacking gel	
H ₂ O	4.6 ml	H ₂ O	6.8 ml
30 % acrylamide / 0.8 % bisacrylamide solution	10 ml	30 % acrylamide / 0.8 % bisacrylamide solution	1.7 ml
Tris (1.5 M, pH 8.0)	5 ml	Tris (1 M, pH 6.8)	1.25 ml
SDS (10 % [w/v])	200 µl	SDS (10 % [w/v])	100 µl
APS (10 % [w/v])	200 µl	APS (10 % [w/v])	100 µl
TEMED	20 µl	TEMED	10 µl

Procedure

Samples were thawed on ice, mixed with Roti[®]-Load 2 loading buffer and denatured for 5 min at 95°C. A prestained protein marker (Fermentas) was used to estimate the molecular masses. Equal sample amounts and a suitable marker volume were loaded onto the gel and separated in electrophoresis buffer (24.8 mM Tris, 1.92 mM glycine, 0.1% [w/v] SDS) for 130 min at 80 V, followed by 2 h at 120 V. Gel

preparation and electrophoresis were carried out using the Bio-Rad Mini PROTEAN system (Bio-Rad, München, Germany).

2.12.3 Blotting

The Mini-Transblot cell (Bio-Rad, München, Germany) system was employed to transfer separated protein samples onto a polyvinylidene fluoride (PVDF) membrane (Immobilon-FL, Millipore, Schwalbach am Taunus, Germany). Prior to blotting, the membrane was incubated for 30 s in methanol. Sponges, blotting papers, the gel and membrane were equilibrated in transfer buffer, followed by gel sandwich preparation. Blotting was carried out at 80 mA overnight. Afterwards, the membrane was incubated in Rockland Blocking Buffer (RBB) for near-infrared Western Blotting (Rockland, Gilbertsville, PA, USA) for 1 h in order to block unspecific binding sites.

2.12.4 Immunodetection

Antibodies were either diluted in PBST (0.1% [v/v] tween 20 in PBS) containing 5% [m/v] dried milk or BSA or RBB according to table 7.

Table 7: Antibody dilutions used for immunodetection.

Antibody	dilution
anti-human p62, rabbit IgG	1:1,000 in PBST + 5% [m/v] BSA
anti-human/mouse PTEN, rabbit IgG	1:500 in PBST + 5% [m/v] BSA
anti-human/mouse Erk, mouse IgG	1:1,000 in RBB
anti-human/mouse pErk, rabbit IgG	1:1,000 in RBB
anti-human/mouse Akt, rabbit IgG	1:1,000 in RBB
anti-human/mouse pAkt, rabbit IgG	1:1,000 in RBB
anti-human/mouse I κ B α , rabbit IgG	1:1,000 in RBB
anti-human tubulin, mouse IgG	1:1,000 in PBST + 5% [m/v] dried milk
IRDye [®] 800CW conjugated goat anti-mouse IgG	1:5,000 in RBB
IRDye [®] 680 conjugated mouse anti-rabbit IgG	1:5,000 in RBB

Membranes were incubated with primary antibodies for 2 h (p62, tubulin) or 3 h (ERK, AKT) at room temperature or overnight at 4°C (pErRK, pAKT, I κ B α , PTEN). Subsequently, they were washed either in PBST + 5% [m/v] dried milk or BSA for p62 and PTEN blots (2 x 5 min), followed by additional washing steps in PBST (2 x 5 min). Afterwards, membranes were incubated with the secondary antibody for 1.5 h at room temperature. After washing twice in PBST and PBS for 5 min, blots were scanned with an Odyssey Infrared Imaging System (LI-COR Bioscience, Bad Homburg, Germany) and relative signal intensities were determined using the Odyssey software.

2.13 Transfection of HepG2 cells

2.13.1 Plasmid transfection

Plasmids were introduced into HepG2 cells using jetPEITM-Hepatocyte transfection reagent according to the manufacturer's guidelines for transfection of hepatocyte cells. Briefly, 10⁴ cells were plated in 0.2 ml growth medium per well in 96 well plates. For each well, 0.25 μ g plasmid DNA was diluted in a total volume of 10 μ l NaCl 150 mM, mixed with 0.8 μ l of jetPEITM-Hepatocyte in 10 μ l NaCl 150 mM and incubated for 15 min at room temperature prior to its addition to HepG2 cells. For p62 overexpression assays, cells were treated 48 h after they were transfected with pcDNA3.1/CT-GFP-TOPO[®] p62-sense or the antisense control construct and harvested 68 h after transfection.

2.13.2 siRNA transfection

For knockdown of p62 by siRNA, cells were reverse transfected with sip62 and control siRNA using INTERFERinTM transfection reagent as recommended by the supplier. In short, 250 nmole siRNA were diluted in 248 μ l serum- and antibiotic-free RPMI-1640, mixed with 2 μ l of INTERFERinTM and incubated at room temperature for 10 min. Afterwards the mixture was transferred to a 12 well plate with 250 μ l per well and HepG2 cells were seeded at a density of 1.25 x 10⁵ cells per well. Experiments were performed 48 h after transfection.

2.14 Determination of mRNA stability

To analyze the effects of the p62 transgene on PTEN and GILZ mRNA stability, the transcription inhibitor actinomycin D (10 µg/ml) was added to primary hepatocytes isolated from p62 transgenic mice. 4 to 10 h thereafter, cells were harvested and RNA was isolated. The relative amount of PTEN and GILZ mRNA was determined by real-time RT-PCR.

2.15 Caspase-3-activity assay

After treatment cells were washed twice with ice-cold PBS, incubated with 70 µl ice-cold lysis buffer (25 mM HEPES, 5 M MgCl₂, 1 M EGTA, 0.1% [v/v] Triton X-100) and frozen at -80°C overnight. Tissue was homogenized in lysis buffer. After thawing on ice, cells were scratched off the culture plates, collected by centrifugation (14,000 rpm, 10 min, 4°C) and 10 µl of the supernatants were transferred to a flat-bottom 96well microtiter plate (TPP, Trasadingen, Switzerland). After dilution with 90 µl substrate buffer (50 mM HEPES, 0.1% [w/v] CHAPS, 1% [w/v] sucrose, pH 7.5), generation of free 7-amino-4-trifluoro-methylcoumarin (AFC) at 37°C was kinetically determined by fluorescence measurement (excitation: 385 nm; emission: 535 nm) using a fluorometer microplate reader (Wallac Victor2, PerkinElmer). Enzyme activity was calculated using an external AFC standard curve. The time point at which highest enzyme activity was measured was set to 100%.

2.16 ELISA

Serum concentrations of the murine cytokines IL-6 and TNF-α were determined using Quantikine® Mouse IL-6 Immunoassay and Quantikine® Mouse TNF-α/TNFSF1A Immunoassay (R&D Systems Europe, Abingdon, United Kingdom) according to the manufacturer's instructions. The plate was read at an absorbance microplate reader (Wallac Victor2, PerkinElmer, Radgau-Jüdsheim, Germany). Total protein concentrations were determined by Bradford protein assay using a Sunrise absorbance reader (Tecan, Mainz, Germany)

2.17 Fatty acid measurement

Murine liver samples were lyophilized to dryness, dissolved in a mixture of 500 μ l methanol/toluene/sulfuric acid (50:50:2 [v/v/v]) and incubated at 55°C overnight. Subsequently, 400 μ l of a 0.5 M NH_4CO_3 , 2 M KCl solution were added to the samples, which were then centrifuged at room temperature, transferred to a GC vial and derivatized with 25 μ l N-methyl-N-(trimethylsilyl)trifluoroacetamide at 37°C for 1 h. Fatty acid analysis was performed on an Agilent 6890N gas chromatograph coupled to an Agilent 5973N mass selective detector (both Agilent Technologies, Waldbronn, Germany) and equipped with a non-polar J&WDB-5HT capillary column. Fatty acid analysis was performed by Dominik Pistorius (Saarland University, Pharmaceutical Biotechnology).

2.18 Human HCC samples

Paraffin-embedded liver samples from HCC patients were obtained from the Institute of Pathology, Saarland University, Homburg, Germany. Clinical patient data are shown in table 8.

Table 8: Clinical data of human HCC samples. m: male, f: female, hemochr.: hemochromatosis n/a: not available.

	age	gender	etiology	BCLC	nodularity	tumor size	grading	follow-up
1	25	m	HBV	C	no	5 cm	G2	death after 3 months
2	65	f	alcohol	B	no	1.1 cm	G2	recurrence 4 months
3	46	f	alcohol	A	yes	9.5 cm	G2	recurrence 4 months
4	82	m	alcohol	B	yes	5.2 cm	G2	recurrence 19 months
5	68	m	HBV	B	no	6 cm	G2	ongoing 19 months
6	21	m	HBV	B	no	5 cm	G2	recurrence 6 months
7	73	m	alcohol	A	yes	8 cm	G3	n/a
8	77	m	cryptogen	A	yes	9 cm	G2	n/a
9	56	f	NASH	A	yes	26 cm	G2	recurrence 6 months
10	57	m	HCV	A	yes	2.2 cm	G2	ongoing 18 months
11	57	f	alcohol	A	yes	4.2 cm	G2	ongoing 8 months
12	64	f	HCV	A	yes	2.2 cm	G2	HCC free 52 months
13	70	m	ASH	A	yes	6.5 cm	G3	ongoing 6 months
14	61	f	alcohol	B	no	3.7 cm	G2	ongoing 10 months
15	68	m	HBV	0	yes	1.6 cm	G2	ongoing 12 months
16	n/a	n/a	n/a	n/a	n/a	n/a	n/a	n/a
17	65	m	alcohol	A	no	2.3 cm	G2	n/a
18	n/a	n/a	n/a	n/a	n/a	n/a	n/a	n/a
19	65	f	alcohol	A	yes	4.2 cm	G1	ongoing 11 months
20	73	f	HCV	B	yes	2.9 cm	G2	ongoing 42 months
21	73	m	hemochr.	A	yes	2.2 cm	G2	ongoing 6 months
22	79	f	porphyria	A	yes	7 cm	G2	recurrence 25 months
23	66	m	alcohol	A	yes	2.7 cm	G1	n/a
24	66	m	alcohol	A	yes	6 cm	G2	ongoing 14 months
25	70	m	NASH	B	yes	13 cm	G3	n/a
26	64	m	NASH	B	no	13 cm	G2	ongoing 7 months
27	67	m	NASH	A	yes	3.4 cm	G2	recurrence 56 months
28	57	f	hemochr.	A	yes	2.1 cm	G2	postoperative death
29	69	m	alcohol	A	yes	3.2 cm	G1	recurrence 6 months
30	71	m	HCV	A	yes	2.4 cm	G2	n/a
31	51	f	HCV	B	no	3 cm	G3	recurrence 23 months
32	68	m	NASH	A	yes	3.5 cm	G2	n/a

2.19 Statistics

Data analysis and statistics were performed using Origin software (OriginPro 8.1G; OriginLabs, Northampton, MA, USA). All data are displayed as mean values \pm SEM. Statistical differences were estimated by independent two-sample t-test unless stated otherwise. Differences were considered statistically significant when p values were less than 0.05.

3 Results

3.1 Effects of p62 on hepatic metabolism

3.1.1 p62 expression in DEN-treated mice

In order to confirm the transgene expression in DEN-treated *p62* transgenic mice real-time RT-PCR was performed to determine *p62* mRNA expression. There was no difference in expression levels between 2.5- and 5-week-old animals (figure 6).

Furthermore, no gender specificity was observed (figure 6).

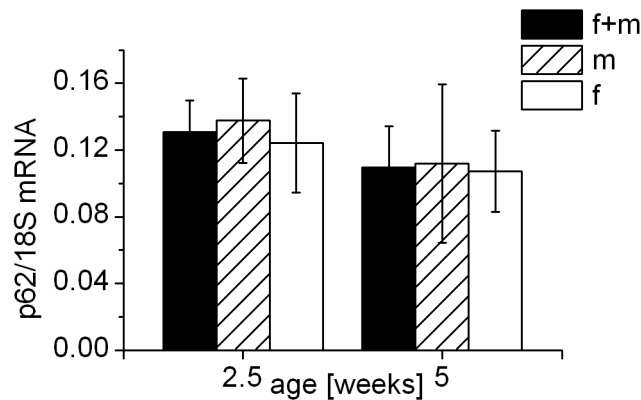


Figure 6: p62 expression in DEN-treated transgenic mice – RNA was isolated from snap-frozen liver tissue and real-time RT-PCR analysis was performed. Data were normalized to 18S. Data show means \pm SEM of 28 (2.5 weeks) and 17 (5 weeks) animals (A). Mice were treated with DEN and sacrificed 48 h later at the indicated age. f+m: female and male mice, m: male mice, f: female mice.

3.1.2 Effect of p62 on the metabolism of fatty acids

The determination of serum parameters of DEN-treated mice revealed a significant increase of triglycerides, HDL, and cholesterol levels in the transgenic group (table 9). Five-week-old transgenic mice also showed decreased glucose levels compared to controls (table 9).

Table 9: Table shows mean serum levels \pm SEM of 28 (2.5 weeks) or 17 (5 weeks) wild-type (co) or transgenic (tg) animals. * $P < 0.05$, ** $P < 0.01$ compared to wild-type (co) at the same age.

	2.5 weeks		5 weeks	
	co	tg	co	tg
AST [U/l]	3,055 \pm 310	3,259 \pm 971	3,510 \pm 384	3,436 \pm 327
ALT [U/l]	571 \pm 105	614 \pm 167	741 \pm 94	613 \pm 80
Glucose [mg/dl]	89.5 \pm 8.3	78.5 \pm 6.1	119.9 \pm 7.1	76.4 \pm 7.8**
Triglycerides [mg/dl]	110.2 \pm 8.9	229.5 \pm 43.3*	82.4 \pm 9.0	115.6 \pm 13.5*
HDL [mg/dl]	44.2 \pm 6.10	75.9 \pm 7.4**	100.0 \pm 10.3	152.5 \pm 13.4**
Cholesterol [mg/dl]	74.1 \pm 9.3	129.9 \pm 12.5**	133.3 \pm 8.6	186.8 \pm 11.2**

Because of the metabolic changes in the transgenic animals it was interesting to investigate the fatty acid composition of liver tissue (table 10). Due to the fact that DEN itself provokes changes in fat metabolism (Canuto 1989), also liver tissues of untreated animals were analysed in comparison. DEN evoked changes in fatty acid composition of wild-type mice leading to increased levels of palmitic acid (16:0), stearic acid (18:0), oleic acid (18:1), linoleic acid (18:2), adrenic acid (22:4), and cholesterol compared to untreated control. Docosapentaenoic acid (22:5) was reduced in DEN-treated *versus* untreated wild-type animals.

Despite these already remarkable changes transgenic animals showed even more pronounced changes upon DEN-treatment: compared to DEN-treated wild-type animals the DEN-treated transgenic group showed significantly increased amounts of oleic acid (18:1), gadoleic acid (20:1), eicosadienoic acid (20:2), eicosatrienoic acid (20:3), eicosapentaenoic acid (20:5), docosapentaenoic acid (22:5), and cholesterol in the liver. Stearic acid (18:0) and docosahexaenoic acid (22:6) were decreased.

In the absence of DEN transgenic mice showed higher amounts of lauric acid (12:0), myristic acid (14:0), palmitic acid (16:0), palmitoleic acid (16:1), stearic acid (18:0), oleic acid (18:1), linoleic acid (18:2), gadoleic acid (20:1), eicosadienoic acid (20:2), eicosatrienoic acid (20:3), adrenic acid (22:4), and cholesterol compared to untreated wild-type mice. These massive changes in both the amount and pattern of fatty acids

in the liver due to p62 expression was hypothesized to change activation of signaling pathways or cytokine production, in which fatty acids are involved.

Table 10: Table shows mean serum levels \pm SEM of 7 (untreated wild-type (co)), 19 (untreated transgenic (tg)), 15 (DEN treated wild-type (co)), and 11 (DEN treated transgenic (tg)) animals 2.5 weeks of age. Liver tissues were lyophilized and analysed by GC-MS. * $P < 0.05$, ** $P < 0.01$, *** $P < 0.001$ compared to untreated control; # $P < 0.05$, ## $P < 0.01$ compared to DEN-treated control.

Fatty acid composition	untreated		DEN-treated	
	co	tg	co	tg
12:0	0.05 \pm 0.05	0.57 \pm 0.13***	0.51 \pm 0.34	0.87 \pm 0.18
14:0	0.32 \pm 0.11	1.48 \pm 0.30***	1.33 \pm 0.84	2.39 \pm 0.42
16:0	16.66 \pm 0.77	25.82 \pm 1.54***	30.01 \pm 4.29**	28.89 \pm 2.12
16:1	0.04 \pm 0.03	0.44 \pm 0.10**	0.87 \pm 0.63	1.36 \pm 0.24
18:0	11.71 \pm 0.20	14.15 \pm 0.44***	17.61 \pm 0.85***	14.09 \pm 0.64##
18:1	5.54 \pm 0.47	15.40 \pm 1.68***	15.00 \pm 2.64**	22.74 \pm 2.56##
18:2	9.75 \pm 0.62	24.46 \pm 2.46***	22.54 \pm 4.92*	30.24 \pm 3.49
20:1	n.d.	0.14 \pm 0.06*	n.d.	0.55 \pm 0.10##
20:2	0.34 \pm 0.07	0.82 \pm 0.14**	0.48 \pm 0.18	1.76 \pm 0.20##
20:3	0.29 \pm 0.07	1.11 \pm 0.16***	0.47 \pm 0.17	1.41 \pm 0.17##
20:4	10.91 \pm 0.26	12.08 \pm 0.65	13.70 \pm 1.10	13.45 \pm 0.54
20:5	n.d.	0.05 \pm 0.05	n.d.	0.39 \pm 0.10##
22:4	0.11 \pm 0.07	0.58 \pm 0.15**	2.69 \pm 1.00*	1.23 \pm 0.22
22:5	2.20 \pm 0.92	2.33 \pm 0.54	0.20 \pm 0.07*	2.43 \pm 0.59##
22:6	1.55 \pm 0.52	0.90 \pm 0.18	1.62 \pm 0.34	0.42 \pm 0.07##
Cholesterol	8.06 \pm 1.18	16.04 \pm 1.60***	17.02 \pm 3.01*	24.21 \pm 2.51#

3.1.3 p62 downregulates PTEN expression

It has been shown previously that the accumulation of fatty acids reduces the expression of the tumor suppressor PTEN (Vinciguerra et al., 2009a). As expected, the *p62* transgenic mice show decreased PTEN expression on both mRNA and protein level at 2.5 weeks of age (figure 7 A, C, D). No gender-specific changes were observed (figure 7 A, C, D). However, in 5-week-old animals protein expression was decreased, but mRNA expression was not altered (figure 7 B, E, F). In transgenic male mice even a slight but non-significant increase in mRNA levels could be noted.

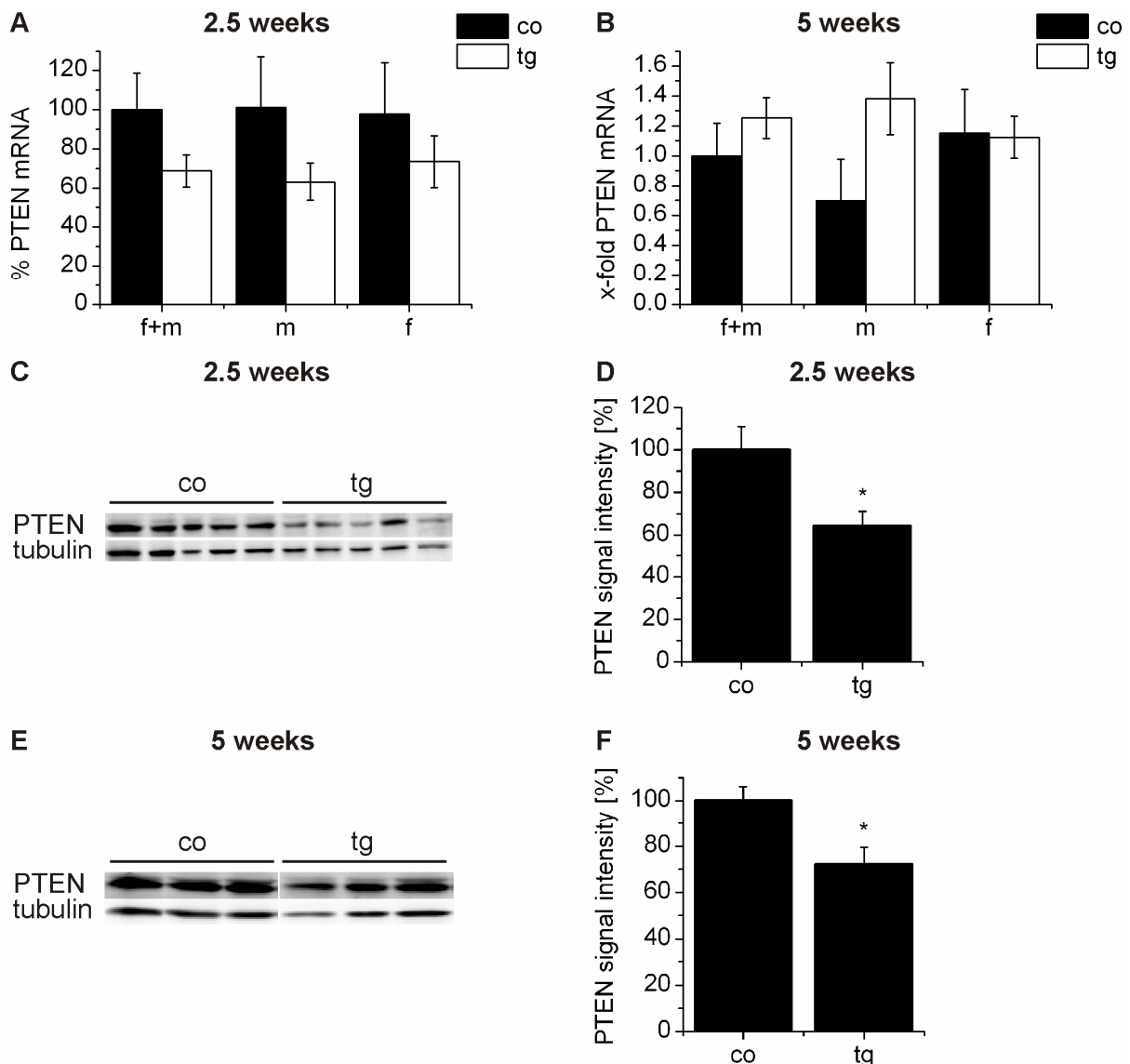


Figure 7: PTEN downregulation in p62 transgenic mice – Wild-type (co) or transgenic (tg) mice were treated with DEN at the age of 2.5 weeks or 5 weeks. A, B: RNA was isolated from liver tissue and real-time RT-PCR was performed. Data were normalized to 18S. Data show means \pm SEM of 28 (2.5 weeks) (A) and 17 (5 weeks) (B) animals. f+m: female and male mice, m: male mice, f: female mice. C-F: Western Blot analysis from liver tissue was performed using tubulin as a loading control. Data show representative blots performed with tissue from 28 (2.5 weeks) (C) and 17 (5 weeks) (E) animals. D, F: PTEN protein signal intensities were quantified and normalized to tubulin values. Data are expressed as percentage of wild-type animals (co) values. * $P < 0.05$ compared to DEN-treated wild-type mice.

Knockdown experiments in HepG2 cells underlined the connection between p62 and PTEN also in the human system: knockdown of *p62* increased *PTEN* expression (figure 8).

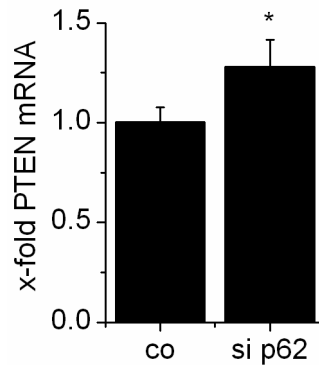


Figure 8: p62 regulates PTEN expression – HepG2 cells were transfected with either random siRNA (co) or p62 siRNA (si p62). After 48 h cells were harvested, RNA was isolated and real-time RT-PCR analysis was performed. Data show means \pm SEM of three independent experiments. * $P < 0.05$ compared to random siRNA.

3.1.4 Expression of glucocorticoid-induced leucine zipper (GILZ)

Elevated GILZ levels have previously been shown to play a role in alcoholic hepatitis (Hamdi et al., 2007). We therefore hypothesized that GILZ might also be a mediator in NASH. Thus, we investigated the expression of *Gilz* mRNA in *p62* transgenic mice. There was in fact an upregulated expression of *Gilz* in DEN-treated transgenic animals, but only at the age of five weeks (figure 9 A, B). This upregulation was more pronounced in male mice (figure 9 B).

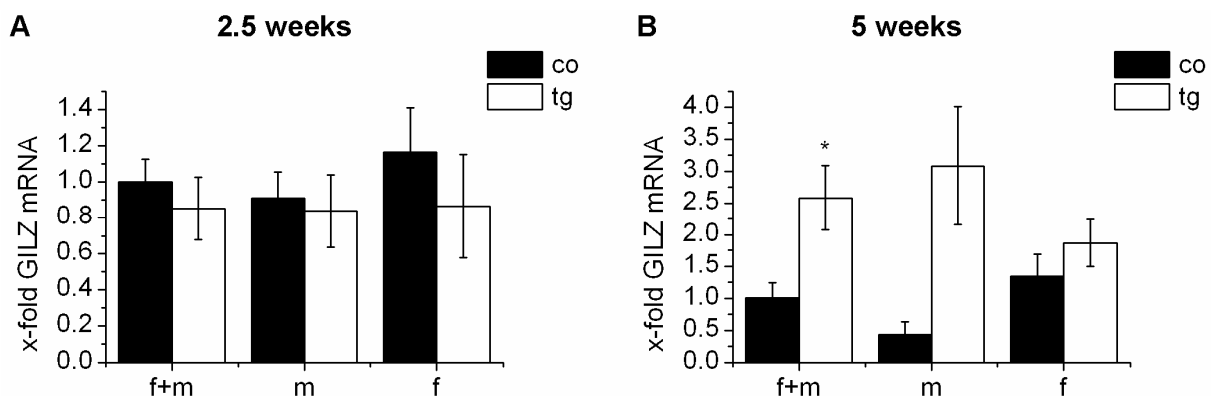


Figure 9: GILZ expression in DEN-treated mice – Wild-type (co) or transgenic (tg) mice were treated with DEN at the age of 2.5 weeks (A) or 5 weeks (B). f+m: female and male mice, m: male mice, f: female mice. A, B: RNA was isolated from liver tissue and real-time RT-PCR analysis was performed. Data were normalized to 18S. Data show means \pm SEM of 28 (2.5 weeks) (A) and 17 (5 weeks) (B) animals. * $P < 0.05$ compared to DEN-treated control mice.

After knockdown of *p62* in HepG2 cells, *GILZ* mRNA was significantly downregulated (figure 10 A). Because *GILZ* mRNA expression is known to be altered *via* changes in its stability (Hoppstädter, 2010), mRNA stability was determined in primary murine hepatocytes from transgenic animals. Transgenic animals displayed a $t_{1/2}$ of *GILZ* mRNA of 9.0 h, whereas *GILZ* mRNA half-life was only 3.5 h in hepatocytes from control mice (figure 10 B).

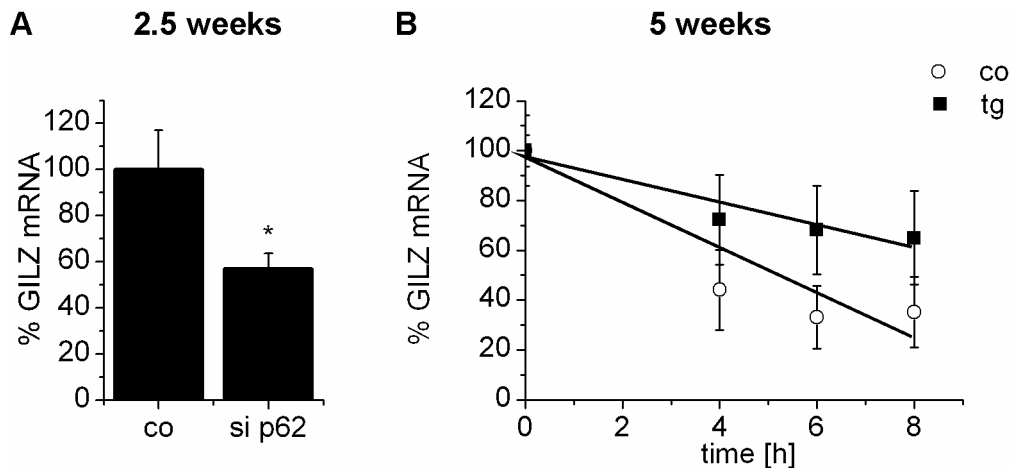


Figure 10: GILZ expression in hepatoma cells and mRNA stability of GILZ - A: HepG2 cells were transfected with either random siRNA (co) or *p62* siRNA (si *p62*). After 48 h cells were harvested, RNA was isolated, and real-time RT-PCR analysis was performed. Data show means \pm SEM of three independent experiments. **B:** RNA of primary murine hepatocytes, which were isolated from co and tg animals and treated with Actinomycin D (10 μ g/ml) for the indicated time points, done by Elisabeth Tybl (Saarland University), was used for real-time RT-PCR analysis. Data show means \pm SEM of hepatocytes from 3 control and 3 transgenic animals. * $P < 0.05$ compared to random siRNA (A) or hepatocytes from control animals (B), respectively.

Due to the altered expression of *GILZ*, known to be a regulator of inflammatory processes, by *p62*, we aimed to investigate the inflammatory response upon *p62* expression in DEN-treated mice.

3.1.5 *p62* induces inflammatory cytokines

In *p62* transgenic animals the transcription factor NF- κ B has been shown to be overexpressed in the cytosol (Tybl et al., 2011). We hypothesized that inflammatory activation, as it can be induced by fatty acids (Mollica et al., 2011), might be amplified in *p62* transgenic animals. Therefore, serum cytokine levels of TNF- α and IL6 were determined by ELISA. A significant increase in TNF- α protein was detected for five-week-old animals (figure 11 B). The observed increase in IL6 levels was not statistically significant, but more pronounced in 2.5-week-old transgenic mice (figure

11 A).

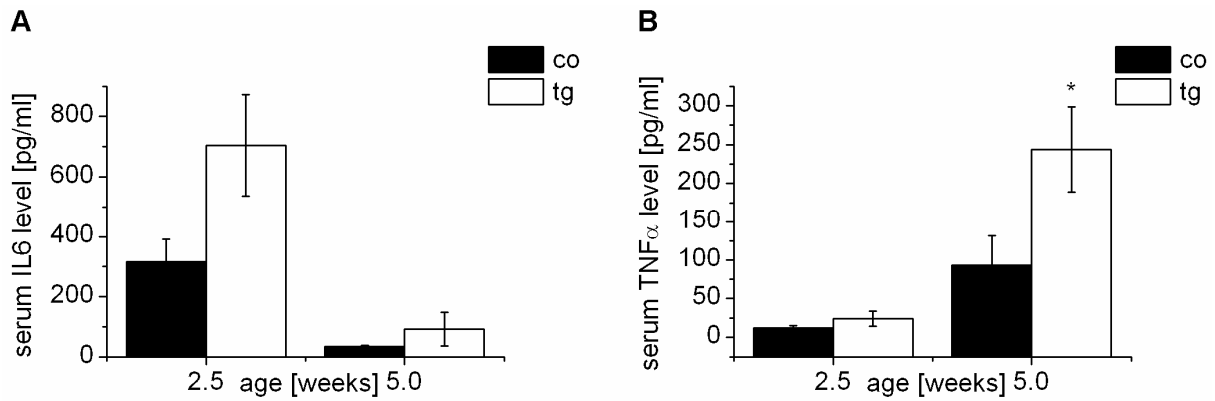


Figure 11: Induction of inflammatory cytokines in p62 transgenic mice – Levels of IL6 (A) and TNF α (B) were analysed in sera of 27 (2.5 weeks) and 9 animals (5 weeks) by ELISA. Data show means \pm SEM. * $P < 0.05$ compared to sera of DEN-treated wild-type (co) mice.

Enhanced cytokine levels are typically transcriptionally induced. Thus, we measured mRNA expression in the livers of DEN-treated animals. Here, we could also observe a tendency of increased *IL6* and *TNF- α* mRNA expression (figure 12 A-D).

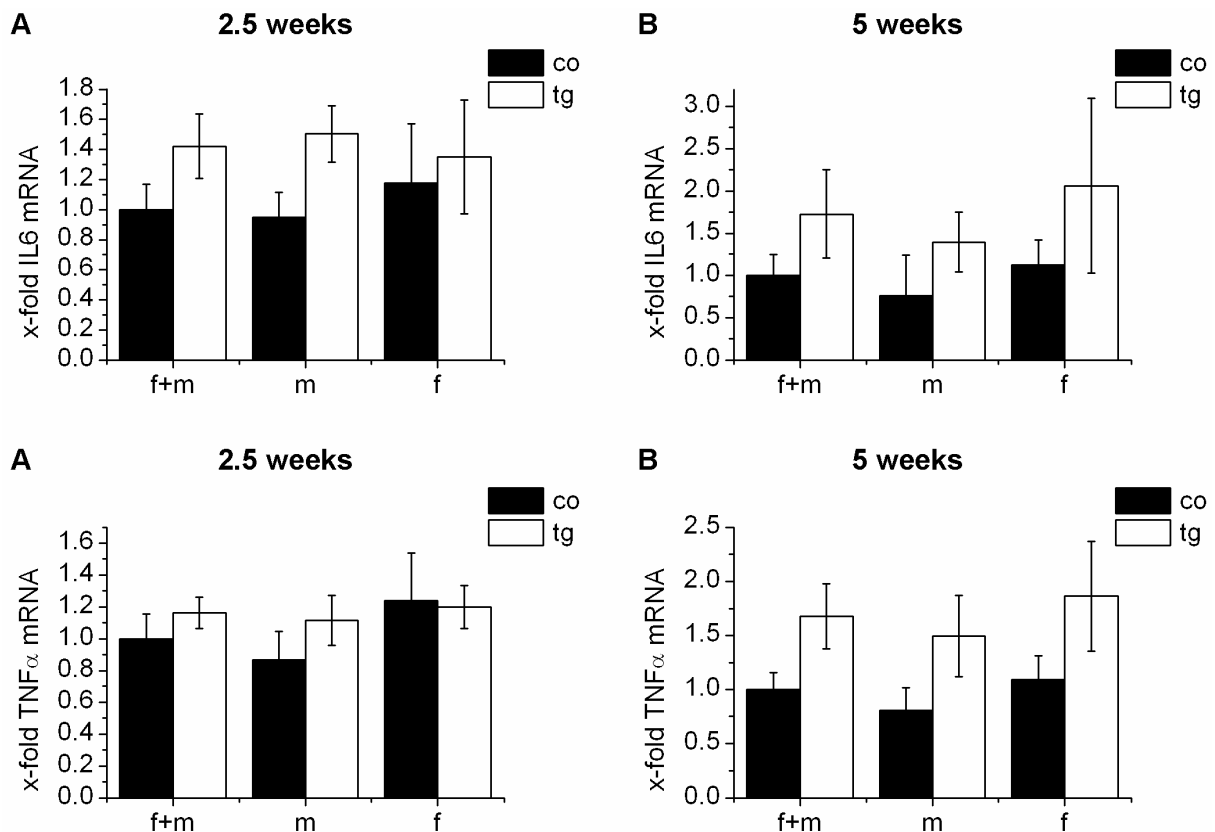


Figure 12: Induction of inflammatory cytokines in p62 transgenic mice – Mice were treated with DEN at the age of 2.5 weeks (A, C) or 5 weeks (B, D). f+m: female and male mice, m: male mice, f: female mice. A-D: RNA was isolated from liver tissue and real-time RT-PCR analysis was performed. Data were normalized to 18S. Data show means \pm SEM of 28 (2.5 weeks) (A, C) and 17 (5 weeks) (B, D) animals.

Transcriptional upregulation of inflammatory cytokines is mediated by transcription factors, nuclear factor κ B (NF- κ B) being the most important one of them. The degradation of NF- κ B-inhibitor (I κ B α) represents a necessary step in the activation of the transcription factor NF- κ B, (Kierner et al., 2002; Vinciguerra et al., 2008). Its degradation could be observed by Western Blot analysis in 2.5-week-old transgenic mice to a higher extent than in control animals (figure 13 A, B). In 5 week old mice, I κ B α levels were not significantly different, but appeared to be slightly lower (figure 13 C, D).

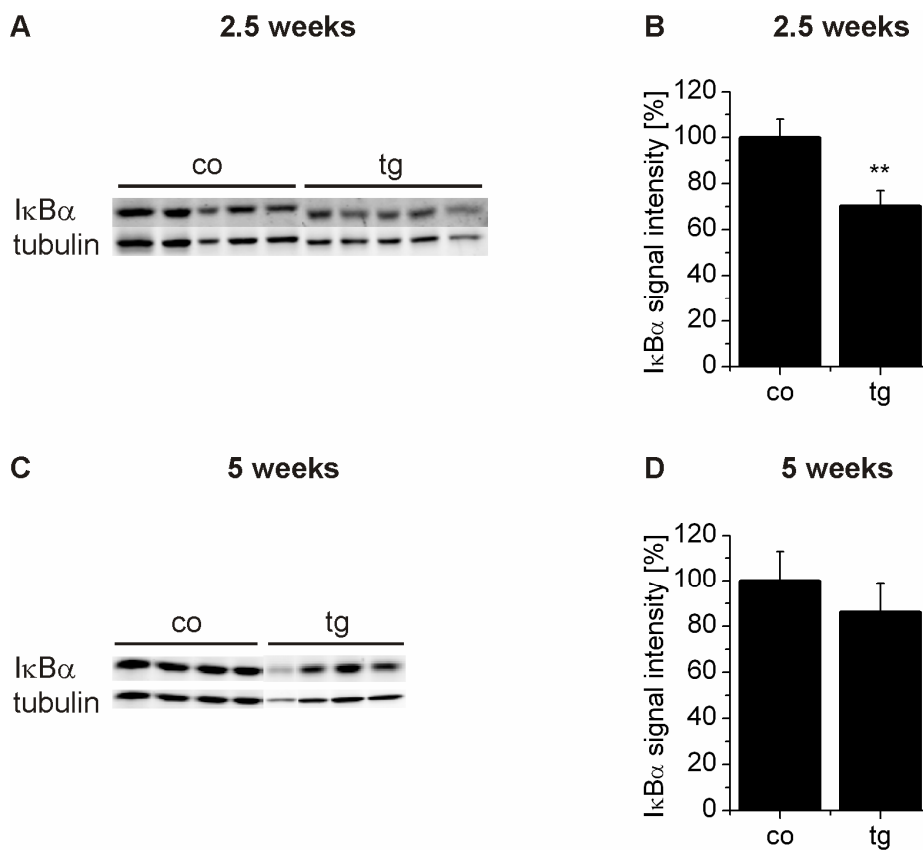


Figure 13: Degradation of I κ B α in p62 transgenic mice – Western Blot analysis from liver tissue was performed using tubulin as a loading control. Data show representatives out of 28 (2.5 weeks) (A, B) and 17 (5 weeks) (C, D) animals. B, D: Relative I κ B α protein signal intensities were quantified and normalized to tubulin values. Data are expressed as percentage of wild-type (co) animal values. ** P < 0.01 compared to DEN-treated wild-type (co) mice.

3.2 Antiapoptotic effect of p62

3.2.1 p62 expression results in high expression of Igf2

Untreated transgenic mice show high *Igf2* levels compared to control animals (Tybl et al. 2011). This was also true for transgenic mice treated with DEN at 2.5 and 5 weeks of age (figure 14). In transgenic females the induction of *Igf2* expression is more pronounced than in males.

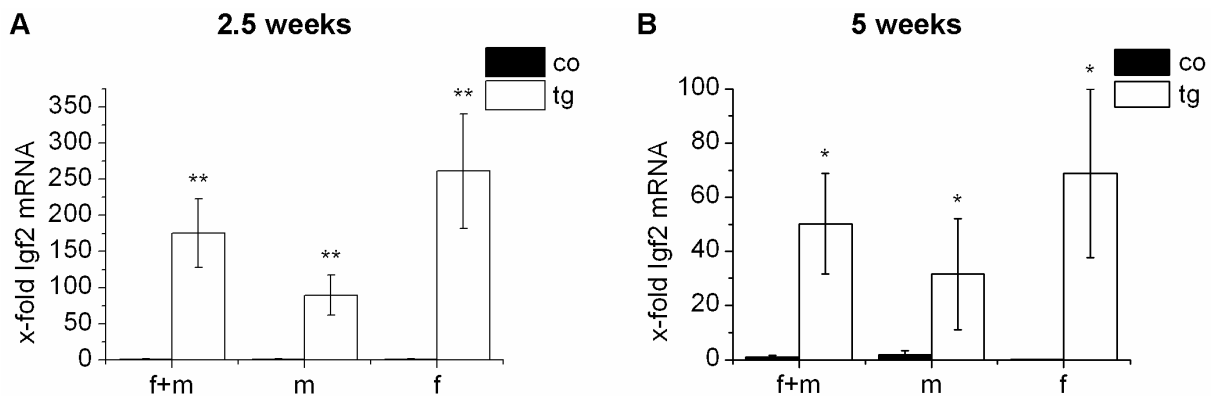


Figure 14: Igf2 expression in DEN treated mice – RNA was isolated from snap-frozen liver tissue and real-time RT-PCR analysis was performed. Data were normalized to 18S. Data show means \pm SEM of 28 (2.5 weeks) and 17 (5 weeks) animals. Mice were treated with DEN at the age of 2.5 weeks (A, B) or 5 weeks (C, D). * $p < 0.05$, ** $p < 0.01$ compared to control mice.

In order to determine whether this increase in *Igf2* expression was due to a switch from normal monoallelic to biallelic expression, five week old heterozygous SD7 mice were treated with DEN and genomic imprinting status was investigated by SNUPE analysis. Expression of *Igf2* remained monoallelic (table 11).

Table 11: Table shows allele-specific index of Igf2 expression after SNUPE-HPLC detection. Values were obtained by determination of the peak heights of the C- and T-extended primers and calculating the ratio $h(C)/h(C) + h(T)$ (5 weeks: 7 transgenic and 1 control animal).

	control	transgenic
Igf2	1.0 \pm 0.0	1.0 \pm 0.0

In figure 15 one representative SNUPE chromatogram is shown.

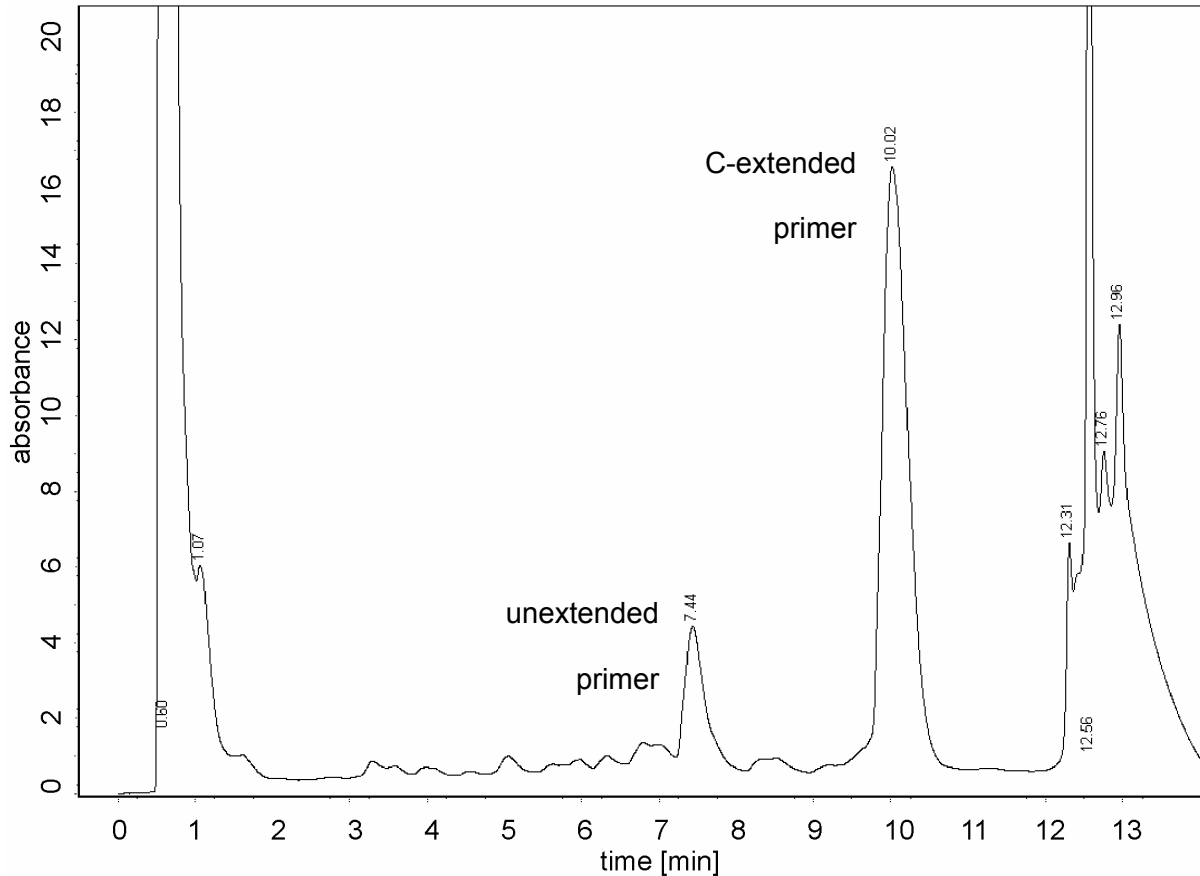


Figure 15: Continuation of genomic imprinting of *Igf2* in *p62* transgenic mice treated with DEN - RNA was isolated from liver tissue and SNUPE analysis was performed. Mice were treated with DEN at the age of 5 weeks. The figure shows a representative SNUPE chromatogram for *Igf2*.

Due to high *Igf2* expression levels in *p62* transgenic mice and because of well described antiapoptotic effects of *Igf2* (Lamonerie et al., 1995), we determined the effect of *p62* on apoptosis. In transgenic mice induction of apoptosis with DEN was reduced compared to wild-type animals (figure 16 A, B).

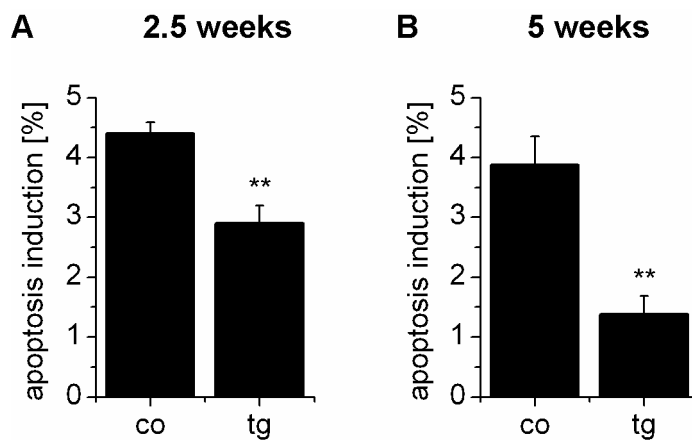


Figure 16: *p62* has an antiapoptotic effect – A, B: Protein lysates were prepared from snap-frozen liver tissue of DEN-treated mice 2.5 (A) or 5 (B) weeks of age and caspase-3-like activity assay was performed. Data show means \pm SEM of 28 (A) or 17 (B) animals. ** $P < 0.01$ compared to DEN-induced apoptosis induction in wild-type (co) animals.

3.2.2 Role of p62 and IGF2 in human HCC

In order to investigate a connection between p62 and IGF2 in human HCC, paraffin-embedded samples of human HCC tissues and matched normal tissues were analysed. *p62* as well as *IGF2* expression was increased in tumor tissues when compared to their respective surrounding tissue (figure 17 A). We also found a positive correlation between *p62* and *IGF2* in tumor tissues (figure 17 B). A comparison of *p62* expression increases between cirrhotic and non-cirrhotic tissue did not indicate differences between the two groups.

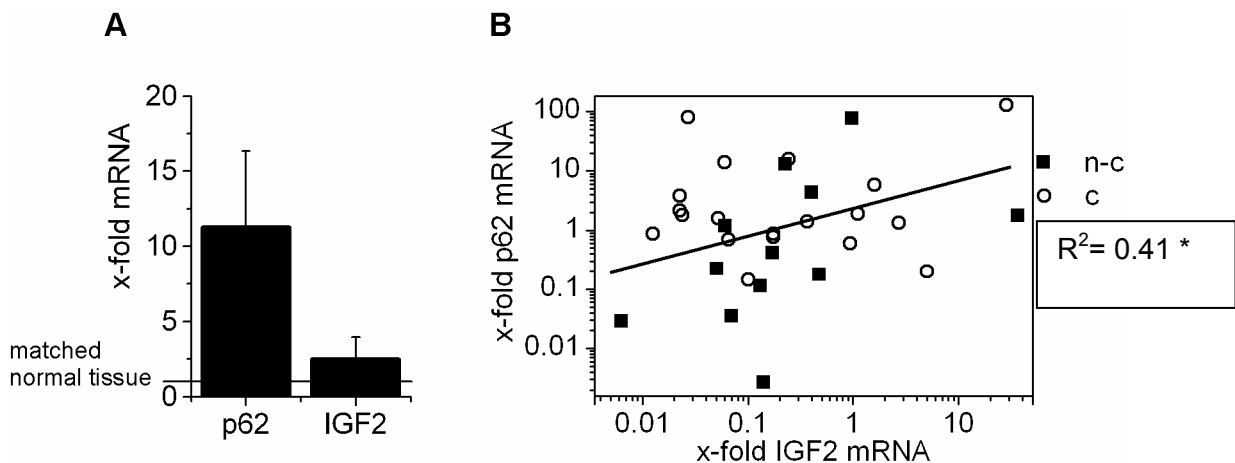


Figure 17: Expression of p62 and IGF2 in human HCC - A, B: RNA was isolated from paraffin-embedded HCC tissues and matched normal tissues and real-time RT-PCR analysis was performed. Data were normalized to β -actin. Data show means \pm SEM (A) or distribution (B) of cirrhotic (c) and non-cirrhotic (n-c) samples from 32 patients. * $P < 0.05$

When comparing absolute *p62* levels from cirrhotic *versus* non-cirrhotic tumor tissue, however, *p62* expression revealed to be higher in tumor tissues surrounded by non-cirrhotic tissue (figure 18 A). Within this non-cirrhotic group tumor tissues revealed a strong correlation between *p62* and *IGF2* (figure 18 B).

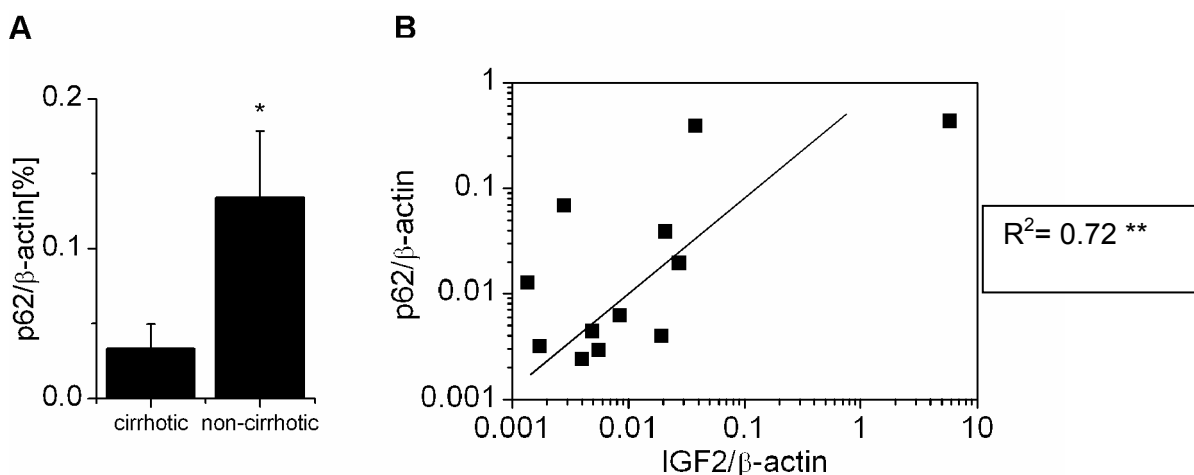


Figure 18: High p62 expression in non-cirrhotic tissue - A, B: RNA was isolated from paraffin embedded HCC tissues and real-time RT-PCR analysis was performed. Data were normalized to β -actin. Data show means \pm SEM of samples from 32 patients (A) or distribution of non-cirrhotic samples from 13 patients (B). * $P < 0.05$ compared to cirrhotic tissues.

Interestingly, the upper third of higher *p62*-expressing samples showed poorer prognosis characterized by an intermediate or advanced Barcelona staging (BCLC B or C), multinodularity, increased tumor size (> 5 cm), and early recurrence (< 20 month) (figure 19).

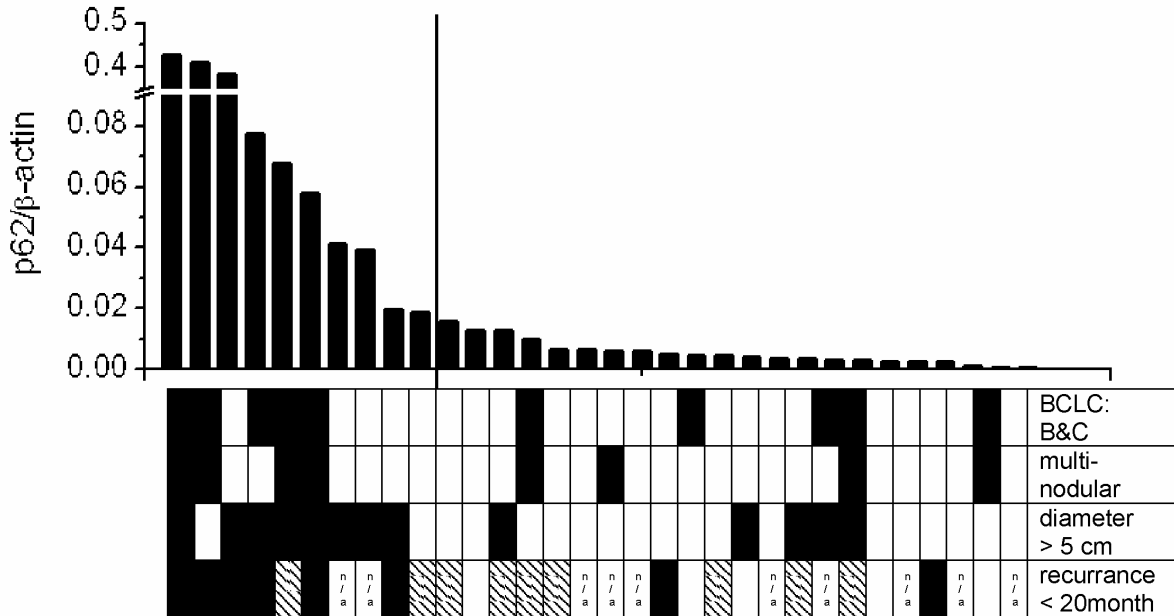


Figure 19: *p62* expression and clinical prognosis - RNA was isolated from paraffin embedded HCC tissues and real-time RT-PCR analysis was performed. Data were normalized to β-actin. Data show *p62* mRNA expression and corresponding clinical data. n/a: not available, black rectangles: applicable, white rectangles: not applicable, striped rectangles: ongoing monitoring less than 20 months.

Table 12 shows *p62* expression of the specific clinical groups.

Table 12: Table shows *p62* expression in HCC tissues and corresponding clinical data. *p62* mRNA expression was determined by real-time RT-PCR analysis from 32 paraffin-embedded HCC tissues. Data show mean ± SEM and median of indicated groups. p-value was calculated by Mann-Whitney U test.

	p62/β-actin			P value
		B/C	0/A	
BLCL				
	mean ± SEM	0.106 ± 0.053	0.030 ± 0.020	
	median	0.034	0.005	0.211
nodularity		multinodular	uninodular	
	mean ± SEM	0.123 ± 0.065	0.030 ± 0.017	
	median	0.034	0.005	0.0984
tumor size (diameter)		> 5 cm	< 5 cm	
	mean ± SEM	0.089 ± 0.043	0.030 ± 0.024	
	median	0.029	0.004	0.0174
recurrence		< 20 months	> 20 months	
	mean ± SEM	0.197 ± 0.075	0.011 ± 0.004	
	median	0.077	0.005	0.0085

3.2.3 Role of IGF2 in anti-apoptotic action of p62

Due to the correlation of high p62 expression with poor prognosis and due to the knowledge of disturbed apoptosis in HCC we aimed to focus in more detail on the mechanisms being responsible for p62's anti-apoptotic action. In order to verify whether the anti-apoptotic action of p62 exists also in the human system, we induced apoptosis in HepG2 cells with doxorubicin after knockdown of p62. Knockdown of p62 in HepG2 cells in fact increased apoptosis upon doxorubicin treatment (figure 20 A). *Vice versa*, overexpression of p62 resulted in a decline of apoptosis in HepG2 cells (figure 20 B). These findings demonstrate antiapoptotic properties of p62 also in human hepatoma cells.

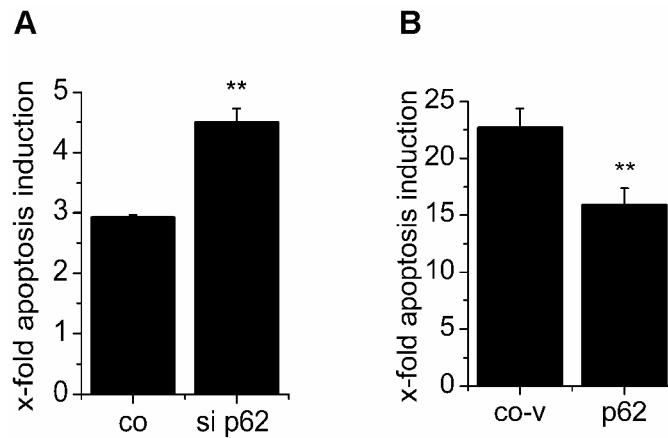


Figure 20: Effect of p62 on apoptosis induction by doxorubicin in hepatoma cells - HepG2 cells were transfected with random siRNA (co) or p62 siRNA (A), or p62 antisense control vector (co-v) or p62 sense vector (B). 48 h after transfection cells were treated with doxorubicin (12.5 µg/ml) for 20 h, lysed, and caspase-3-like activity assay was performed. Data were normalized to untreated control cells. Data show means \pm SEM of 3 independent experiments. ** $p < 0.01$ compared to respective control.

Due to the correlation between *p62* and *IGF2* expression we aimed to clarify whether the antiapoptotic effect of *p62* is *IGF2*-dependent. We first used an siRNA approach to test whether *IGF2* expression is causally linked to *p62*. In fact, *IGF2* expression was downregulated after knockdown of *p62* in HepG2 cells (figure 21).

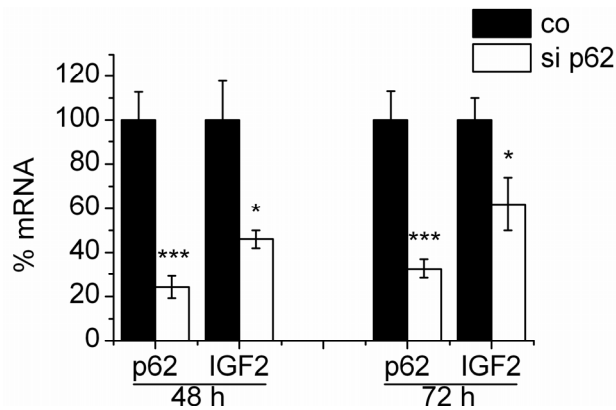


Figure 21: A: Cells were transfected with random siRNA (co) or p62 siRNA (si p62). 48 h and 72 h after transfection cells were lysed, RNA was isolated and real-time RT-PCR was performed. Data were normalized to β -actin. Data show means \pm SEM. * $p < 0.05$, *** $p < 0.001$ compared to transfection reagent control (co). Experiments were performed by Elisabeth Tybl (Saarland University).

To elucidate whether the observed antiapoptotic effect of *p62* in HepG2 cells is due to higher *IGF2* expression and activation of *IGF2*-dependent PI3-K/AKT signalling, we used a neutralizing *IGF2*-antibody as well as inhibitors of the PI3-K/AKT pathway. However, neither the *IGF2*-antibody nor the widely used PI3-K-inhibitors Ly294002 and wortmannin affected the reduced induction of apoptosis caused by overexpression of *p62* (figure 22).

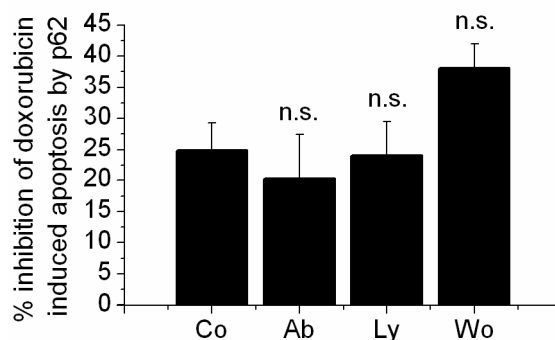


Figure 22: Antiapoptotic effect of p62 is independent of IGF2 signaling – HepG2 cells were treated with doxorubicin (12.5 μ g/ml) for 20 h after pretreatment with either 4.6 ng Igf2 antibody (Ab) for 2 h or PI3K-inhibitors (Ly294002 (Ly) 10 μ M and wortmannin (Wo) 800 nM) for 1 h, 48 h after transfection with either p62 antisense control vector (co-v) or p62 sense vector (p62). Cells were lysed and caspase-3-like activity assay was performed. Data are expressed as percent inhibition of doxorubicin-induced apoptosis in p62 versus co-v transfected cells. Data show means \pm SEM of 3 independent experiments. n.s.: not significantly different from doxorubicin-treated p62-transfected control cells (co).

The lack of effect of PI3-K/AKT signaling suggested no involvement of this pathway in p62-facilitated anti-apoptotic action. Still, p62 transgenic animals showed elevated Akt phosphorylation at the age of 5 weeks (Tybl et al., 2011). We therefore investigated whether p62 influences AKT also in hepatoma cells. However, Western Blot analysis did not show any effect on AKT phosphorylation after knockdown or overexpression of p62 in HepG2 cells. (figure 23).

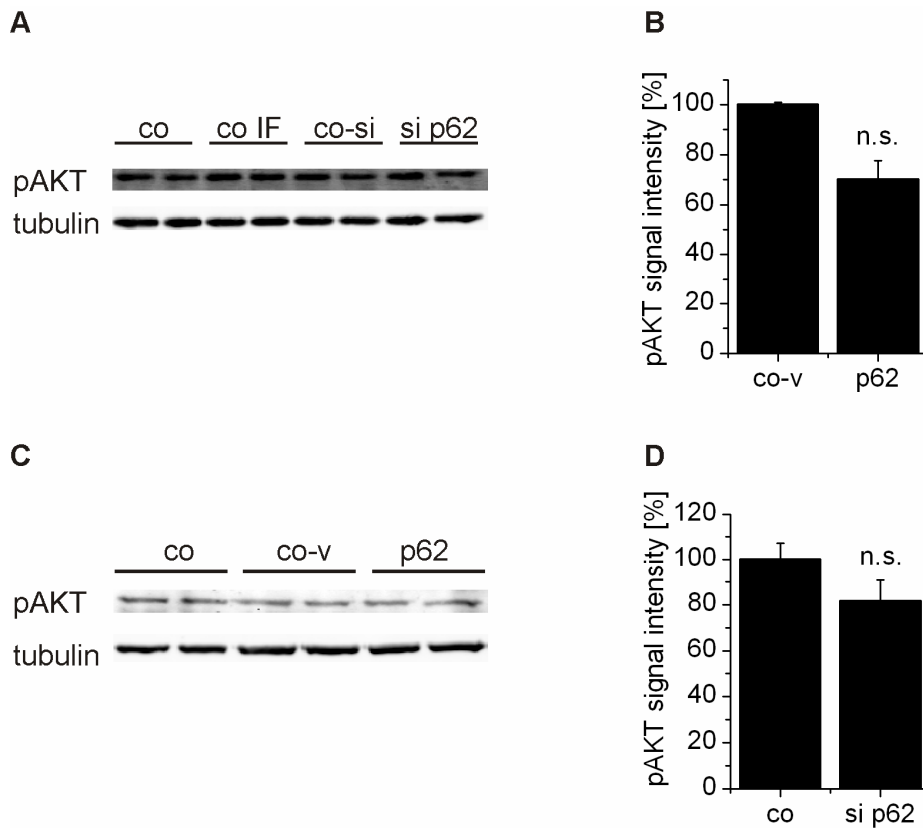


Figure 23: No alterations in AKT phosphorylation by p62 – A, B: HepG2 cells were transfected with either random siRNA (co-si) or p62 siRNA (si p62), treated only with transfection reagent Interferin® (co IF) or left untreated (co). **C, D:** HepG2 cells were transfected with either p62 antisense control vector (co-v) or p62 sense vector or left untreated (co). Cells were harvested and Western Blot analysis was performed using tubulin as a loading control. Data show representative blots out of two (C) or three (A) independent experiments. **B, D:** Relative pAKT protein signal intensities were quantified and normalized to tubulin values. Data are expressed as percentage of co-si or co-v values. n.s.: not significantly different from co (B) or co-v (D).

In addition to the unchanged levels of phosphorylated AKT in hepatoma cells, there was no change regarding Akt activity in DEN-treated transgenic mice compared to control animals (figure 24 A-D) at 2.5 and 5 weeks of age.

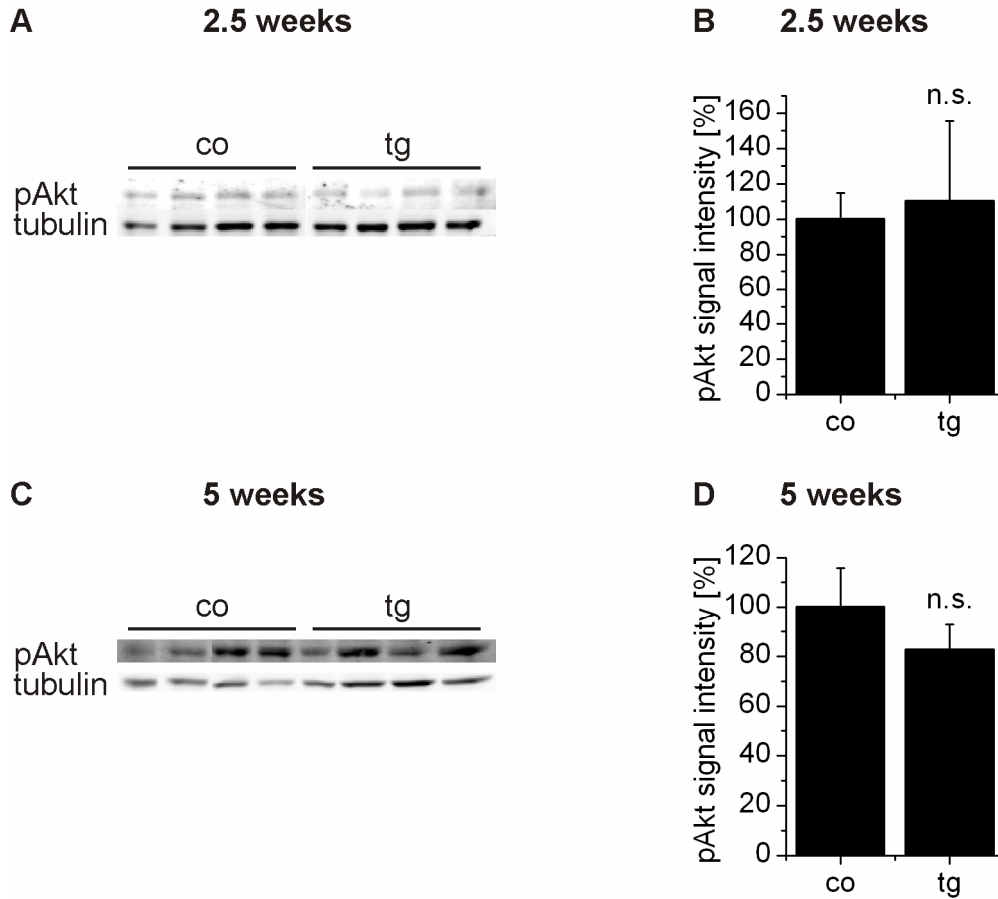


Figure 24: No alterations in AKT phosphorylation by p62 – Western Blot analysis from liver tissue was performed using tubulin as a loading control. Data show representative blots performed with tissue from 28 (2.5 weeks) (A, B) and 17 (5 weeks) (C, D) animals. B, D: Relative pAkt protein signal intensities were quantified and normalized to tubulin values. Data are expressed as percentage of control animal (co) values. n.s.: not significantly different from wild-type mice (co).

3.2.4 The antiapoptotic effect of p62 is facilitated *via* ERK phosphorylation

Since we could exclude PI3K/AKT to mediate p62-facilitated anti-apoptotic action, we hypothesized that ERK as another important survival pathway in hepatocytes might play a role. In fact, Western Blot analysis showed increased levels of phosphorylated ERK1/2 (pERK) in HepG2 cells overexpressing p62 (figure 25 A, B) and decreased levels of pERK in respective knockdown experiments (figure 25 C-F).

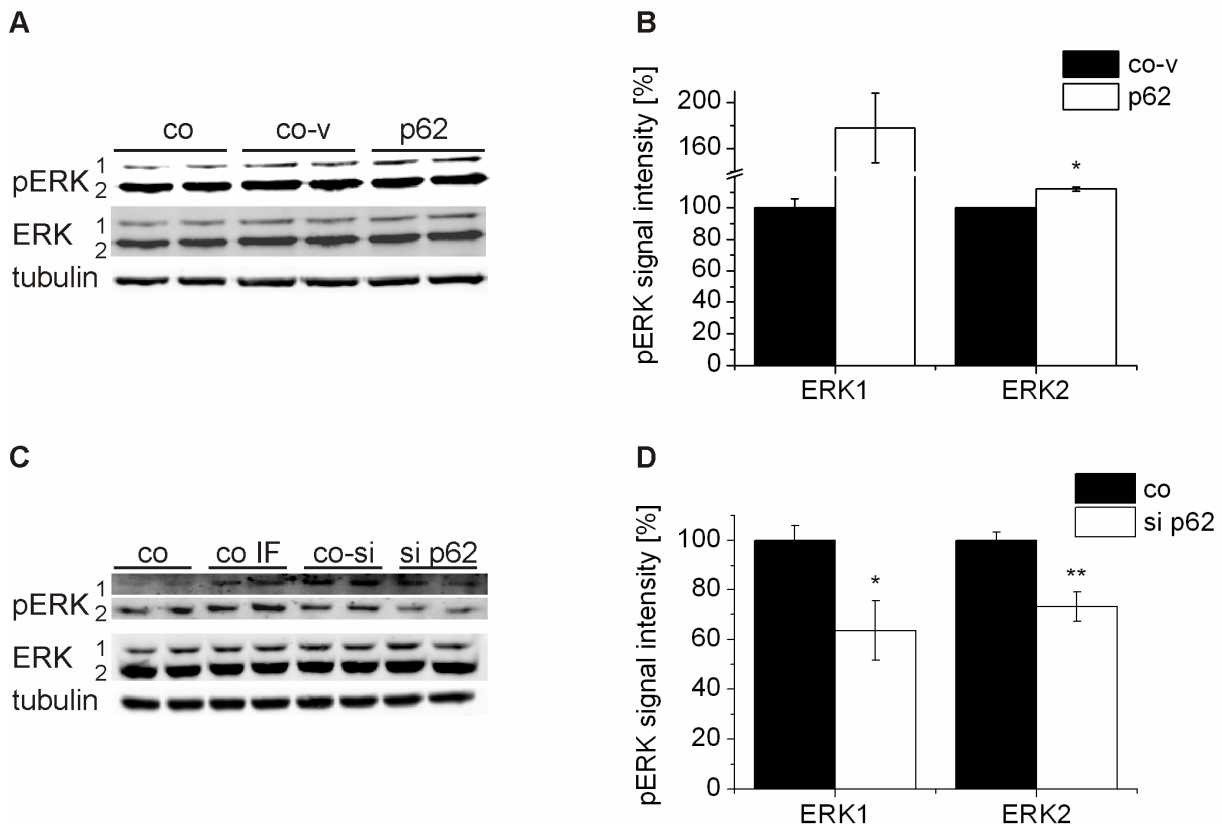


Figure 25: p62 increases ERK1/2 phosphorylation – A, B: HepG2 cells were transfected with either p62 antisense control vector (co-v) or p62 sense vector or left untreated (co). C, D: HepG2 cells were transfected with either random siRNA (co-si) or p62 siRNA (si p62), treated only with tranfection reagent Interferin® (co IF) or left untreated (co). Cells were harvested and Western Blot analysis was performed using tubulin as a loading control. Data show one representative blot out of two (A, B) or six (C, D) independent experiments. B, D: Relative pERK protein signal intensities were quantified and normalized to total ERK values. Data are expressed as percentage of co-v or co-si values. * p < 0.05, ** p < 0.01 compared to respective control.

We then tested the role of ERK activation in the antiapoptotic effect of p62. Therefore, p62 overexpressing cells were treated with the ERK inhibitors PD98059 and U126. The protecting effect of p62 against apoptosis was completely abrogated (figure 26). Again, p62 action was independent of IGF2 since the antibody did not affect apoptosis protection (figure 26).

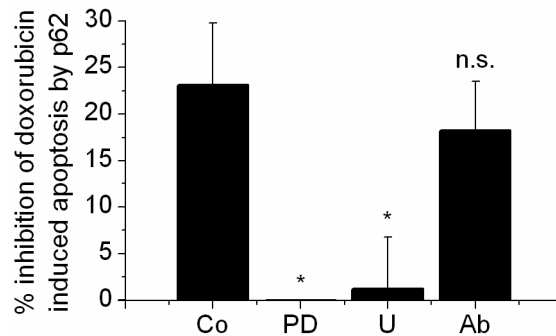


Figure 26: The antiapoptotic effect of p62 is facilitated *via* ERK1/2 phosphorylation – HepG2 cells were treated with doxorubicin (12.5 µg/ml) for 20 h after pretreatment with either 4.6 ng IGF2 antibody (Ab) for 2 h or ERK1/2-inhibitors (PD98059 (PD) 10 µM and U126 (U) 10 µM) for 1 h 48 h after transfection with either p62 antisense control vector (co-v) or p62 sense vector (p62). Afterwards, cells were lysed and caspase-3-like activity was determined. Data are expressed as percent inhibition of doxorubicin-induced apoptosis in p62 versus co-v transfected cells. Data show means ± SEM of 3 independent experiments. * $p < 0.05$, n.s.: not significant compared doxorubicin-treated p62-transfected control cells (co).

Furthermore, ERK2 was slightly but not significantly activated in transgenic mice treated with DEN at the age of 2.5 weeks (figure 27 A, B).

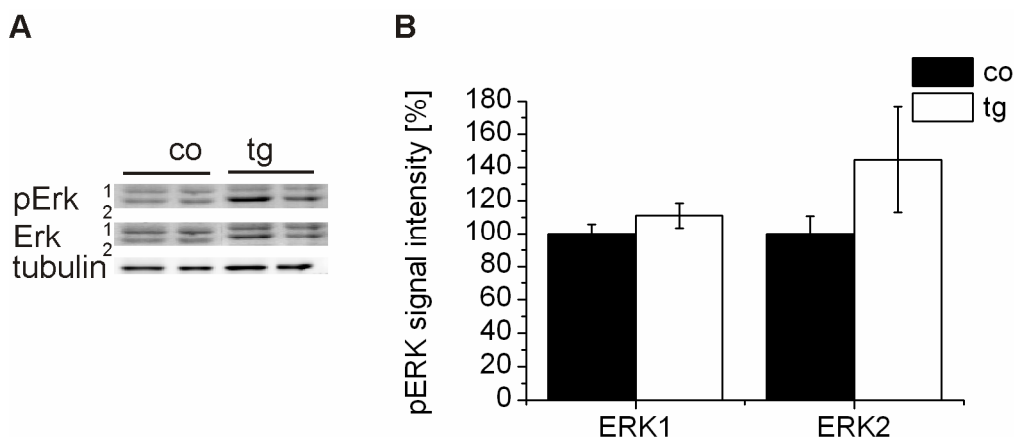


Figure 27: ERK phosphorylation in DEN-treated mice - Western Blot analysis from liver tissue was performed using tubulin as a loading control. Data show one representative blot performed with tissue from 28 animals. B: Relative pErk protein signal intensities were quantified and normalized to total Erk values. Data are expressed as percentage of control animal (co) values.

3.3 Role of *H19* in HCC

3.3.1 *H19* expression in DEN-treated mice

Untreated transgenic mice show high *H19* levels compared to control animals (Tybl et al. 2011). This was also true for transgenic mice treated with DEN (figure 28) at 2.5 and 5 weeks of age. *H19* expression did not differ between both genders in transgenic mice, but rather in the control group, in which females showed higher expression than male mice.

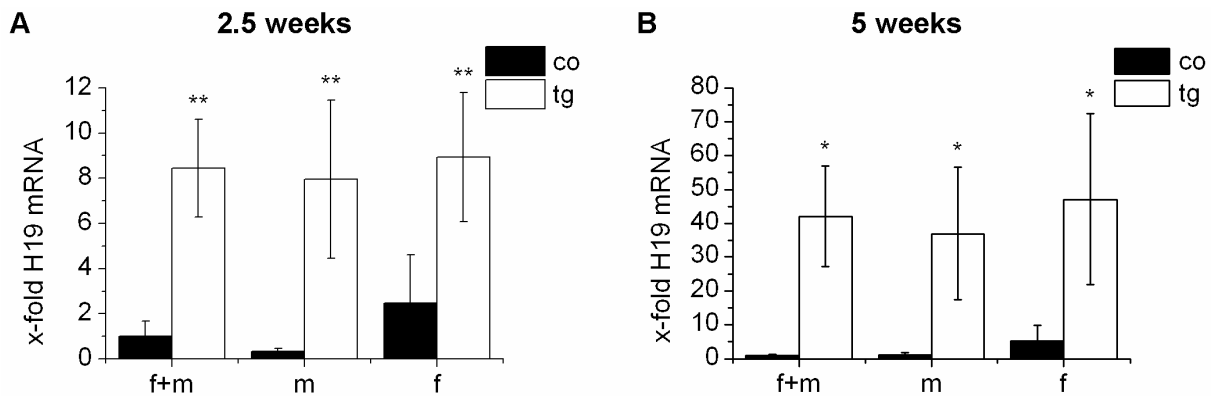


Figure 28: *H19* expression in DEN-treated mice – RNA was isolated from snap-frozen liver tissue and real-time RT-PCR analysis was performed. Data were normalized to 18S. Data show means \pm SEM of 28 (2.5 weeks) and 17 (5 weeks) animals. Mice were treated with DEN at the age of 2.5 weeks (A) or 5 weeks (B). f+m: female and male mice, m: male mice, f: female mice. * $p < 0.05$, ** $p < 0.01$ compared to wild-type (co) mice.

In order to determine if the increase in *H19* expression was due to a switch from normal monoallelic to biallelic expression, five-week-old heterozygous SD7 mice were treated with DEN and genomic imprinting status was investigated by SNUPE analysis. Expression of *H19* remained monoallelicly (table 13).

Table 13: Table shows allele-specific index of *H19* and *IGF2* expression after SNUPE-HPLC detection. Values were obtained by determination of the peak heights of the C- and T-extended primers and calculating the ratio $h(C)/h(C)+h(T)$ (5 weeks: 7 transgenic and 1 control animal).

	control	transgenic
H19	1.0 \pm 0.0	1.0 \pm 0.0

In figure 29 one representative SNUPE chromatogram is shown.

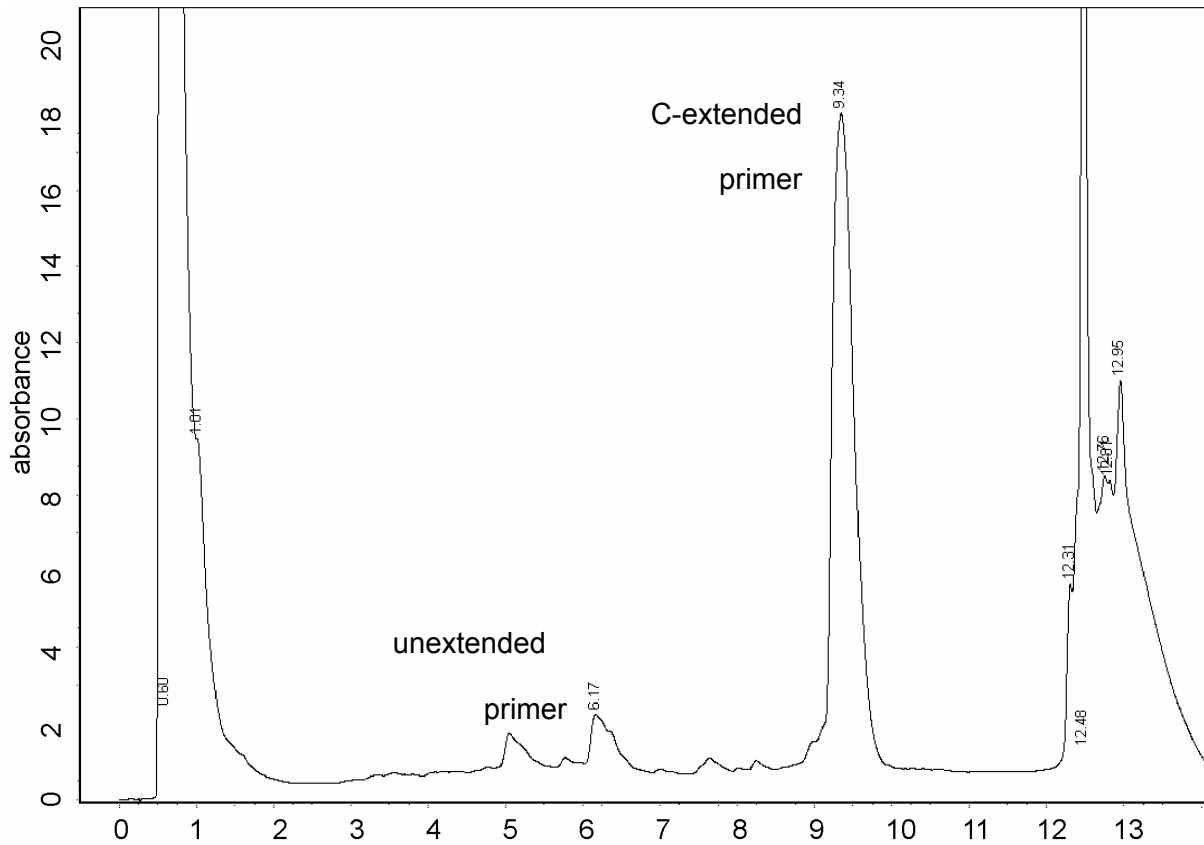


Figure 29: Continuation of genomic imprinting in p62 transgenic mice treated with DEN - RNA was isolated from frozen liver tissue and SNUPE analysis was performed. Mice were treated with DEN at the age of 5 weeks. The figure shows one representative SNUPE chromatogram for H19.

In control mice administration of DEN induced a decline in *H19* RNA expression (figure 30). In DEN-treated transgenic mice *H19* RNA was still highly expressed, but strongly reduced compared to untreated transgenic animals (figure 30).

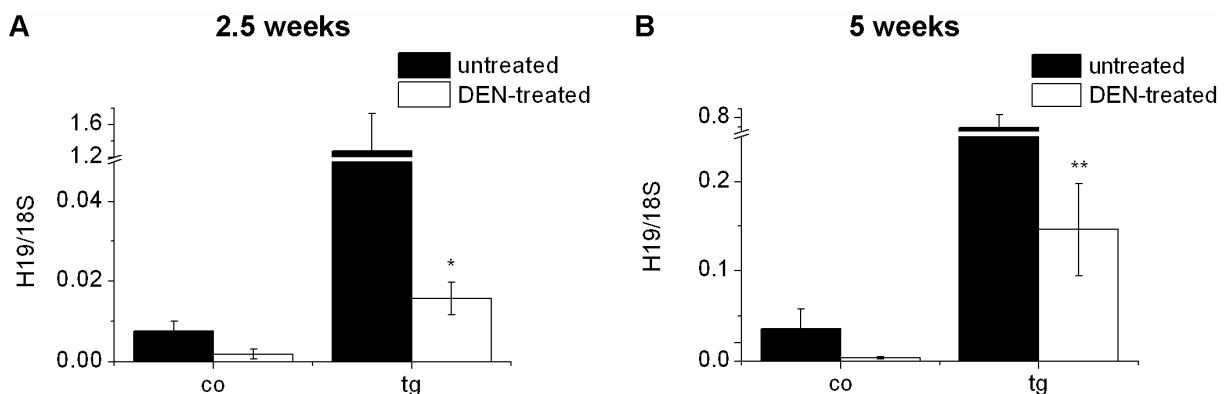


Figure 30: Effect of DEN treatment on H19 expression in mice – RNA was isolated from liver tissue and real-time RT-PCR analysis was performed. Data were normalized to 18S. Data show means \pm SEM of 9 (2.5 weeks, untreated), 12 (2.5 weeks, DEN-treated), 14 (5 weeks, untreated), and 10 (5 weeks, DEN-treated) animals. Mice were treated with DEN at the age of 2.5 weeks (A) or 5 weeks (B). * $p < 0.05$, ** $p < 0.01$ compared to untreated animals of the respective genotype.

3.3.2 H19 expression in human HCC

Investigation of human HCC samples revealed a significant decrease in *H19* RNA expression in tumor tissue compared to surrounding normal tissue (figure 31).

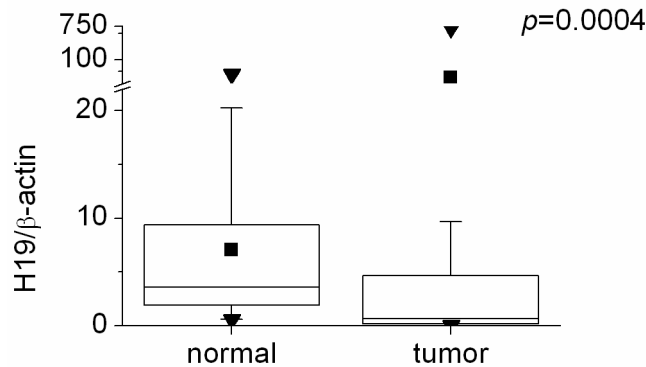


Figure 31: H19 expression in human HCC - RNA was isolated from paraffin embedded HCC tissues and real-time RT-PCR analysis was performed. Data were normalized to β -actin. Data are presented as 25th and 75th percentile boxes with arithmetic medians (square), geometric median (line), and 10th and 90th percentiles as rhombi. Data were generated out of a set of samples from 32 patients. *p*-value was calculated by Mann-Whitney U test.

Due to the fact that epigenetic variations of *H19* and *IGF2* have been reported in several types of cancer, RFLP analysis on HCC tissues was performed (table 14). In figure 32 representative agarose gels of RFLP analysis are shown.

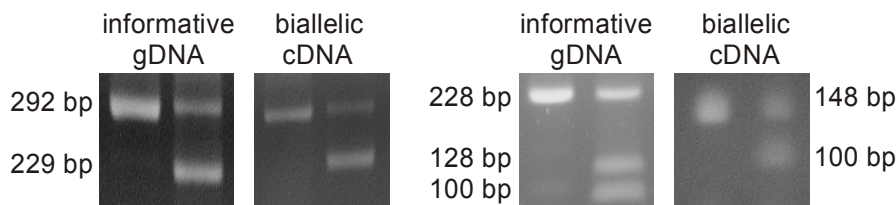


Figure 32: RFLP analysis of human HCC samples – gDNA and RNA were isolated, PCR was performed, gDNA and cDNA was digested with restriction enzymes and agarose gel electrophoresis was performed. Figure shows one representative gel for *IGF2* (left) and *H19* (right).

Table 14: Table shows proportion of samples with biallelic expression determined by RFLP analysis. RFLP analysis was performed on cDNA samples of corresponding informative gDNA samples of 32 HCC tissues and matched normal tissues.

	normal		tumor	
	biallelic	informative	biallelic	informative
IGF2	4/10	10/32	6/10	10/32
H19	3/9	9/32	3/9	9/32

Samples, which had alterations in imprinting status did not show specific changes in

total IGF2 or H19 mRNA expression. Interestingly, however, samples with biallelic expression of IGF2 showed significantly higher H19 expression than monoallelic samples (figure 33).

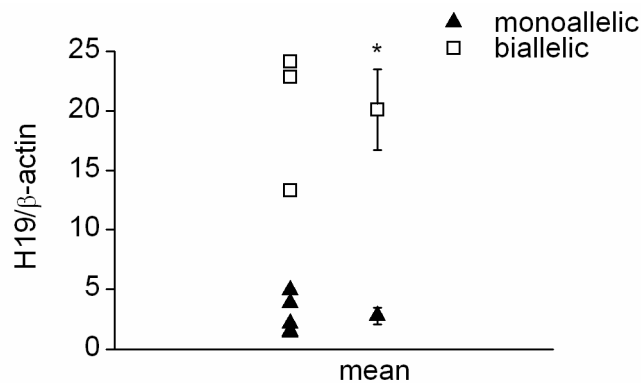


Figure 33: Distribution of H19 expression in samples with mono- or biallelic IGF2 expression. RNA was isolated from paraffin embedded HCC tissues and matched normal tissues and real-time RT-PCR analysis was performed. Data were normalized to β -actin. Data show distribution of values and means \pm SEM of 10 samples, which were informative for RFLP analysis. * $p < 0.05$ compared to tissues expressing IGF2 monoallelicly.

3.3.3 H19 expression in hepatoma cells

Since *H19* expression was decreased both upon DEN-treatment as well as in human HCC samples, we hypothesized a tumor suppressor activity for *H19*. Therefore, we tested the connection between *H19* expression and chemosensitivity in hepatoma cells. Comparison of two hepatoma cell lines, HepG2 and HUH-7, revealed higher basal *H19* RNA levels in HUH-7 cells (figure 34 A). HUH-7 cells were more sensitive to doxorubicin-induced cell death determined by MTT-assay (figure 34 B).

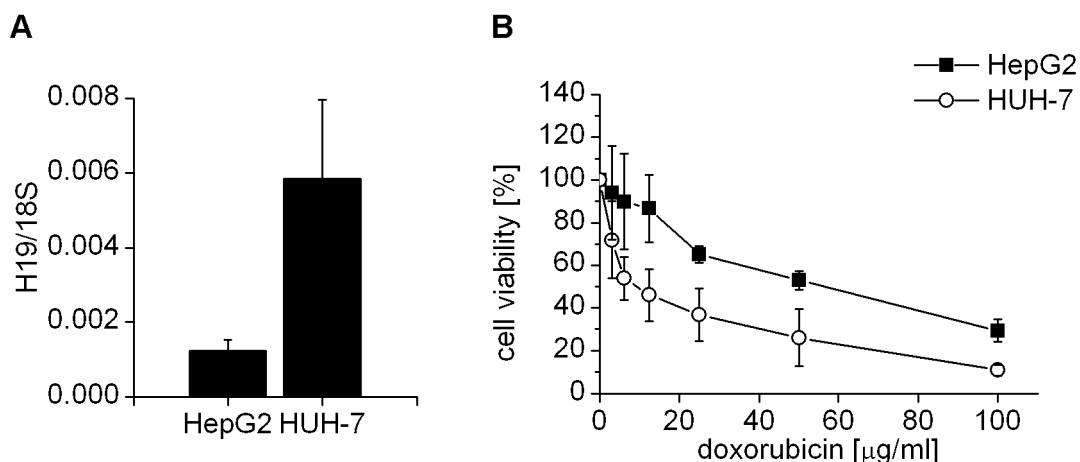


Figure 34: H19 expression and chemosensitivity – A: RNA was isolated and real-time RT-PCR was performed (by Elisabeth Tybl, Saarland University). Data show means \pm SEM of 6 independent experiments. **B:** Cells were treated with indicated concentrations [μ g/ml] of doxorubicin for 24 h and cell viability was determined by MTT-assay. Data show means \pm SEM of 2 independent experiments.

In order to verify the connection between *H19* expression and response to chemotherapeutics, we performed an *H19* siRNA-knockdown in HepG2 cells (figure 35 A). Knockdown of *H19* resulted in reduced caspase-3-like activity in HepG2 cells (figure 35 B).

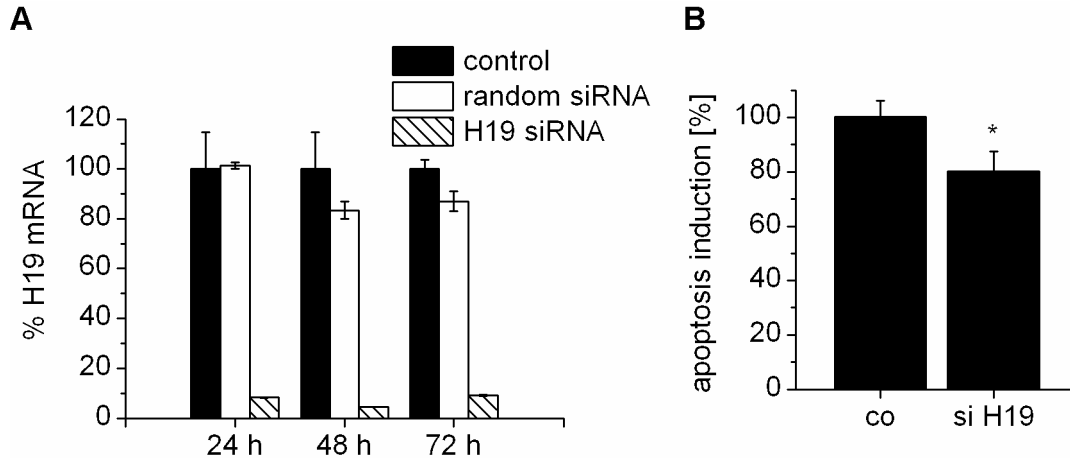


Figure 35: Effect of H19 on apoptosis induction by doxorubicin in hepatoma cells - HepG2 cells were either left untreated (control) or transfected with random siRNA (random si) or H19 siRNA (H19 si). **A:** At the indicated time points, cells were harvested, RNA was isolated and real-time RT-PCR was performed. Data were normalized to β -actin. **B:** 48 h after transfection cells were treated with doxorubicin (12.5 μ g/ml) for 20 h, lysed and caspase-3-like activity assay was performed. Data were normalized to cells transfected with random siRNA. Data show means \pm SEM of 3 independent experiments. * $P < 0.05$ compared to respective control.

Treatment with the demethylating agent 5-azacytidine strongly increased *H19* expression (figure 36 A) suggesting that *H19* expression is suppressed by DNA promoter methylation in this tumor cell line. Interestingly, the expression of the tumor-promoting growth factor *IGF2* was suppressed under the same conditions (figure 36 B).

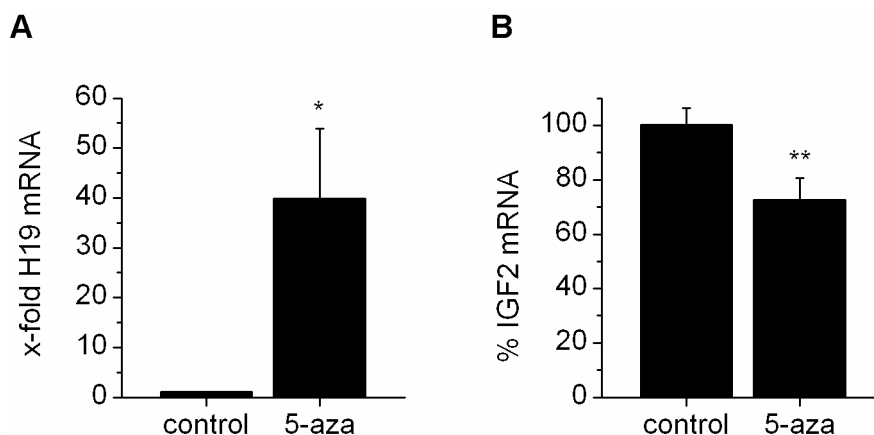


Figure 36: Effect of 5'-azacytidine on H19 and IGF2 expression in hepatoma cells - HepG2 cells were either left untreated (control) or treated with ... μ M 5'-azacytidine for ... (5-aza). RNA was isolated and real-time RT-PCR was performed. RNA isolation and H19 real-time RT-PCR was kindly performed by Rebecca Risch (Saarland University). Data were normalized to β -actin. Data show means \pm SEM of three independent experiments. * $p < 0.05$, ** $p < 0.01$ compared to untreated control.

4 Discussion

4.1 Effects of p62 on metabolism and inflammation

p62 can be regarded as an oncofetal protein because of its exclusive expression in HCC cancer nodules and its appearance in fetal liver (Lu et al., 2001). Functional implications of the protein have as yet been almost unknown. We recently presented a first phenotypic characterization of liver-specific overexpression of human p62 in transgenic mice (Tybl et al., 2011). Although no evidence of spontaneous tumor formation upon *p62* overexpression was detected, a hint on an impact of p62 on liver pathogenesis was given by histological fat staining, which revealed the phenotype of a fatty liver in *p62* transgenic mice. Whereas the fatty liver in *p62* transgenic mice can be regarded as a benign condition, the “second hit” towards the progression of NASH, resulting from inflammation, is missing. Within this project the DEN-model with a short period of treatment, which imitates an early stage of liver damage with inflammation, was exhibited as a second hit in transgenic animals and compared to wild-type mice.

4.1.1 Effects of p62 on fatty acid metabolism

Fatty acids can be regarded as essential components of cellular growth and survival. Therefore, tumor tissues of different origin contain high levels of lipids in comparison to normal tissues due to a distinct increase in lipogenesis (Kuhajda, 2000; Menendez and Lupu, 2007). The enhanced cholesterol and triglyceride plasma levels in *p62* transgenic mice were a first hint on changes in the fat metabolism of these animals. The amount of cholesterol in liver tissues was doubled in untreated transgenic animals compared to wild-type mice and 1.4-fold increased in DEN-treated transgenic mice compared to treated control. In human HCC tissues cholesterol levels were also found to be doubled compared to normal liver tissues (Eggens and Elmberger, 1990). Hypertriglyceridemia was reported to be connected to decreased lipoprotein lipase activity, which was observed in hepatoma bearing rats (Carbo et al., 1994). In esophageal carcinomas hyperlipidemia could be correlated with a higher risk of metastases (Sako et al., 2004). Given that information, we had a closer look on the fatty acid composition of the liver tissue of *p62* transgenic animals.

DEN itself has been reported to change fatty acid metabolism in rats (Canuto et al., 1986). Hyperlipidemia and changes in hepatic fatty acid composition has also been

observed in DEN-treated rats (Ramakrishnan et al., 2008). Therefore, the effect of DEN-treatment in control animals was investigated in detail. In fact, most of the fatty acids were increased due to DEN-treatment, except for docosapentanoic acid, which was decreased.

The liver tissue of untreated *p62* transgenic mice showed increased levels in almost all fatty acids, except of docosahexanoic acid (22:6), indicating a general enhancement of storage and/or synthesis of fatty acids in the transgenics.

Interestingly, the group of DEN-treated *p62* transgenic mice showed a different pattern. Palmitic acid (16:0) was not altered in the DEN-treated transgenic animals, whereas slightly higher levels of palmitoleic acid (16:1) were determined, resulting in an increased palmitoleic acid (16:1) to palmitic acid (16:0) ratio. Such an increased ratio has already been shown for human NAFLD and NASH tissues compared to control livers (Puri et al., 2009). In DEN-treated *p62* transgenic mice, a rise in oleic acid levels could be observed which is in concordance with findings in NASH patients (Puri et al., 2009). In a matrigel assay treatment with oleic acid induced the invasion of breast cancer cells into the gel, which demonstrates a role of oleic acid in tumor invasiveness (Byon et al., 2009). Though incorporated oleic acid was shown to protect against oxygen-induced cytotoxicity *in vitro* (Kinter et al., 1996), which is important regarding the inflammatory properties of fatty acids due to generation of reactive oxygen species, oleic as well as palmitoleic acid is able to decrease expression of the tumor suppressor PTEN (Vinciguerra et al., 2009b). Both the higher palmitoleic acid to palmitic acid ratio as well as the increased amount of oleic acid have been reported to reflect an activation of the stearoyl-CoA desaturase (SCD) system (De Alaniz and Marra, 1994; Ntambi and Miyazaki, 2004). One could therefore hypothesize that SCD activity is enhanced in *p62* transgenic animals. This is supported by decreased levels of stearic acid in DEN-treated transgenic mice, with stearic acid being the source for conversion to oleic acid by SCD. In HCC tissues it was demonstrated that the ratio of stearic acid to unsaturated C18 acids is lower in tumor tissue compared to non-tumorous tissue (Wood et al., 1985).

Eicosapentaenoic acid (20:5) has been described to ameliorate steatohepatitis and HCC in PTEN-deficient mice (Ishii et al., 2009). However, we found increased levels of eicosapentaenoic acid in DEN-treated *p62* transgenic mice. We suggest that this might be some kind of counter-regulation in this complex metabolic system.

Docosapentaenoic acid (22:5) was significantly increased in DEN-treated transgenic animals, which corresponds to higher levels in NAFLD and NASH (Puri et al., 2009). The downstream product of docosapentaenoic acid, docosahexaenoic acid (22:6), was decreased in DEN-treated *p62* transgenics suggesting dysfunction of the metabolizing steps in peroxisomes corresponding to human NAFLD and NASH (Puri et al., 2009). In breast cancer cells treatment with docosahexaenoic acid caused enhanced expression of the peroxisome proliferator-activated receptor γ (PPAR γ) and a subsequent decrease in NF- κ B activity (Horia and Watkins, 2007). Metabolites of docosahexaenoic acid were identified as potent PPAR γ agonists with antidiabetic activity. In contrast, however, untreated *p62* transgenic mice had an improved glucose tolerance (Tybl et al., 2011). In addition, lower glucose levels were measured in the DEN-treated transgenic animals compared to control mice. The reason for this might partly be the conversion of glucose to fatty acids in *de novo* lipogenesis, which is denoted by increased levels of palmitoleic acid (Hellerstein et al., 1996). Interestingly, insulin hypersensitivity was also found in PTEN deficient mice (Stiles et al., 2004), which show a similar fatty acid composition of the liver as our untreated *p62* transgenic mice (Horie et al., 2004).

Taken together, these findings suggest that *p62* might lead to shorter tumor initiation and progression times due to its impact on fat metabolism and the fatty acid pattern of the liver.

4.1.2 *p62* downregulates PTEN

Fatty acids have been shown to inhibit the tumor suppressor PTEN (Vinciguerra et al., 2009b). PTEN was first identified as a tumor suppressor, which is frequently mutated in several cancers including HCC (Chow and Baker, 2006; Dong-Dong et al., 2003; Hu et al., 2003). PTEN downregulation is achieved by different mechanisms, among which are epigenetic alterations, genetic mutations, and reduction of mRNA and protein expression. Several transcription factors act in *PTEN* regulation: p53 and PPAR γ upregulate *PTEN* transcription by binding to its promoter (Stambolic et al., 2001; Zhang et al., 2006), whereas NF- κ B and c-Jun negatively regulate *PTEN* transcription (Hettinger et al., 2007; Vasudevan et al., 2004). We have already shown that PTEN mRNA and protein is downregulated in untreated *p62* transgenic mice (Tybl et al., 2011). This is also true for DEN-treated *p62* transgenic animals.

Interestingly, in five-week-old mice mRNA levels were not decreased in contrast to protein levels, suggesting an involvement of microRNAs in p62-induced inhibition of PTEN (Vinciguerra et al., 2009b)

PTEN was shown to regulate the IGF system *via* insulin-like growth factor binding-proteins (IGFBPs) in gastric cancer cells (Yi et al., 2005). In a hepatoma cell line it was also shown that PTEN expression inversely correlates with IGF2 expression (Kang-Park et al., 2003), proving that PTEN has several implications in the IGF system in both ways, i.e. IGF2-dependent and independent, without direct dephosphorylation of AKT. The higher extent of *PTEN* expression in five weeks old male mice compared to females could therefore explain the lower *Igf2* expression in male mice.

Our findings show that p62 decreases PTEN expression in both early liver damage *in vivo* as well as in hepatoma cells *in vitro*, and therefore affects a crucial tumor suppressor gene in liver disease and cancer.

4.1.3 Interaction of p62 and GILZ

Thirty-four years ago a fatty liver was diagnosed in patients after long-term treatment with glucocorticoids. These livers showed pathohistological features of alcoholic hepatitis (Itoh et al., 1977). In the following years, hepatic steatosis could be linked to Cushing's syndrome (Rockall et al., 2003). Recently, it was demonstrated that glucocorticoids increase both activity and expression of lipogenic enzymes (Cai et al.). Glucocorticoids can therefore be regarded as important inducers of NAFLD. Several of the beneficial, i.e. anti-inflammatory actions of glucocorticoids have been linked to critically depend on GILZ (Ayroldi and Riccardi, 2009). In this context it is interesting to note that GILZ expression was suggested to be responsible for beneficial effects of glucocorticoid treatment in patients with alcoholic hepatitis (Hamdi et al., 2007). In NASH patients GILZ levels were reported to negatively correlate with the amount of liver lesions (Boujedidi, 2010).

We investigated the connection between p62 and *GILZ* expression. In five weeks old *p62* transgenic mice we found increased *Gilz* expression. This increase in *Gilz* mRNA expression can be regulated by both transcriptional and post-transcriptional mechanisms. Post-transcriptional modulation is commonly procured by changes in

mRNA stability, which allows cells to dynamically adapt gene expression to environmental challenges (Wilusz and Wilusz, 2004). Thus, we used primary hepatocytes isolated from transgenic and control animals to investigate changes in mRNA stability. In fact, *Gilz* mRNA stability was increased in hepatocytes of transgenic origin compared to control hepatocytes. Interestingly, the IMP family members IMP1 and IMP3 were previously described to prolong the half-life of *CD44* mRNA (Vikesaa et al., 2006) and the RNA-binding protein AUF1 was found to directly interact with IMP2 (Moraes et al., 2003). This information suggests an important role for IMPs in post-transcriptional control of gene expression.

Little is known about the functional implications of GILZ in tumorigenesis and cancer. In ovarian cancer tissues GILZ was shown to promote tumor cell proliferation due to increased AKT activation (Redjimi et al., 2009). Contrarily, GILZ expression is essential for induction of apoptosis in multiple myeloma by glucocorticoids and inhibition of the PI3K/AKT pathway results in upregulated GILZ expression (Grugan et al., 2008). Thus, the role of GILZ seems to be specific for the type of cancer. Interestingly, GILZ has been reported to inhibit Raf-1 phosphorylation, which results in the suppression of ERK phosphorylation (Ayroldi et al., 2002) suggesting an antagonizing role of GILZ for p62. However, in HCC functional implications of GILZ in tumorigenesis and the interaction of p62 and GILZ need to be further investigated.

Similar to glucocorticoid treatment, GILZ is able to inhibit the production of inflammatory mediators (Berrebi et al., 2003). GILZ inhibits the translocation of NF- κ B to the nucleus due to a direct interaction with the NF- κ B subunits (Ayroldi et al., 2001). Increased *Gilz* expression in five-week-old *p62* transgenic mice could contribute to higher levels of I κ B α compared to 2.5-week-old mice *via* inhibition of NF- κ B. Therefore, we next investigated the inflammatory actions in *p62* transgenic animals.

4.1.4 p62 induces inflammatory cytokines

In a mouse model it has been shown that obesity-promoted HCC development is dependent on enhanced production of the tumor-promoting cytokines IL-6 and TNF- α , which cause hepatic inflammation (Park et al., 2010). Also in DEN-treated mice IL6 has been shown to be strongly upregulated and to be causally involved in

tumorigenesis (Naugler et al., 2007). We therefore investigated the inflammatory response in DEN-treated *p62* transgenic mice. In fact, we found increased IL6 levels in DEN-treated *p62* transgenic mice compared to control. Interestingly, IL6 signaling has antiapoptotic effects in myeloma cells (Catlett-Falcone et al., 1999) and high IL6 levels have been demonstrated to cause resistance against apoptosis in chronic inflammatory diseases (Atreya, 2000; Yamamoto et al., 2000). Also the risk of Hodgkin lymphoma is associated with IL6 levels (Cozen et al., 2004). In a cell culture model treatment with a neutralizing IL6 antibody retarded tumorigenesis (Ancrile et al., 2007). These findings underline that the increased IL6 levels in response to liver damage due to DEN-treatment potentiate the risk of HCC development. Regarding HCC as a result of a long-term liver inflammation, *p62* could accelerate tumor initiation due to an increased inflammatory response to liver-damaging stimuli. Increased IL6 expression can also contribute to the observed reduction in PTEN expression by activating the transcription factor STAT3, which leads to inhibition of PTEN *via* induction of microRNA miR-21 (Iliopoulos et al.). Since ERKs are downstream targets of IL6 (Pricola et al., 2009), IL6 might even amplify the *p62*-induced ERK activation in DEN-treated transgenic animals compared to control mice.

The role of TNF- α in cancer is controversial. TNF- α has been shown to have tumor-promoting effects (Mocellin et al., 2005), but also anti-tumor actions have been described (Van Etten et al., 2003; van Horssen et al., 2006). Our data showed increased TNF- α levels in DEN-treated *p62* transgenic mice. For HCC, a rodent model revealed obesity to promote tumorigenesis by enhancing both IL6 and TNF- α expression (Park et al., 2010). Both cytokines can activate the transcription factor NF- κ B, which has been described to play a role in cancer development and progression (Dolcet et al., 2005; He and Karin). We have recently demonstrated increased cytoplasmatic expression of NF- κ B in *p62* transgenic mice (Tybl et al., 2011). Here, we show decreased levels of I κ B α in *p62* transgenic animals treated with DEN, modeling a pretumorous state of liver disease. I κ B α -degradation is responsible for NF- κ B-activation (Kierner et al., 2002; Vinciguerra et al., 2008) and the IKK-complex, which triggers phosphorylation of I κ B α , has been demonstrated to be necessary for the malignant transformation to HCC in the liver (Jiang et al., 2009). Therefore, *p62* affects tumor initiation and progression *via* changes in the inflammatory response, especially through activation of NF- κ B.

4.2 Antiapoptotic effect of p62

4.2.1 p62 expression in human HCC

In a knockout mouse model the IMP family member IMP1 was demonstrated to be essential for normal growth and development (Hansen et al., 2004). For *p62*, we observed an 11-fold increased expression in tumor tissues compared to matched normal tissues. In fact, enhanced *p62* mRNA expression was found in 53% of HCC tissues (17/32). In the literature, aberrant expression of the protein p62 was described for 30% (Lu et al., 2001; Zhang and Chan, 2002), but also for 61.5% of HCCs (Su et al., 2005). Autoantibodies against p62 were detected in 21% of HCC patients (Zhang et al., 1999) and in several other types of cancer (Zhang et al., 2001). The high amount of *p62*-positive tumor tissues in our study could be explained by the sensitivity of the method, which was used. Real-time RT-PCR is much more sensitive than protein quantification methods like Western Blot, ELISA or immunohistochemistry. In addition, variation in the proportion of p62-positive cases could be due to a different set of samples. HCC can be the result of a variety of underlying diseases, such as viral hepatitis, alcoholic or non-alcoholic steatohepatitis. We used samples with mixed etiology, whereas other reports on p62 in HCC did not give any information on disease etiology. Molecular mechanisms regarding these precursor conditions and the respective tumor progression can be completely different.

IMP3 was suggested as a prognostic marker for tumor malignancy and prognosis (Hutchinson, 2010). Also for p62 we observed a correlation between *p62* expression and poor prognosis. High *p62* expression was observed in tissues from tumors, which were categorized as intermediate (B) or advanced (C) by using the BLCL staging system. These categories include multinodularity and increased tumor size (Forner et al.). Also early recurrence of tumors with high p62 expression underlined the more severe status of disease. Interestingly, *p62* expression was increased specifically in non-cirrhotic HCCs. Okuda et al. observed lower differentiation in tumors of non-cirrhotic livers (Okuda et al., 1982). In HCCs from non-cirrhotic livers the existence of dysplastic lesions has been reported (Grando-Lemaire et al., 1999), which are now established as precancerous pathological changes (Kojiro and Roskams, 2005). One study reported a prevalence of 26.8% of dysplasia in HCCs in non-cirrhotic livers (Okuda et al., 1989). Absence of cirrhosis was also related to increased tumor size and faster tumor growth (Trevisani et al., 1995; Van Roey et al.,

2000). These findings combined with the observation, that elevated levels of α -fetoprotein, the common marker for HCC, are more frequent in cirrhotic tumors (Trevisani et al., 1995; Van Roey et al., 2000), display p62 as a useful marker for HCC, especially for HCC developing in the non-cirrhotic liver.

The balance between survival and apoptosis is often disrupted due to antiapoptotic signals occurring in cancer (Fabregat et al., 2007). During hepatocarcinogenesis apoptosis is diminished compared to proliferation resulting in an early expansion of neoplastic hepatocytes (Park et al., 2001). Interestingly, both knockdown and overexpression of p62 in hepatoma cells verified an antiapoptotic effect of p62. DEN-treatment of *p62* transgenic and control mice indicated this antiapoptotic action of p62 also *in vivo*. As mentioned before, investigation of human HCC tissues revealed higher *p62* expression in non-cirrhotic *versus* non-cirrhotic tissues. Cirrhosis development critically depends on the activation of hepatic stellate cells (Canbay et al., 2004). The activation of hepatic stellate cells, connected to inflammation, increases hepatocyte apoptosis (Canbay et al., 2004). Persistent activation of hepatic stellate cells results in exacerbation of hepatocyte apoptosis, hepatic inflammation, and progression to liver cirrhosis (Guicciardi and Gores, 2005). In regenerative cirrhotic nodules, 14% showed higher rates of apoptosis than proliferation (Park et al., 2010). In contrast, hepatocarcinogenesis and promotion of HCC is characterized by defective apoptosis and increased cell proliferation (Guicciardi and Gores, 2005). Taken together, the antiapoptotic effects p62 seem to have implications in tumor initiation and promotion, especially in the non-cirrhotic liver.

4.2.2 Mechanism of the anti-apoptotic action of p62

We recently reported that liver-specific transgenic *p62* expression in mice leads to enhanced *Igf2* expression in liver tissue (Tybl et al., 2011). *IGF2* is a well known antiapoptotic factor, overexpressed in HCC (Cariani et al., 1988b; Liu et al., 1997; Scharf and Braulke, 2003; Schirmacher et al., 1992; Tovar et al., 2010), and demonstrated to be an inducer of angiogenesis and vasculogenesis (Kim et al., 1998; Maeng et al., 2009). Overexpression of imprinted genes can be induced by two different mechanisms: higher transcription levels of the active allele or reactivation of the silenced allele resulting in biallelic expression of the gene. In murine hepatocellular carcinoma cell lines LOI of *Igf2* has been reported (Ooasa et al.,

1998). Regarding the influence of DEN on *Igf2* expression, we determined the allelic expression of *Igf2* in the transgenic mice. As reported before for untreated animals (Tybl et al., 2011), no switch to biallelic expression in the transgenics was observed upon DEN-treatment. In fact, it has been reported that IGF2 expression is unrelated to its imprinting status in colorectal cancer (Cheng et al.).

The increased expression of the transcriptional regulator *Aire* determined in untreated animals is most likely responsible for the high expression of *Igf2* in *p62* transgenic animals (Tybl et al., 2011). *Igf2* was described to be highly regulated by *Aire* expression (Johnnidis et al., 2005). Although *Aire* has been described to be found in hepatocytes to a high extent (Halonen et al., 2001), functional implications of *Aire* expression in the liver are as yet completely unknown. *Aire* is known to act gender-specifically (Hässler et al., 2006), which explains the higher expression of *Igf2* in female transgenic mice, although *p62* levels were similar in males and females.

HCC is characterized by alterations in several important cellular signaling pathways including the PI3-K- and the ERK-pathway (Whittaker et al.). Constitutive activation of the PI3-K/AKT signalling pathway has been firmly established as a major determinant of tumor cell growth and survival in several tumors (Chen et al., 2005). In HepG2 cells IGF1 has been demonstrated to have the ability to reverse apoptotic signaling by activation of the PI3-K/AKT signalling (Alexia et al., 2006). IGF1 binds to the IGF1 receptor whose autophosphorylation is followed by phosphorylation of intracellular targets and finally leads to activation of the PI3-K and the ERK pathway (Pollak et al., 2004).

We demonstrate that *p62* expression in HCC correlates with IGF2 expression in tumor tissue. IGF2 was also demonstrated to act *via* the PI3-K/AKT pathway (Liang et al.). Unexpectedly, the altered *Igf2* expression in DEN-treated *p62* transgenic mice did not result in an increased activation of Akt. In untreated transgenic animals, we reported increased Akt phosphorylation in five-week-old animals. Younger or older animals, however, did not show altered phosphor-Akt levels (Tybl et al., 2011). Unchanged phosphorylation levels after both *p62* knockdown and overexpression in HepG2 cells were in concordance with this observation. Due to highly increased levels of *Igf2* mRNA in *p62* transgenic animals, one would expect an IGF2-dependent action of *p62*. However, our data clearly indicate that the antiapoptotic effect is IGF2/PI3-K/AKT-independent and rather facilitated *via* ERK phosphorylation.

Silencing ERK1/2 expression using RNA interference led to suppression of ovarian tumor cell proliferation (Steinmetz et al., 2004). One report displayed aberrant ERK phosphorylation in 69% of HCCs (Huynh et al., 2003). In a rodent model tumor growth and apoptosis resistance of intraperitoneally applied hepatoma cells was enhanced by overexpression of MEK1 (Huynh et al., 2003). Schmitz et al. showed increased ERK1/2 phosphorylation, especially in HCCs with poor prognosis (Schmitz et al., 2008). Also Caja et al. reported that overactivation of the MAPK pathway in liver tumor cells might play a role in initiation and development of HCC through resistance to apoptosis (Caja et al., 2009).

ERK phosphorylation is not only altered in malignant tissue, but also in patients with severe chronic hepatitis B (Han et al., 2008), suggesting a transition step to HCC. In fact, in the context of both HBV- and HCV-infection, activation of the ERK pathway was demonstrated to enhance cell cycle progression, cell proliferation, and survival (Ewings et al., 2007; Zhao et al., 2005). We demonstrate for the first time that ERK phosphorylation in a hepatoma cell line, which leads to resistance against apoptosis, is due to expression of the IMP p62. In line with these findings, ERK also seems to be involved in modulating drug resistance of HCC cells (Yan et al., 2009). Clinical relevance is underlined by the suggestion of a combined doxorubicin and ERK targeted therapy for enhanced anti-cancer effects in HCC (Choi et al., 2008).

Only in 2.5 week old DEN-treated *p26* transgenic mice we could observe a slight but not significant increase solely in ERK2 phosphorylation. Interestingly, only ERK2 has been reported to be a pivotal mediator of hepatocyte cell cycle progression both *in vitro* and *in vivo*: whereas Erk1 knockout and knockdown had no effect on rodent hepatocyte proliferation, specific Erk2 knockdown abolished cell cycle progression (Frémin et al., 2007). Regarding liver cancer, two recent studies revealed knockdown of ERK2 but not ERK1 abolishes liver tumor cell proliferation *in vitro* as well as growth of xenografted tumors in rodents (Bessard et al., 2008; Gailhouste et al., 2010). Also in fibroblasts, ERK2 seems to have a positive role in controlling cell proliferation, whereas ERK1 could probably affect the overall signaling by antagonizing ERK2 activity (Vantaggiato et al., 2006). Another study proved the competition between ERK1 and ERK2 for their binding and activation by MEKs with an ERK1 knockout which was accompanied by an increase in ERK2 signaling (Mazzucchelli et al., 2002). Conversely, silencing ERK1 expression alone is sufficient

to significantly decrease tumor cell viability (Zeng et al., 2005). Given this information, Erk2 activation might be more important in DEN-induced carcinogenesis.

Taken together, ERK activation due to p62 expression seems to display a prominent step in liver pathogenesis considering the multiple targets of ERK.

4.3 Role of *H19* in HCC

In our previous study we reported that transgenic p62 expression in mice leads to overexpression of *H19* (Tybl et al., 2011). Also in DEN-treated mice *H19* is still highly expressed. Interestingly, however, in the livers of DEN-treated p62 transgenic mice *H19* was overexpressed to a lower extent, when compared to our data from untreated transgenic mice (Tybl et al., 2011). The role of *H19* in tumorigenesis is controversially discussed. *H19* was described as both an oncogene (Matouk et al., 2007) and a tumor suppressor gene (Hao et al., 1993; Yoshimizu et al., 2008). In human HCC samples we found decreased expression of *H19* in tumor tissue compared to surrounding normal tissue. Cui et al. showed that inactivation of *H19* resulted in blastema overgrowth in Wilms' tumorigenesis (Cui et al., 1997). Investigation of different hepatoma cell lines also indicated a tumor suppressor activity for *H19*. We observed different basal levels of *H19* in two hepatoma cell lines, HepG2 and HUH-7. HUH-7 cells, which had higher expression levels of *H19*, were more sensitive to doxorubicin. This is in concordance with the literature (Lee et al., 2002).

Our findings corroborate the tumor suppressor activity of *H19*. We speculate that the expression of *H19* could be responsible for the lack of tumor development in untreated p62 transgenic animals. In order to test this hypothesis, p62 transgenic mice will be crossed with *H19* deficient animals in the future. The mechanisms involved in the biological activities of *H19* remain elusive. *H19* was already shown to bind IMP1 (Nielsen et al., 2004; Runge et al., 2000) and might also interact with other IMPs, such as p62. Another mechanism of the action of *H19* may be *via* induction of miRNAs (Cai and Cullen, 2007).

The imprinted genes *IGF2* and *H19* often show coordinate, reciprocal regulation (Reik et al., 2001; Vernucci et al., 2004). In the human liver imprinting analysis is more complex due to biallelic expression of *IGF2* in the adult liver (Davies, 1994; Ekstrom et al., 1995), but monoallelic expression of *H19*. Interestingly, in the HCC samples which displayed biallelic *IGF2* expression, *H19* was significantly overexpressed compared to samples with abnormal monoallelic expression. In the fetal liver *IGF2* is transcribed from P2, P3, and P4 promoters from the paternal allele. In the adult liver transcription is switched to P1 promoter resulting in biallelic expression of *IGF2* (Kalscheuer et al., 1993; Vu and Hoffman, 1994). Therefore, our

findings further support the hypothesis about *H19* being a tumor suppressor, which is downregulated in samples showing epigenetic changes of the *IGF2* gene by monoallelic expression. Classification of the observed biallelic expression as normal adult expression would need a promoter analysis to distinguish between a fetal and an adult promoter methylation pattern (Li et al., 1997; Wu et al., 2008). Transcripts from the fetal promoters have been reported to be highly expressed in HCC (Cariani et al., 1988b; Nardone et al., 1996).

The fact that also surrounding non-tumorous tissue showed an aberrant imprinting status of *IGF2* and *H19* indicate that epigenetic changes could predict cancer risk or disease progression (Couvert et al., 2008; Kaneda et al., 2007). It is noteworthy that both DNMT1 and DNMT3a are upregulated in human HCCs (Lin et al., 2001; Saito et al., 2001) and methylation abnormalities in the DMR of the *IGF2* locus were detected in HCC (Poirier et al., 2003). Thus, changes in DNA methylation might have a great influence on the dysregulated expression of *IGF2* and *H19* (Thorgeirsson and Grisham, 2002). We therefore performed expression analysis of *IGF2* and *H19* in HepG2 cells after treatment with the demethylating substance azacytidine, which was shown to affect human *IGF2* promoter P3 and P4 in colorectal cancer (Hu et al., 1996). Whereas *H19* was strongly upregulated, *IGF2* mRNA was downregulated. This further supports a regulation of *Igf2* by *H19*, which was also observed in both *H19* transgenic and knockout mice (Gabory et al., 2009).

5 Summary

Summary

Primary liver cancers including hepatocellular carcinoma (HCC) have dramatically increased in the last years. Although HCC is prevalent in Asian and African countries, incidence of HCC and mortality is also rising in most industrialized countries. Patients suffering from diseases of the metabolic syndrome complex show an increasing incidence of HCC.

The IMP p62 was found as an autoantigen in an HCC patient. Functional implications of p62, however, have as yet been almost completely unknown.

Samples from HCC patients showed increased *p62* expression, especially in non-cirrhotic tissue. *p62* expression correlated with *IGF2* expression, suggesting IGF2-dependent actions for p62. The antiapoptotic effect of p62 in both human hepatoma cells as well as *p62* transgenic mice, which express p62 liver-specifically, however, turned out to be IGF2-independent. Investigations on the underlying mechanism revealed that antiapoptotic signalling is due to ERK activation.

Although *p62* transgenic mice develop a fatty liver, no tumors are formed during life time. Therefore, we wanted to employ a second hit to promote liver damage in these animals. Intraperitoneal application of the carcinogen DEN, which is a common HCC model, was used. In *p62* transgenic mice a downregulation of the tumor suppressor PTEN was observed, which can make the liver more susceptible to tumorigenesis. Additionally, increased levels of inflammatory cytokines were measured in livers of transgenic mice. An enhanced inflammatory response can indicate a more severe liver damage. Interestingly, the fatty acid composition of the DEN treated *p62* transgenic mice compared to control animals was changed in a comparable pattern to NASH patients compared to NAFLD patients.

Although these observations would indicate a spontaneous tumor development in *p62* transgenic mice, tumor formation does not occur in untreated transgenic animals. The reason for the inhibition of tumor initiation could be the high levels of *H19* RNA in *p62* transgenic mice. In human HCC samples *H19* was downregulated in tumor tissue compared to normal tissue. In hepatoma cells knockdown of *H19* led to increased resistance against doxorubicin, suggesting a tumor suppressor role of *H19* in HCC.

Taken together, this characterization of IMP p62 provides new insight into possible functional targets of p62 and its influence on liver disease. Regarding clinical aspects, a further characterization of the role of p62 in liver pathogenesis as well as in tumor initiation and progression can lead to new diagnostic and treatment options.

This work was supported by the Deutsche Krebshilfe (grant #107751).

6 References

- Alexia, C., Fourmatgeat, P., Delautier, D. and Groyer, A. (2006) Insulin-like growth factor-I stimulates H4II rat hepatoma cell proliferation: Dominant role of PI-3'K/Akt signaling. *Experimental Cell Research*, **312**, 1142.
- Ancrile, B., Lim, K.H. and Counter, C.M. (2007) Oncogenic Ras-induced secretion of IL6 is required for tumorigenesis. *Genes and Development*, **21**, 1714.
- Arkan, M.C., Hevener, A.L., Greten, F.R., Maeda, S., Li, Z.W., Long, J.M., Wynshaw-Boris, A., Poli, G., Olefsky, J. and Karin, M. (2005) IKK- β links inflammation to obesity-induced insulin resistance. *Nature Medicine*, **11**, 191.
- Atreya, R. (2000) IL-6 trans-signaling mediates T cell resistance against apoptosis in Crohn's disease. *Biomedicine and Pharmacotherapy*, **54**, 417.
- Avila, M.A., Berasain, C., Sangro, B. and Prieto, J. (2006) New therapies for hepatocellular carcinoma. *Oncogene*, **25**, 3866.
- Ayroldi, E., Migliorati, G., Bruscoli, S., Marchetti, C., Zollo, O., Cannarile, L., D'Adamio, F. and Riccardi, C. (2001) Modulation of T-cell activation by the glucocorticoid-induced leucine zipper factor via inhibition of nuclear factor κ B. *Blood*, **98**, 743.
- Ayroldi, E. and Riccardi, C. (2009) Glucocorticoid-induced leucine zipper (GILZ): A new important mediator of glucocorticoid action. *FASEB Journal*, **23**, 3649.
- Ayroldi, E., Zollo, O., Macchiarulo, A., Di Marco, B., Marchetti, C. and Riccardi, C. (2002) Glucocorticoid-induced leucine zipper inhibits the Raf-extracellular signal-regulated kinase pathway by binding to Raf-1. *Molecular and Cellular Biology*, **22**, 7929.
- Bell, A.C. and Felsenfeld, G. (2000) Methylation of a CTCF-dependent boundary controls imprinted expression of the Igf2 gene. *Nature*, **405**, 482.
- Berrebi, D., Bruscoli, S., Cohen, N., Foussat, A., Migliorati, G., Bouchet-Delbos, L., Maillot, M.C., Portier, A., Couderc, J., Galanaud, P., Peuchmaur, M., Riccardi, C. and Emilie, D. (2003) Synthesis of glucocorticoid-induced leucine zipper (GILZ) by macrophages: An anti-inflammatory and immunosuppressive mechanism shared by glucocorticoids and IL-10. *Blood*, **101**, 729.
- Bessard, A., Framin, C., Ezan, F., Fautrel, A., Gailhouste, L. and Baffet, G. (2008) RNAi-mediated ERK2 knockdown inhibits growth of tumor cells in vitro and in vivo. *Oncogene*, **27**, 5315.
- Biddinger, S.B., Almind, K., Miyazaki, M., Kokkotou, E., Ntambi, J.M. and Kahn, C.R. (2005) Effects of diet and genetic background on sterol regulatory element-binding protein-1c, stearoyl-CoA desaturase 1, and the development of the metabolic syndrome. *Diabetes*, **54**, 1314.
- Bosch, F.X., Ribes, J., Díaz, M. and Cléries, R. (2004) Primary liver cancer: Worldwide incidence and trends. *Gastroenterology*, **127**, S5.
- Boujedidi, H., Bigorgne, A., Cassard-Doulcier, A.-M., Bouchet-Delbos, L., Naveau, S., Hamdi, H., Durand-Gasselini, I. Rousset, S., Douard, R., Chevallier, J.-M., Emilie D., Perlemuter, G. (2010) Glucocorticoid-induced leucine zipper (GILZ): a key protein in the sensitization of fatty liver to LPS in obesity. *poster presentation at The International Liver Congress*, **abstract**.
- Brannan, C.I., Dees, E.C., Ingram, R.S. and Tilghman, S.M. (1990) The product of the H19 gene may function as an RNA. *Molecular and Cellular Biology*, **10**, 28.
- Browning, J.D., Szczepaniak, L.S., Dobbins, R., Nuremberg, P., Horton, J.D., Cohen, J.C., Grundy, S.M. and Hobbs, H.H. (2004) Prevalence of hepatic steatosis in an urban population in the United States: Impact of ethnicity. *Hepatology*, **40**, 1387.
- Bunney, T.D. and Katan, M. Phosphoinositide signalling in cancer: Beyond PI3K and PTEN. *Nature Reviews Cancer*, **10**, 342.

- Byon, C.H., Hardy, R.W., Ren, C., Ponnazhagan, S., Welch, D.R., McDonald, J.M. and Chen, Y. (2009) Free fatty acids enhance breast cancer cell migration through plasminogen activator inhibitor-1 and SMAD4. *Laboratory Investigation*, **89**, 1221.
- Cai, D., Yuan, M., Frantz, D.F., Melendez, P.A., Hansen, L., Lee, J. and Shoelson, S.E. (2005) Local and systemic insulin resistance resulting from hepatic activation of IKK- β and NF- κ B. *Nature Medicine*, **11**, 183.
- Cai, X. and Cullen, B.R. (2007) The imprinted H19 noncoding RNA is a primary microRNA precursor. *RNA*, **13**, 313.
- Cai, Y., Song, Z., Wang, X., Jiao, H. and Lin, H. (2011) Dexamethasone-induced hepatic lipogenesis is insulin dependent in chickens (*Gallus gallus domesticus*). *Stress*, **in press**.
- Caja, L., Sancho, P., Bertran, E., Iglesias-Serret, D., Gil, J. and Fabregat, I. (2009) Overactivation of the MEK/ERK pathway in liver tumor cells confers resistance to TGF- β -induced cell death through impairing up-regulation of the NADPH oxidase NOX4. *Cancer Research*, **69**, 7595.
- Canbay, A., Friedman, S. and Gores, G.J. (2004) Apoptosis: The Nexus of Liver Injury and Fibrosis. *Hepatology*, **39**, 273.
- Cantley, L.C. and Neel, B.G. (1999) New insights into tumor suppression: PTEN suppresses tumor formation by restraining the phosphoinositide 3-kinase/AKT pathway. *Proc Natl Acad Sci U S A*, **96**, 4240-4245.
- Canuto, R.A., Biocca, M.E., Muzio, G. and Dianzani, M.U. (1986) Changes of fatty acid composition of phospholipids during diethylnitrosamine carcinogenesis in rat liver. *Cell Biology International Reports*, **10**, 472.
- Carbo, N., Costelli, P., Tessitore, L., Bagby, G.J., Lopez-Soriano, F.J., Baccino, F.M. and Argiles, J.M. (1994) Anti-tumour necrosis factor-alpha treatment interferes with changes in lipid metabolism in a tumour cachexia model. *Clinical Science*, **87**, 349.
- Cardone, M.H., Roy, N., Stennicke, H.R., Salvesen, G.S., Franke, T.F., Stanbridge, E., Frisch, S. and Reed, J.C. (1998) Regulation of cell death protease caspase-9 by phosphorylation. *Science*, **282**, 1318-1321.
- Cariani, E., Lasserre, C., Seurin, D., Hamelin, B., Kemeny, F., Franco, D., Czech, M.P., Ullrich, A. and Brechot, C. (1988a) Differential expression of insulin-like growth factor II mRNA in human primary liver cancers, benign liver tumors, and liver cirrhosis. *Cancer Research*, **48**, 6844.
- Cariani, E., Lasserre, C., Seurin, D., Hamelin, B., Kemeny, F., Franco, D., Czech, M.P., Ullrich, A. and Brechot, C. (1988b) Differential Expression of Insulin-like Growth Factor II mRNA in Human Primary Liver Cancers, Benign Liver Tumors, and Liver Cirrhosis. *Cancer Res*, **48**, 6844-6849.
- Catlett-Falcone, R., Landowski, T.H., Oshiro, M.M., Turkson, J., Levitzki, A., Savino, R., Ciliberto, G., Moscinski, L., Fernández-Luna, J.L., Nuaez, G., Dalton, W.S. and Jove, R. (1999) Constitutive activation of Stat3 signaling confers resistance to apoptosis in human U266 myeloma cells. *Immunity*, **10**, 105.
- Chang, F., Steelman, L.S., Lee, J.T., Shelton, J.G., Navolanic, P.M., Blalock, W.L., Franklin, R.A. and McCubrey, J.A. (2003) Signal transduction mediated by the Ras//Raf//MEK//ERK pathway from cytokine receptors to transcription factors: potential targeting for therapeutic intervention. *Leukemia*, **17**, 1263.
- Chao, J.A., Patskovsky, Y., Patel, V., Levy, M., Almo, S.C. and Singer, R.H. (2010) ZBP1 recognition of β -actin zipcode induces RNA looping. *Genes and Development*, **24**, 148.

- Charalambous, M., Menheniott, T.R., Bennett, W.R., Kelly, S.M., Dell, G., Dandolo, L. and Ward, A. (2004) An enhancer element at the *Igf2/H19* locus drives gene expression in both imprinted and non-imprinted tissues. *Developmental Biology*, **271**, 488.
- Chen, Y.L., Law, P.Y. and Loh, H.H. (2005) Inhibition of P13K/Akt signaling: An emerging paradigm for targeted cancer therapy. *Current Medicinal Chemistry - Anti-Cancer Agents*, **5**, 575.
- Cheng, Y.W., Idrees, K., Shattock, R., Khan, S.A., Zeng, Z., Brennan, C.W., Paty, P. and Barany, F. Loss of imprinting and marked gene elevation are 2 forms of aberrant *IGF2* expression in colorectal cancer. *International Journal of Cancer*, **127**, 568.
- Choi, J., Yip-Schneider, M., Albertin, F., Wiesenauer, C., Wang, Y. and Schmidt, C.M. (2008) The Effect of Doxorubicin on MEK-ERK Signaling Predicts Its Efficacy in HCC. *Journal of Surgical Research*, **150**, 219.
- Chow, L.M.L. and Baker, S.J. (2006) PTEN function in normal and neoplastic growth. *Cancer Letters*, **241**, 184.
- Christiansen, J., Kolte, A.M., Hansen, T.V.O. and Nielsen, F.C. (2009) *IGF2* mRNA-binding protein 2: Biological function and putative role in type 2 diabetes. *Journal of Molecular Endocrinology*, **43**, 187.
- Cortez-Pinto, H., Jesus, L., Barros, H., Lopes, C., Moura, M.C. and Camilo, M.E. (2006) How different is the dietary pattern in non-alcoholic steatohepatitis patients? *Clinical Nutrition*, **25**, 816.
- Couvert, P., Carrié, A., Pariès, J., Vaysse, J., Miroglio, A., Kerjean, A., Nahon, P., Chelly, J., Trinchet, J.C., Beaugrand, M. and Ganne-Carrié, N. (2008) Liver insulin-like growth factor 2 methylation in hepatitis C virus cirrhosis and further occurrence of hepatocellular carcinoma. *World Journal of Gastroenterology*, **14**, 5419.
- Covey, T.M., Edes, K., Coombs, G.S., Virshup, D.M. and Fitzpatrick, F.A. Alkylation of the tumor suppressor PTEN activates Akt and β -catenin signaling: A mechanism linking inflammation and oxidative stress with cancer. *PLoS ONE*, **5**.
- Cozen, W., Gill, P.S., Ingles, S.A., Masood, R., Martínez-Maza, O., Cockburn, M.G., Gauderman, W.J., Pike, M.C., Bernstein, L., Nathwani, B.N., Salam, M.T., Danley, K.L., Wang, W., Gage, J., Gundell-Miller, S. and Mack, T.M. (2004) *IL-6* levels and genotype are associated with risk of young adult Hodgkin lymphoma. *Blood*, **103**, 3216.
- Crespo, J., Cayoen, A., Fernandez-Gil, P., Hernandez-Guerra, M., Mayorga, M., Domnguez-Dez, A., Fernandez-Escalante, J.C. and Pons-Romero, F. (2001) Gene expression of tumor necrosis factor α and TNF-receptors, p55 and p75, in nonalcoholic steatohepatitis patients. *Hepatology*, **34**, 1158.
- Crews, C.M. and Erikson, R.L. (1992) Purification of a murine protein-tyrosine/threonine kinase that phosphorylates and activates the Erk-1 gene product: Relationship to the fission yeast *byr1* gene product. *Proceedings of the National Academy of Sciences of the United States of America*, **89**, 8205.
- Cruz-Correa, M., Cui, H., Giardiello, F.M., Powe, N.R., Hylind, L., Robinson, A., Hutcheon, D.F., Kafonek, D.R., Brandenburg, S., Wu, Y., He, X. and Feinberg, A.P. (2004) Loss of Imprinting of Insulin Growth Factor II Gene: A Potential Heritable Biomarker for Colon Neoplasia Predisposition. *Gastroenterology*, **126**, 964.
- Cui, H., Cruz-Correa, M., Giardiello, F.M., Hutcheon, D.F., Kafonek, D.R., Brandenburg, S., Wu, Y., He, X., Powe, N.R. and Feinberg, A.P. (2003) Loss

- of IGF2 imprinting: A potential marker of colorectal cancer risk. *Science*, **299**, 1753.
- Cui, H., Hedborg, F., He, L., Nordenskjöld, A., Sandstedt, B., Pfeifer-Ohlsson, S. and Ohlsson, R. (1997) Inactivation of H19, an imprinted and putative tumor repressor gene, is a preneoplastic event during Wilms' tumorigenesis. *Cancer Research*, **57**, 4469.
- Datta, S.R., Dudek, H., Tao, X., Masters, S., Fu, H., Gotoh, Y. and Greenberg, M.E. (1997) Akt phosphorylation of BAD couples survival signals to the cell-intrinsic death machinery. *Cell*, **91**, 231-241.
- Davies, H., Bignell, G.R., Cox, C., Stephens, P., Edkins, S., Clegg, S., Teague, J., Woffendin, H., Garnett, M.J., Bottomley, W., Davis, N., Dicks, E., Ewing, R., Floyd, Y., Gray, K., Hall, S., Hawes, R., Hughes, J., Kosmidou, V., Menzies, A., Mould, C., Parker, A., Stevens, C., Watt, S., Hooper, S., Wilson, R., Jayatilake, H., Gusterson, B.A., Cooper, C., Shipley, J., Hargrave, D., Pritchard-Jones, K., Maitland, N., Chenevix-Trench, G., Riggins, G.J., Bigner, D.D., Palmleri, G., Cossu, A., Flanagan, A., Nicholson, A., Ho, J.W.C., Leung, S.Y., Yuen, S.T., Weber, B.L., Seigler, H.F., Darrow, T.L., Paterson, H., Marais, R., Marshall, C.J., Wooster, R., Stratton, M.R. and Futreal, P.A. (2002) Mutations of the BRAF gene in human cancer. *Nature*, **417**, 949.
- Davies, S.M. (1994) Developmental regulation of genomic imprinting of the IGF2 gene in human liver. *Cancer Research*, **54**, 2560.
- Day, C.P. (2006) Genetic and environmental susceptibility to non-alcoholic fatty liver disease. *Digestive Diseases*, **28**, 255.
- De Alaniz, M.J.T. and Marra, C.A. (1994) Role of $\Delta 9$ desaturase activity in the maintenance of high levels of monoenoic fatty acids in hepatoma cultured cells. *Molecular and Cellular Biochemistry*, **137**, 85.
- de Lima, V.M.R., Oliveira, C.P.M.S., Alves, V.A.F., Chammas, M.C., Oliveira, E.P., Stefano, J.T., de Mello, E.S., Cerri, G.G., Carrilho, F.J. and Caldwell, S.H. (2008) A rodent model of NASH with cirrhosis, oval cell proliferation and hepatocellular carcinoma. *Journal of Hepatology*, **49**, 1055.
- Dent, P. and Grant, S. (2001) Pharmacologic interruption of the mitogen-activated extracellular-regulated kinase/mitogen-activated protein kinase signal transduction pathway: Potential role in promoting cytotoxic drug action. *Clinical Cancer Research*, **7**, 775.
- Di Cristofano, A., Pesce, B., Cordon-Cardo, C. and Pandolfi, P.P. (1998) Pten is essential for embryonic development and tumour suppression. *Nature Genetics*, **19**, 348.
- Diehl, J.A., Cheng, M., Roussel, M.F. and Sherr, C.J. (1998) Glycogen synthase kinase-3 β regulates cyclin D1 proteolysis and subcellular localization. *Genes Dev*, **12**, 3499-3511.
- Dolcet, X., Llobet, D., Pallares, J. and Matias-Guiu, X. (2005) NF- κ B in development and progression of human cancer. *Virchows Archiv*, **446**, 475.
- Dong-Dong, L., Xi-Ran, Z. and Xiang-Rong, C. (2003) Expression and significance of new tumor suppressor gene PTEN in primary liver cancer. *Journal of Cellular and Molecular Medicine*, **7**, 67.
- Donnelly, K.L., Smith, C.I., Schwarzenberg, S.J., Jessurun, J., Boldt, M.D. and Parks, E.J. (2005) Sources of fatty acids stored in liver and secreted via lipoproteins in patients with nonalcoholic fatty liver disease. *Journal of Clinical Investigation*, **115**, 1343.
- Drewell, R.A., Brenton, J.D., Ainscough, J.F.X., Barton, S.C., Hilton, K.J., Arney, K.L., Dandolo, L. and Surani, M.A. (2000) Deletion of a silencer element disrupts

- H19 imprinting independently of a DNA methylation epigenetic switch. *Development*, **127**, 3419.
- Duvoux, C. (1998) Epidemiology and diagnosis of hepatocellular carcinoma in cirrhosis. *Epidemiologie et diagnostic des carcinomes hepatocellulaires sur cirrhose*, **52**, 511.
- Eggens, I. and ElMBERger, P.G. (1990) Studies on the polyisoprenoid composition in hepatocellular carcinomas and its correlation with their differentiation. *APMIS*, **98**, 535.
- Ekstrom, T.J., Cui, H., Li, X. and Ohlsson, R. (1995) Promoter-specific IGF2 imprinting status and its plasticity during human liver development. *Development*, **121**, 309.
- Emuss, V., Garnett, M., Mason, C. and Marais, R. (2005) Mutations of C-RAF are rare in human cancer because C-RAF has a low basal kinase activity compared with B-RAF. *Cancer Research*, **65**, 9719.
- Ewings, K.E., Hadfield-Moorhouse, K., Wiggins, C.M., Wickenden, J.A., Balmanno, K., Gilley, R., Degenhardt, K., White, E. and Cook, S.J. (2007) ERK1/2-dependent phosphorylation of Bim (EL) promotes its rapid dissociation from Mcl-1 and Bcl-x (L). *EMBO Journal*, **26**, 2856.
- Fabregat, I., Roncero, C. and Fernández, M. (2007) Survival and apoptosis: A dysregulated balance in liver cancer. *Liver International*, **27**, 155.
- Farrell, G.C. and Larter, C.Z. (2006) Nonalcoholic fatty liver disease: From steatosis to cirrhosis. *Hepatology*, **43**.
- Feldstein, A.E., Werneburg, N.W., Canbay, A., Guicciardi, M.E., Bronk, S.F., Rydzewski, R., Burgart, L.J. and Gores, G.J. (2004) Free fatty acids promote hepatic lipotoxicity by stimulating TNF- α expression via a lysosomal pathway. *Hepatology*, **40**, 185.
- Feng, D.Y., Zheng, H., Tan, Y. and Cheng, R.X. (2001) Effect of phosphorylation of MAPK and Stat3 and expression of c-fos and c-jun proteins on hepatocarcinogenesis and their clinical significance. *World Journal of Gastroenterology*, **7**, 33.
- Forner, A., Reig, M.E., Rodriguez De Lope, C. and Bruix, J. Current strategy for staging and treatment: The BCLC update and future prospects. *Seminars in Liver Disease*, **30**, 61.
- Freeman, D.J., Li, A.G., Wei, G., Li, H.H., Kertesz, N., Lesche, R., Whale, A.D., Martinez-Diaz, H., Rozengurt, N., Cardiff, R.D., Liu, X. and Wu, H. (2003) PTEN tumor suppressor regulates p53 protein levels and activity through phosphatase-dependent and -independent mechanisms. *Cancer Cell*, **3**, 117.
- Frémin, C., Ezan, F., Boisselier, P., Bessard, A., Pagès, G., Pouysségur, J. and Baffet, G. (2007) ERK2 but not ERK1 plays a key role in hepatocyte replication: An RNAi-mediated ERK2 knockdown approach in wild-type and ERK1 null hepatocytes. *Hepatology*, **45**, 1035.
- Frevel, M.A.E., Hornberg, J.J. and Reeve, A.E. (1999) A potential imprint control element: Identification of a conserved 42 bp sequence upstream of H19. *Trends in Genetics*, **15**, 216.
- Fujiwara, Y., Hoon, D.S., Yamada, T., Umeshita, K., Gotoh, M., Sakon, M., Nishisho, I. and Monden, M. (2000) PTEN / MMAC1 mutation and frequent loss of heterozygosity identified in chromosome 10q in a subset of hepatocellular carcinomas. *Jpn J Cancer Res*, **91**, 287-292.
- Gabory, A., Ripoché, M.A., Le Digarcher, A., Watrin, F., Ziyat, A., Forné, T., Jammes, H., Ainscough, J.F.X., Surani, M.A., Journot, L. and Dandolo, L.

- (2009) H19 acts as a trans regulator of the imprinted gene network controlling growth in mice. *Development*, **136**, 3413.
- Gabory, A., Ripoche, M.A., Yoshimizu, T. and Dandolo, L. (2006a) The H19 gene: regulation and function of a non-coding RNA. *Cytogenet. Genome Res.*, **113**, 188-193.
- Gabory, A., Ripoche, M.A., Yoshimizu, T. and Dandolo, L. (2006b) The H19 gene: Regulation and function of a non-coding RNA. *Cytogenetic and Genome Research*, **113**, 188.
- Gailhouste, L., Ezan, F., Bessard, A., Frémin, C., Rageul, J., Langouët, S. and Baffet, G. (2010) RNAi-mediated MEK1 knock-down prevents ERK1/2 activation and abolishes human hepatocarcinoma growth in vitro and in vivo. *International Journal of Cancer*, **126**, 1367.
- Giannoukakis, N., Deal, C., Paquette, J., Goodyer, C.G. and Polychronakos, C. (1993) Parental genomic imprinting of the human IGF2 gene. *Nature Genetics*, **4**, 98.
- Gollob, J.A., Wilhelm, S., Carter, C. and Kelley, S.L. (2006) Role of Raf Kinase in Cancer: Therapeutic Potential of Targeting the Raf/MEK/ERK Signal Transduction Pathway. *Seminars in Oncology*, **33**, 392.
- Grando-Lemaire, V., Guettier, C., Chevret, S., Beaugrand, M. and Trinchet, J.C. (1999) Hepatocellular carcinoma without cirrhosis in the West: Epidemiological factors and histopathology of the non-tumorous liver. *Journal of Hepatology*, **31**, 508.
- Grugan, K.D., Ma, C., Singhal, S., Krett, N.L. and Rosen, S.T. (2008) Dual regulation of glucocorticoid-induced leucine zipper (GILZ) by the glucocorticoid receptor and the PI3-kinase/AKT pathways in multiple myeloma. *The Journal of Steroid Biochemistry and Molecular Biology*, **110**, 244.
- Guicciardi, M.E. and Gores, G.J. (2005) Apoptosis: A mechanism of acute and chronic liver injury. *Gut*, **54**, 1024.
- Halonen, M., Pelto-Huikko, M., Eskelin, P., Peltonen, L., Ulmanen, I. and Kolmer, M. (2001) Subcellular location and expression pattern of autoimmune regulator (Aire), the mouse orthologue for human gene defective in autoimmune polyendocrinopathy candidiasis ectodermal dystrophy (APECED). *Journal of Histochemistry and Cytochemistry*, **49**, 197.
- Hamdi, H., Bigorgne, A., Naveau, S., Balian, A., Bouchet-Delbos, L., Cassard-Doulcier, A.M., Maillot, M.C., Durand-Gasselín, I., Prévot, S., Delaveaucoupet, J., Emilie, D. and Perlemuter, G. (2007) Glucocorticoid-induced leucine zipper: A key protein in the sensitization of monocytes to lipopolysaccharide in alcoholic hepatitis. *Hepatology*, **46**, 1986.
- Hammer, N.A., Hansen, T.v.O., Byskov, A.G., Rajpert-De Meyts, E., Grondahl, M.L., Bredkjaer, H.E., Wewer, U.M., Christiansen, J. and Nielsen, F.C. (2005) Expression of IGF-II mRNA-binding proteins (IMPs) in gonads and testicular cancer. *Reproduction*, **130**, 203-212.
- Han, M., Yan, W., Guo, W., Xi, D., Zhou, Y., Li, W., Gao, S., Liu, M., Levy, G., Luo, X. and Ning, Q. (2008) Hepatitis B virus-induced hFGL2 transcription is dependent on c-Ets-2 and MAPK signal pathway. *Journal of Biological Chemistry*, **283**, 32715.
- Hansen, T.V.O., Hammer, N.A., Nielsen, J., Madsen, M., Dalbaeck, C., Wewer, U.M., Christiansen, J. and Nielsen, F.C. (2004) Dwarfism and Impaired Gut Development in Insulin-Like Growth Factor II mRNA-Binding Protein 1-Deficient Mice. *Mol. Cell. Biol.*, **24**, 4448-4464.

- Hao, Y., Crenshaw, T., Moulton, T., Newcomb, E. and Tycko, B. (1993) Tumour-suppressor activity of H19 RNA. *Nature*, **365**, 764.
- Harden, T.K. and Sondek, J. (2006) Regulation of phospholipase C isozymes by Ras superfamily GTPases. *Annual Review of Pharmacology and Toxicology*, Vol. 46, p. 355.
- Hässler, S., Ramsey, C., Karlsson, M.C., Larsson, D., Herrmann, B., Rozell, B., Backheden, M., Peltonen, L., Kämpe, O. and Winqvist, O. (2006) Aire-deficient mice develop hematopoietic irregularities and marginal zone B-cell lymphoma. *Blood*, **108**, 1941.
- He, G. and Karin, M. NF- κ B and STAT3- key players in liver inflammation and cancer. *Cell Research*, **21**, 159.
- Hellerstein, M.K., Schwarz, J.M. and Neese, R.A. (1996) Regulation of hepatic de novo lipogenesis in humans. *Annual Review of Nutrition*, Vol. 16, p. 523.
- Hettinger, K., Vikhanskaya, F., Poh, M.K., Lee, M.K., de Belle, I., Zhang, J.T., Reddy, S.A.G. and Sabapathy, K. (2007) c-Jun promotes cellular survival by suppression of PTEN. *Cell Death and Differentiation*, **14**, 218.
- Hoppstädter, J., Diesel, B., Eifler, L.K., Schmid, T., Brüne, B., Kiemer, A.K. (2010) Downregulation of Glucocorticoid Leucine Zipper in alveolar macrophages upon Toll-like receptor activation occurs MyD88-dependently. *submitted*.
- Horia, E. and Watkins, B.A. (2007) Complementary actions of docosahexaenoic acid and genistein on COX-2, PGE2 and invasiveness in MDA-MB-231 breast cancer cells. *Carcinogenesis*, **28**, 809.
- Horie, Y., Suzuki, A., Kataoka, E., Sasaki, T., Hamada, K., Sasaki, J., Mizuno, K., Hasegawa, G., Kishimoto, H., Iizuka, M., Naito, M., Enomoto, K., Watanabe, S., Mak, T.W. and Nakano, T. (2004) Hepatocyte-specific Pten deficiency results in steatohepatitis and hepatocellular carcinomas. *Journal of Clinical Investigation*, **113**, 1774.
- Hoshino, R., Chatani, Y., Yamori, T., Tsuruo, T., Oka, H., Yoshida, O., Shimada, Y., Ari-I, S., Wada, H., Fujimoto, J. and Kohno, M. (1999) Constitutive activation of the 41-/43-kDa mitogen-activated protein kinase signaling pathway in human tumors. *Oncogene*, **18**, 813.
- Hu, J.F., Vu, T.H. and Hoffman, A.R. (1996) Promoter-specific modulation of insulin-like growth factor II genomic imprinting by inhibitors of DNA methylation. *Journal of Biological Chemistry*, **271**, 18253.
- Hu, T.H., Huang, C.C., Lin, P.R., Chang, H.W., Ger, L.P., Lin, Y.W., Changchien, C.S., Lee, C.M. and Tai, M.H. (2003) Expression and prognostic role of tumor suppressor gene PTEN/MMAC1/TEP1 in hepatocellular carcinoma. *Cancer*, **97**, 1929.
- Hutchinson, L. (2010) Medical oncology: IMP3 is a novel prognostic marker for colon cancer. *Nature Reviews Clinical Oncology*, **7**, 123.
- Huynh, H., Nguyen, T.T.T., Chow, K.-H.P., Tan, P.H., Soo, K.C. and Tran, E. (2003) Over-expression of the mitogen-activated protein kinase (MAPK) kinase (MEK)-MAPK in hepatocellular carcinoma: Its role in tumor progression and apoptosis. *BMC Gastroenterology*, **3**, 19.
- Hwang, Y.H., Choi, J.Y., Kim, S., Chung, E.S., Kim, T., Koh, S.S., Lee, B., Bae, S.H., Kim, J. and Park, Y.M. (2004) Over-expression of c-raf-1 proto-oncogene in liver cirrhosis and hepatocellular carcinoma. *Hepatology Research*, **29**, 113.
- Iliopoulos, D., Jaeger, S.A., Hirsch, H.A., Bulyk, M.L. and Struhl, K. STAT3 Activation of miR-21 and miR-181b-1 via PTEN and CYLD Are Part of the Epigenetic Switch Linking Inflammation to Cancer. *Molecular Cell*, **39**, 493.

- Ishii, H., Horie, Y., Ohshima, S., Anezaki, Y., Kinoshita, N., Dohmen, T., Kataoka, E., Sato, W., Goto, T., Sasaki, J., Sasaki, T., Watanabe, S., Suzuki, A. and Ohnishi, H. (2009) Eicosapentaenoic acid ameliorates steatohepatitis and hepatocellular carcinoma in hepatocyte-specific Pten-deficient mice. *Journal of Hepatology*, **50**, 562.
- Ishizaki, T., Yoshie, M., Yaginuma, Y., Tanaka, T. and Ogawa, K. (2003) Loss of Igf2 imprinting in monoclonal mouse hepatic tumor cells is not associated with abnormal methylation patterns for the H19, Igf2, and Kvlqt1 differentially methylated regions. *Journal of Biological Chemistry*, **278**, 6222.
- Ito, Y., Sasaki, Y., Horimoto, M., Wada, S., Tanaka, Y., Kasahara, A., Ueki, T., Hirano, T., Yamamoto, H., Fujimoto, J., Okamoto, E., Hayashi, N. and Hori, M. (1998) Activation of mitogen-activated protein kinases/extracellular signal-regulated kinases in human hepatocellular carcinoma. *Hepatology*, **27**, 951.
- Itoh, S., Igarashi, M., Tsukada, Y. and Ichinoe, A. (1977) Nonalcoholic fatty liver with alcoholic hyalin after long-term glucocorticoid therapy. *Acta Hepato-Gastroenterologica*, **24**, 415.
- Jelinek, T., Dent, P., Sturgill, T.W. and Weber, M.J. (1996) Ras-induced activation of Raf-1 is dependent on tyrosine phosphorylation. *Molecular and Cellular Biology*, **16**, 1027.
- Jeng, Y.M., Chang, C.C., Hu, F.C., Chou, H.Y., Kao, H.L., Wang, T.H. and Hsu, H.C. (2008a) RNA-binding protein insulin-like growth factor II mRNA-binding protein 3 expression promotes tumor invasion and predicts early recurrence and poor prognosis in hepatocellular carcinoma. *Hepatology (Baltimore, Md.)*, **48**, 1118-1127.
- Jeng, Y.M., Chang, C.C., Hu, F.C., Chou, H.Y., Kao, H.L., Wang, T.H. and Hsu, H.C. (2008b) RNA-binding protein insulin-like growth factor II mRNA-binding protein 3 expression promotes tumor invasion and predicts early recurrence and poor prognosis in hepatocellular carcinoma. *Hepatology (Baltimore, Md.)*, **48**, 1118.
- Jiang, R., Xia, Y., Li, J., Deng, L., Zhao, L., Shi, J., Wang, X. and Sun, B. (2009) High expression levels of IKK α and IKK β are necessary for the malignant properties of liver cancer. *International Journal of Cancer*, **126**, 1263.
- Johnnidis, J.B., Venanzi, E.S., Taxman, D.J., Ting, J.P.Y., Benoist, C.O. and Mathis, D.J. (2005) Chromosomal clustering of genes controlled by the aire transcription factor. *Proceedings of the National Academy of Sciences of the United States of America*, **102**, 7233-7238.
- Juan, V., Crain, C. and Wilson, C. (2000) Evidence for evolutionarily conserved secondary structure in the H19 tumor suppressor RNA. *Nucl. Acids Res.*, **28**, 1221-1227.
- Kalscheuer, V.M., Mariman, E.C., Schepens, M.T., Rehder, H. and Ropers, H.H. (1993) The insulin-like growth factor type-2 receptor gene is imprinted in the mouse but not in humans. *Nature Genetics*, **5**, 74.
- Kaneda, A., Wang, C.J., Cheong, R., Timp, W., Onyango, P., Wen, B., Iacobuzio-Donahue, C.A., Ohlsson, R., Andraos, R., Pearson, M.A., Sharov, A.A., Longo, D.L., Ko, M.S.H., Levchenko, A. and Feinberg, A.P. (2007) Enhanced sensitivity to IGF-II signaling links loss of imprinting of IGF2 to increased cell proliferation and tumor risk. *Proceedings of the National Academy of Sciences of the United States of America*, **104**, 20926.
- Kang-Park, S., Lee, Y.I. and Lee, Y.I. (2003) PTEN modulates insulin-like growth factor II (IGF-II)-mediated signaling; the protein phosphatase activity of PTEN downregulates IGF-II expression in hepatoma cells. *FEBS Letters*, **545**, 203.

- Kawamura, N., Nagai, H., Bando, K., Koyama, M., Matsumoto, S., Tajiri, T., Onda, M., Fujimoto, J., Ueki, T., Konishi, N., Shiba, T. and Emi, M. (1999) PTEN/MMAC1 mutations in hepatocellular carcinomas: somatic inactivation of both alleles in tumors. *Jpn J Cancer Res*, **90**, 413-418.
- Kiemer, A.K., Weber, N.C. and Vollmar, A.M. (2002) Induction of I°B : Atrial natriuretic peptide as a regulator of the NF- κ B pathway. *Biochemical and Biophysical Research Communications*, **295**, 1068.
- Kim, K.-S. and Lee, Y.-I. (1997) Biallelic expression of the H19 and IGF2 genes in hepatocellular carcinoma. *Cancer Letters*, **119**, 143.
- Kim, K.W., Bae, S.K., Lee, O.H., Bae, M.H., Lee, M.J. and Park, B.C. (1998) Insulin-like growth factor II induced by hypoxia may contribute to angiogenesis of human hepatocellular carcinoma. *Cancer Research*, **58**, 348.
- Kinter, M., Spitz, D.R. and Roberts, R.J. (1996) Oleic acid incorporation protects cultured hamster fibroblasts from oxygen-induced cytotoxicity. *Journal of Nutrition*, **126**, 2952.
- Kistner, A., Gossen, M., Zimmermann, F., Jerecic, J., Ullmer, C., Lübbert, H. and Bujard, H. (1996) Doxycycline-mediated quantitative and tissue-specific control of gene expression in transgenic mice. *Proceedings of the National Academy of Sciences of the United States of America*, **93**, 10933.
- Kojiro, M. and Roskams, T. (2005) Early hepatocellular carcinoma and dysplastic nodules. *Seminars in Liver Disease*, **25**, 133.
- Kolch, W., Kotwaliwale, A., Vass, K. and Janosch, P. (2002) The role of Raf kinases in malignant transformation. *Expert reviews in molecular medicine*, **4**, 1.
- Koutsari, C. and Lazaridis, K.N. Emerging genes associated with the progression of nonalcoholic fatty liver disease. *Hepatology*, **52**, 807.
- Kuhajda, F.P. (2000) Fatty-acid synthase and human cancer: new perspectives on its role in tumor biology. *Nutrition*, **16**, 202.
- Kurukuti, S., Tiwari, V.K., Tavoosidana, G., Pugacheva, E., Murrell, A., Zhao, Z., Lobanenkov, V., Reik, W. and Ohlsson, R. (2006) CTCF binding at the H19 imprinting control region mediates maternally inherited higher-order chromatin conformation to restrict enhancer access to Igf2. *Proceedings of the National Academy of Sciences of the United States of America*, **103**, 10684.
- Lamonerie, T., Lavielle, C., De Galle, B., Binoux, M. and Brisson, O. (1995) Constitutive or inducible overexpression of the IGF-2 gene in cells of a human colon carcinoma cell line. *Experimental Cell Research*, **216**, 342.
- Landgraf, P., Rusu, M., Sheridan, R., Sewer, A., Iovino, N., Aravin, A., Pfeffer, S., Rice, A., Kamphorst, A.O., Landthaler, M., Lin, C., Socci, N.D., Hermida, L., Fulci, V., Chiaretti, S., Foà, R., Schliwka, J., Fuchs, U., Novosel, A., Müller, R.U., Schermer, B., Bissels, U., Inman, J., Phan, Q., Chien, M., Weir, D.B., Choksi, R., De Vita, G., Frezzetti, D., Trompeter, H.I., Hornung, V., Teng, G., Hartmann, G., Palkovits, M., Di Lauro, R., Wernet, P., Macino, G., Rogler, C.E., Nagle, J.W., Ju, J., Papavasiliou, F.N., Benzing, T., Lichter, P., Tam, W., Brownstein, M.J., Bosio, A., Borkhardt, A., Russo, J.J., Sander, C., Zavolan, M. and Tuschl, T. (2007) A Mammalian microRNA Expression Atlas Based on Small RNA Library Sequencing. *Cell*, **129**, 1401.
- Lee, H.C., Tian, B., Sedivy, J.M., Wands, J.R. and Kim, M. (2006) Loss of Raf Kinase Inhibitor Protein Promotes Cell Proliferation and Migration of Human Hepatoma Cells. *Gastroenterology*, **131**, 1208.
- Lee, T., Lau, T. and Ng, I. (2002) Doxorubicin-induced apoptosis and chemosensitivity in hepatoma cell lines. *Cancer Chemotherapy and Pharmacology*, **49**, 78.

- Leicht, D.T., Balan, V., Kaplun, A., Singh-Gupta, V., Kaplun, L., Dobson, M. and Tzivion, G. (2007) Raf kinases: Function, regulation and role in human cancer. *Biochimica et Biophysica Acta - Molecular Cell Research*, **1773**, 1196.
- Leighton, P.A., Saam, J.R., Ingram, R.S., Stewart, C.L. and Tilghman, S.M. (1995) An enhancer deletion affects both H19 and Igf2 expression. *Genes and Development*, **9**, 2079.
- Lewis, A., Mitsuya, K., Umlauf, D., Smith, P., Dean, W., Walter, J., Higgins, M., Feil, R. and Reik, W. (2004) Imprinting on distal chromosome 7 in the placenta involves repressive histone methylation independent of DNA methylation. *Nat Genet*, **36**, 1291.
- Li, X., Nong, Z., Ekström, C., Larsson, E., Nordlinder, H., Hofmann, W.J., Trautwein, C., Odenthal, M., Dienes, H.P., Ekström, T.J. and Schirmacher, P. (1997) Disrupted IGF2 promoter control by silencing of promoter P1 in human hepatocellular carcinoma. *Cancer Research*, **57**, 2048.
- Liang, L., Guo, W.H., Esquiliano, D.R., Asai, M., Rodriguez, S., Giraud, J., Kushner, J.A., White, M.F. and Lopez, M.F. Insulin-like growth factor 2 and the insulin receptor, but not insulin, regulate fetal hepatic glycogen synthesis. *Endocrinology*, **151**, 741.
- Lin, C.H., Hsieh, S.Y., Sheen, I.S., Lee, W.C., Chen, T.C., Shyu, W.C. and Liaw, Y.F. (2001) Genome-wide hypomethylation in hepatocellular carcinogenesis. *Cancer Research*, **61**, 4238.
- Liu, P., Terradillos, O., Renard, C.A., Feldmann, G., Buendia, M.A. and Bernuau, D. (1997) Hepatocarcinogenesis in woodchuck hepatitis virus/c-myc mice: Sustained cell proliferation and biphasic activation of insulin-like growth factor II. *Hepatology*, **25**, 874.
- Lu, M., Nakamura, R.M., Dent, E.D., Zhang, J.-Y., Nielsen, F.C., Christiansen, J., Chan, E.K.L. and Tan, E.M. (2001) Aberrant Expression of Fetal RNA-Binding Protein p62 in Liver Cancer and Liver Cirrhosis. *Am J Pathol*, **159**, 945-953.
- Lu, Z.L., Luo, D.Z. and Wen, J.M. (2005) Expression and significance of tumor-related genes in HCC. *World Journal of Gastroenterology*, **11**, 3850.
- Maehama, T. and Dixon, J.E. (1998) The tumor suppressor, PTEN/MMAC1, dephosphorylates the lipid second messenger, phosphatidylinositol 3,4,5-trisphosphate. *Journal of Biological Chemistry*, **273**, 13375.
- Maeng, Y.S., Choi, H.J., Kwon, J.Y., Park, Y.W., Choi, K.S., Min, J.K., Kim, Y.H., Suh, P.G., Kang, K.S., Won, M.H., Kim, Y.M. and Kwon, Y.G. (2009) Endothelial progenitor cell homing: Prominent role of the IGF2-IGF2R-PLC2/2 axis. *Blood*, **113**, 233.
- Malhi, H., Bronk, S.F., Werneburg, N.W. and Gores, G.J. (2006) Free fatty acids induce JNK-dependent hepatocyte lipoapoptosis. *Journal of Biological Chemistry*, **281**, 12093.
- Matouk, I.J., DeGroot, N., Mezan, S., Ayesh, S., Abu-Lail, R., Hochberg, A. and Galun, E. (2007) The H19 non-coding RNA is essential for human tumor growth. *PLoS ONE*, **2**.
- Matteoni, C.A., Younossi, Z.M., Gramlich, T., Boparai, N., Yao Chang, L. and McCullough, A.J. (1999) Nonalcoholic fatty liver disease: A spectrum of clinical and pathological severity. *Gastroenterology*, **116**, 1413.
- Mazzucchelli, C., Vantaggiato, C., Ciamei, A., Fasano, S., Pakhotin, P., Krezel, W., Welzl, H., Wolfer, D.P., Pagã's, G., Valverde, O., Marowsky, A., Porrazzo, A., Orban, P.C., Maldonado, R., Ehrenguber, M.U., Cestari, V., Lipp, H.P., Chapman, P.F., Pouyssegur, J. and Brambilla, R. (2002) Knockout of ERK1

- MAP kinase enhances synaptic plasticity in the striatum and facilitates striatal-mediated learning and memory. *Neuron*, **34**, 807.
- McAvoy, N.C., Ferguson, J.W., Campbell, I.W. and Hayes, P.C. (2006) Non-alcoholic fatty liver disease: Natural history, pathogenesis and treatment. *British Journal of Diabetes and Vascular Disease*, **6**, 251.
- McGlynn, K.A., Tsao, L., Hsing, A.W., Devesa, S.S. and Fraumeni Jr, J.F. (2001) International trends and patterns of primary liver cancer. *International Journal of Cancer*, **94**, 290.
- McKillop, I.H., Schmidt, C.M., Cahill, P.A. and Sitzmann, J.V. (1997) Altered expression of mitogen-activated protein kinases in a rat model of experimental hepatocellular carcinoma. *Hepatology*, **26**, 1484.
- Menendez, J.A. and Lupu, R. (2007) Fatty acid synthase and the lipogenic phenotype in cancer pathogenesis. *Nat Rev Cancer*, **7**, 763.
- Meng, F., Henson, R., Wehbe-Janek, H., Ghoshal, K., Jacob, S.T. and Patel, T. (2007) MicroRNA-21 Regulates Expression of the PTEN Tumor Suppressor Gene in Human Hepatocellular Cancer. *Gastroenterology*, **133**, 647.
- Mercer, K., Giblett, S., Green, S., Lloyd, D., Dias, S.D., Plumb, M., Marais, R. and Pritchard, C. (2005) Expression of endogenous oncogenic V600E/B-raf induces proliferation and developmental defects in mice and transformation of primary fibroblasts. *Cancer Research*, **65**, 11493.
- Mocellin, S., Rossi, C.R., Pilati, P. and Nitti, D. (2005) Tumor necrosis factor, cancer and anticancer therapy. *Cytokine and Growth Factor Reviews*, **16**, 35.
- Mollica, M.P., Lionetti, L., Putti, R., Cavaliere, G., Gaita, M. and Barletta, A. (2011) From chronic overfeeding to hepatic injury: Role of endoplasmic reticulum stress and inflammation. *Nutrition, Metabolism and Cardiovascular Diseases*.
- Moraes, K.C.M., Quresma, A.J.C., Maehns, K. and Kobarg, J. (2003) Identification and characterization of proteins that selectively interact with isoforms of the mRNA binding protein AUF1 (hnRNP D). *Biological Chemistry*, **384**, 25.
- Mori, H., Sakakibara, S.-i., Imai, T., Nakamura, Y., Iijima, T., Suzuki, A., Yuasa, Y., Takeda, M. and Okano, H. (2001) Expression of mouse Igf2 mRNA-binding protein 3 and its implications for the developing central nervous system. *Journal of Neuroscience Research*, **64**, 132.
- Morrison, D.K. and Cutler, R.E. (1997) The complexity of Raf-1 regulation. *Current Opinion in Cell Biology*, **9**, 174.
- Nardone, G., Romano, M., Calabro, A., Pedone, P.V., De Sio, I., Persico, M., Budillon, G., Bruni, C.B., Riccio, A. and Zarrilli, R. (1996) Activation of fetal promoters of insulinlike growth factor II gene in hepatitis C virus-related chronic hepatitis, cirrhosis, and hepatocellular carcinoma. *Hepatology*, **23**, 1304.
- Naugler, W.E., Sakurai, T., Kim, S., Maeda, S., Kim, K., Elsharkawy, A.M. and Karin, M. (2007) Gender Disparity in Liver Cancer Due to Sex Differences in MyD88-Dependent IL-6 Production. *Science*, **317**, 121-124.
- Neuschwander-Tetri, B.A. and Caldwell, S.H. (2003) Nonalcoholic steatohepatitis: Summary of an AASLD Single Topic Conference. *Hepatology*, **37**, 1202.
- Nielsen, J., Christiansen, J., Lykke-Andersen, J., Johnsen, A.H., Wewer, U.M. and Nielsen, F.C. (1999) A family of insulin-like growth factor II mRNA-binding proteins represses translation in late development. *Molecular and Cellular Biology*, **19**, 1262.
- Nielsen, J., Kristensen, M.A., Willemoës, M., Nielsen, F.C. and Christiansen, J. (2004) Sequential dimerization of human zipcode-binding protein IMP1 on

- RNA: a cooperative mechanism providing RNP stability. *Nucleic Acids Research*, **32**, 4368-4376.
- Nonomura, N., Miki, T., Nishimura, K., Kanno, N., Kojima, Y. and Okuyama, A. (1997a) Altered imprinting of the H19 and insulin-like growth factor II genes in testicular tumors. *Journal of Urology*, **157**, 1977.
- Nonomura, N., Nishimura, K., Miki, T., Kanno, N., Kojima, Y., Yokoyama, M. and Okuyama, A. (1997b) Loss of imprinting of the insulin-like growth factor II gene in renal cell carcinoma. *Cancer Research*, **57**, 2575.
- Ntambi, J.M. and Miyazaki, M. (2004) Regulation of stearoyl-CoA desaturases and role in metabolism. *Progress in Lipid Research*, **43**, 91.
- Okuda, K., Nakashima, T., Kojiro, M., Kondo, Y. and Wada, K. (1989) Hepatocellular carcinoma without cirrhosis in Japanese patients. *Gastroenterology*, **97**, 140.
- Okuda, K., Nakashima, T., Sakamoto, K., Ikari, T., Hidaka, H., Kubo, Y., Sakuma, K., Motoike, Y., Okuda, H. and Obata, H. (1982) Hepatocellular carcinoma arising in noncirrhotic and highly cirrhotic livers: A comparative study of histopathology and frequency of hepatitis B markers. *Cancer*, **49**, 450.
- Ooasa, T., Karasaki, H., Kanda, H., Nomura, K., Kitagawa, T. and Ogawa, K. (1998) Loss of imprinting of the insulin-like growth factor II gene in mouse hepatocellular carcinoma cell lines. *Molecular Carcinogenesis*, **23**, 248.
- Page, J.M. and Harrison, S.A. (2009) NASH and HCC. *Clinics in Liver Disease*, **13**, 631.
- Park, E.J., Lee, J.H., Yu, G.Y., He, G., Ali, S.R., Holzer, R.G., Å–sterreicher, C.H., Takahashi, H. and Karin, M. (2010) Dietary and Genetic Obesity Promote Liver Inflammation and Tumorigenesis by Enhancing IL-6 and TNF Expression. *Cell*, **140**, 197.
- Park, Y.N., Chae, K.J., Kim, Y.B., Park, C. and Theise, N. (2001) Apoptosis and proliferation in hepatocarcinogenesis related to cirrhosis. *Cancer*, **92**, 2733.
- Pekow, J.R., Bhan, A.K., Zheng, H. and Chung, R.T. (2007) Hepatic steatosis is associated with increased frequency of hepatocellular carcinoma in patients with hepatitis C-related cirrhosis. *Cancer*, **109**, 2490.
- Persad, S., Attwell, S., Gray, V., Delcommenne, M., Troussard, A., Sanghera, J. and Dedhar, S. (2000) Inhibition of integrin-linked kinase (ILK) suppresses activation of protein kinase B/Akt and induces cell cycle arrest and apoptosis of PTEN-mutant prostate cancer cells. *Proceedings of the National Academy of Sciences of the United States of America*, **97**, 3207.
- Pikarsky, E., Porat, R.M., Stein, I., Abramovitch, R., Amit, S., Kasem, S., Gutkovich-Pyest, E., Urieli-Shoval, S., Galun, E. and Ben-Neriah, Y. (2004) NF- κ B functions as a tumour promoter in inflammation-associated cancer. *Nature*, **431**, 461.
- Poirier, K., Chalas, C., Tissier, F., Couvert, P., Mallet, V., Carrie, A., Marchio, A., Sarli, D., Gicquel, C., Chaussade, S., Beljord, C., Chelly, J., Kerjean, A. and Terris, B. (2003) Loss of parental-specific methylation at the IGF2 locus in human hepatocellular carcinoma. *Journal of Pathology*, **201**, 473.
- Pollak, M.N., Schernhammer, E.S. and Hankinson, S.E. (2004) Insulin-like growth factors and neoplasia. *Nature Reviews Cancer*, **4**, 505.
- Pricola, K.L., Kuhn, N.Z., Haleem-Smith, H., Song, Y. and Tuan, R.S. (2009) Interleukin-6 maintains bone marrow-derived mesenchymal stem cell stemness by an ERK1/2-dependent mechanism. *Journal of Cellular Biochemistry*, **108**, 577.
- Puri, P., Wiest, M.M., Cheung, O., Mirshahi, F., Sargeant, C., Min, H.K., Contos, M.J., Sterling, R.K., Fuchs, M., Zhou, H., Watkins, S.M. and Sanyal, A.J.

- (2009) The plasma lipidomic signature of nonalcoholic steatohepatitis. *Hepatology*, **50**, 1827.
- Purohit, V., Gao, B. and Song, B.-J. (2009) Molecular Mechanisms of Alcoholic Fatty Liver. *Alcoholism: Clinical and Experimental Research*, **33**, 191.
- Qian, H.L., Peng, X.X., Chen, S.H., Ye, H.M. and Qui, J.H. (2005) p62 expression in primary carcinomas of the digestive system. *World Journal of Gastroenterology*, **11**, 1788.
- Qian, J., Yao, D., Dong, Z., Wu, W., Qiu, L., Yao, N., Li, S., Bian, Y., Wang, Z. and Shi, G. Characteristics of hepatic IGF-II expression and monitored levels of circulating IGF-II mRNA in metastasis of hepatocellular carcinoma. *American Journal of Clinical Pathology*, **134**, 799.
- Rachmilewitz, J., Goshen, R., Ariel, I., Schneider, T., De Groot, N. and Hochberg, A. (1992) Parental imprinting of the human H19 gene. *FEBS Letters*, **309**, 25.
- Rainier, S., Dobry, C.J. and Feinberg, A.P. (1995) Loss of Imprinting in Hepatoblastoma. *Cancer Res*, **55**, 1836-1838.
- Rainier, S., Johnson, L.A., Dobry, C.J., Ping, A.J., Grundy, P.E. and Feinberg, A.P. (1993) Relaxation of imprinted genes in human cancer. *Nature*, **362**, 747.
- Ramakrishnan, G., Elinos-Báez, C.M., Jagan, S., Augustine, T.A., Kamaraj, S., Anandakumar, P. and Devaki, T. (2008) Silymarin downregulates COX-2 expression and attenuates hyperlipidemia during NDEA-induced rat hepatocellular carcinoma. *Molecular and Cellular Biochemistry*, **313**, 53.
- Redjimi, N., Gaudin, F., Touboul, C., Emilie, D., Pallardy, M., Biola-Vidamment, A., Fernandez, H., Prevot, S., Balabanian, K. and Machelon, V. (2009) Identification of glucocorticoid-induced leucine zipper as a key regulator of tumor cell proliferation in epithelial ovarian cancer. *Molecular Cancer*, **8**, 83.
- Reik, W., Dean, W. and Walter, J. (2001) Epigenetic reprogramming in mammalian development. *Science*, **293**, 1089.
- Roberts, L.R. and Gores, G.J. (2005) Hepatocellular carcinoma: Molecular pathways and new therapeutic targets. *Seminars in Liver Disease*, **25**, 212.
- Rockall, A.G., Sohaib, S.A., Evans, D., Kaltsas, G., Isidori, A.M., Monson, J.P., Besser, G.M., Grossman, A.B. and Reznick, R.H. (2003) Hepatic steatosis in Cushing's syndrome: A radiological assessment using computed tomography. *European Journal of Endocrinology*, **149**, 543.
- Runge, S., Nielsen, F.C., Nielsen, J., Lykke-Andersen, J., Wewer, U.M. and Christiansen, J. (2000) H19 RNA Binds Four Molecules of Insulin-like Growth Factor II mRNA-binding Protein. *J. Biol. Chem.*, **275**, 29562-29569.
- Saito, Y., Kanai, Y., Sakamoto, M., Saito, H., Ishii, H. and Hirohashi, S. (2001) Expression of mRNA for DNA methyltransferases and methyl-CpG-binding proteins and DNA methylation status on CpG islands and pericentromeric satellite regions during human hepatocarcinogenesis. *Hepatology*, **33**, 561.
- Sako, A., Kitayama, J., Kaisaki, S. and Nagawa, H. (2004) Hyperlipidemia is a risk factor for lymphatic metastasis in superficial esophageal carcinoma. *Cancer Letters*, **208**, 43.
- Scharf, J.G. and Braulke, T. (2003) The Role of the IGF Axis in Hepatocarcinogenesis. *Hormone and Metabolic Research*, **35**, 685.
- Schirmacher, P., Held, W.A., Yang, D., Chisari, F.V., Rustum, Y. and Rogler, C.E. (1992) Reactivation of insulin-like growth factor II during hepatocarcinogenesis in transgenic mice suggests a role in malignant growth. *Cancer Research*, **52**, 2549.

- Schmidt, C.M., McKillop, I.H., Cahill, P.A. and Sitzmann, J.V. (1997) Increased MAPK expression and activity in primary human hepatocellular carcinoma. *Biochemical and Biophysical Research Communications*, **236**, 54.
- Schmitz, K.J., Wohlschlaeger, J., Lang, H., Sotiropoulos, G.C., Malago, M., Steveling, K., Reis, H., Cicinnati, V.R., Schmid, K.W. and Baba, H.A. (2008) Activation of the ERK and AKT signalling pathway predicts poor prognosis in hepatocellular carcinoma and ERK activation in cancer tissue is associated with hepatitis C virus infection. *Journal of Hepatology*, **48**, 83.
- Schofield, P.N., Lee, A., Hill, D.J., Cheetham, J.E., James, D. and Stewart, C. (1991) Tumour suppression associated with expression of human insulin-like growth factor II. *British Journal of Cancer*, **63**, 687.
- Schuijter, M.M., Bataille, F., Weiss, T.S., Hellerbrand, C. and Bosserhoff, A.K. (2006) Raf kinase inhibitor protein is downregulated in hepatocellular carcinoma. *Oncology reports*, **16**, 451.
- Seger, R., Ahn, N.G., Posada, J., Munar, E.S., Jensen, A.M., Cooper, J.A., Cobb, M.H. and Krebs, E.G. (1992) Purification and characterization of mitogen-activated protein kinase activator(s) from epidermal growth factor-stimulated A431 cells. *Journal of Biological Chemistry*, **267**, 14373.
- Sepp-Lorenzino, L. (1998) Structure and function of the insulin-like growth factor I receptor. *Breast Cancer Research and Treatment*, **47**, 235.
- Sherman, M. (2005) Hepatocellular carcinoma: Epidemiology, risk factors, and screening. *Seminars in Liver Disease*, **25**, 143.
- Shimano, H., Horton, J.D., Hammer, R.E., Shimomura, I., Brown, M.S. and Goldstein, J.L. (1996) Overproduction of cholesterol and fatty acids causes massive liver enlargement in transgenic mice expressing truncated SREBP-1a. *Journal of Clinical Investigation*, **98**, 1575.
- Shoelson, S.E., Lee, J. and Goldfine, A.B. (2006) Inflammation and insulin resistance. *Journal of Clinical Investigation*, **116**, 1793.
- Stambolic, V., MacPherson, D., Sas, D., Lin, Y., Snow, B., Jang, Y., Benchimol, S. and Mak, T.W. (2001) Regulation of PTEN transcription by p53. *Molecular Cell*, **8**, 317.
- Stambolic, V., Suzuki, A., de la Pompa, J.L., Brothers, G.M., Mirtsos, C., Sasaki, T., Ruland, J., Penninger, J.M., Siderovski, D.P. and Mak, T.W. (1998) Negative regulation of PKB/AKT-dependent cell survival by tumor suppressor PTEN. *Cell*, **95**, 29 - 39.
- Steenman, M.J.C., Rainier, S., Dobry, C.J., Grundy, P., Horon, I.L. and Feinberg, A.P. (1994) Loss of imprinting of IGF2 is linked to reduced expression and abnormal methylation of H19 in Wilms' tumour. *Nature Genetics*, **7**, 433.
- Steinmetz, R., Wagoner, H.A., Zeng, P., Hammond, J.R., Hannon, T.S., Meyers, J.L. and Pescovitz, O.H. (2004) Mechanisms regulating the constitutive activation of the extracellular signal-regulated kinase (ERK) signaling pathway in ovarian cancer and the effect of ribonucleic acid interference for ERK1/2 on cancer cell proliferation. *Molecular Endocrinology*, **18**, 2570.
- Stickel, F. and Hellerbrand, C. (2010) Non-alcoholic fatty liver disease as a risk factor for hepatocellular carcinoma: Mechanisms and implications. *Gut*, **59**, 1303.
- Stiles, B., Wang, Y., Stahl, A., Bassilian, S., Lee, W.P., Kim, Y.J., Sherwin, R., Devaskar, S., Lesche, R., Magnuson, M.A. and Wu, H. (2004) Live-specific deletion of negative regulator Pten results in fatty liver and insulin hypersensitivity. *Proceedings of the National Academy of Sciences of the United States of America*, **101**, 2082.

- Sturgill, T.W. and Ray, L.B. (1986) Muscle proteins related to microtubule associated protein-2 are substrates for an insulin-stimulatable kinase. *Biochemical and Biophysical Research Communications*, **134**, 565.
- Su, Y., Qian, H., Zhang, J., Wang, S., Shi, P. and Peng, X. (2005) The diversity expression of p62 in digestive system cancers. *Clinical Immunology*, **116**, 118.
- Tadokoro, K., Fujii, H., Inoue, T. and Yamada, M. (1991) Polymerase chain reaction (PCR) for detection of Apal polymorphism at the insulin like growth factor II gene (IGF2). *Nucleic Acids Research*, **19**, 6967.
- Takeda, S., Kondo, M., Kumada, T., Koshikawa, T., Ueda, R., Nishio, M., Osada, H., Suzuki, H., Nagatake, M., Washimi, O., Takagi, K., Takahashi, T., Nakao, A. and Takahashi, T. (1996) Allelic-expression imbalance of the insulin-like growth factor 2 gene in hepatocellular carcinomas and underlying disease. *Oncogene*, **12**, 1589.
- Tamguney, T. and Stokoe, D. (2007) New insights into PTEN. *Journal of Cell Science*, **120**, 4071.
- Tannapfel, A., Sommerer, F., Benicke, M., Katalinic, A., Uhlmann, D., Witzigmann, H., Hauss, J. and Wittekind, C. (2003) Mutations of the BRAF gene in cholangiocarcinoma but not in hepatocellular carcinoma. *Gut*, **52**, 706.
- Thorgeirsson, S.S. and Grisham, J.W. (2002) Molecular pathogenesis of human hepatocellular carcinoma. *Nature Genetics*, **31**, 339.
- Thorvaldsen, J.L., Duran, K.L. and Bartolomei, M.S. (1998) Deletion of the H19 differentially methylated domain results in loss of imprinted expression of H19 and Igf2. *Genes and Development*, **12**, 3693.
- Tierling, S., Dalbert, S., Schoppenhorst, S., Tsai, C.E., Oliger, S., Ferguson-Smith, A.C., Paulsen, M. and Walter, J. (2006) High-resolution map and imprinting analysis of the Gtl2-Dnchc1 domain on mouse chromosome 12. *Genomics*, **87**, 225.
- To, M.D., Perez-Losada, J., Mao, J.H. and Balmain, A. (2005) Crosstalk between Pten and Ras signaling pathways in tumor development. *Cell Cycle*, **4**, 1185.
- Tovar, V., Alsinet, C., Villanueva, A., Hoshida, Y., Chiang, D.Y., Solé, M., Thung, S., Moyano, S., Toffanin, S., Mínguez, B., Cabellos, L., Peix, J., Schwartz, M., Mazzaferro, V., Bruix, J. and Llovet, J.M. (2010) IGF activation in a molecular subclass of hepatocellular carcinoma and pre-clinical efficacy of IGF-1R blockage. *Journal of Hepatology*, **52**, 550.
- Trevisani, F., D'Intino, P.E., Caraceni, P., Pizzo, M., Stefanini, G.F., Mazziotti, A., Grazi, G.L., Gozzetti, G., Gasbarrini, G. and Bernardi, M. (1995) Etiologic factors and clinical presentation of hepatocellular carcinoma: Differences between cirrhotic and noncirrhotic Italian patients. *Cancer*, **75**, 2220.
- Tsochatzis, E.A., Manolakopoulos, S., Papatheodoridis, G.V. and Archimandritis, A.J. (2009) Insulin resistance and metabolic syndrome in chronic liver diseases: Old entities with new implications. *Scandinavian Journal of Gastroenterology*, **44**, 6.
- Tybl, E., Shi, F.-D., Kessler, S.M., Tierling, S., Walter, J., Bohle, R.M., Wieland, S., Zhang, J., Tan, E.M. and Kiemer, A.K. (2011) Overexpression of the IGF2-mRNA binding protein p62 in transgenic mice induces a steatotic phenotype. *Journal of Hepatology*, **In Press, Corrected Proof**.
- Uchida, K., Kondo, M., Takeda, S., Osada, H., Takahashi, T., Nakao, A. and Takahashi, T. (1997) Altered transcriptional regulation of the insulin-like growth factor 2 gene in human hepatocellular carcinoma. *Molecular Carcinogenesis*, **18**, 193.

- Van Etten, B., De Vries, M.R., Van Ijken, M.G.A., Lans, T.E., Guetens, G., Ambagtsheer, G., Van Tiel, S.T., De Boeck, G., De Bruijn, E.A., Eggermont, A.M.M. and Ten Hagen, T.L.M. (2003) Degree of tumour vascularity correlates with drug accumulation and tumour response upon TNF- α -based isolated hepatic perfusion. *British Journal of Cancer*, **88**, 314.
- van Horssen, R., ten Hagen, T.L.M. and Eggermont, A.M.M. (2006) TNF- α in Cancer Treatment: Molecular Insights, Antitumor Effects, and Clinical Utility. *Oncologist*, **11**, 397-408.
- Van Roey, G., Fevery, J. and Van Steenberghe, W. (2000) Hepatocellular carcinoma in Belgium: Clinical and virological characteristics of 154 consecutive cirrhotic and non-cirrhotic patients. *European Journal of Gastroenterology and Hepatology*, **12**, 61.
- Vantaggiato, C., Formentini, I., Bondanza, A., Bonini, C., Naldini, L. and Brambilla, R. (2006) ERK1 and ERK2 mitogen-activated protein kinases affect Ras-dependent cell signaling differentially. *Journal of Biology*, **5**.
- Vasudevan, K.M., Gurumurthy, S. and Rangnekar, V.M. (2004) Suppression of PTEN Expression by NF- κ B Prevents Apoptosis. *Mol. Cell. Biol.*, **24**, 1007-1021.
- Vernucci, M., Cerrato, F., Besnard, N., Casola, S., Pedone, P.V., Bruni, C.B. and Riccio, A. (2000) The H19 endodermal enhancer is required for Igf2 activation and tumor formation in experimental liver carcinogenesis. *Oncogene*, **19**, 6376.
- Vernucci, M., Cerrato, F., Pedone, P.V., Dandolo, L., Bruni, C.B. and Riccio, A. (2004) Developmentally regulated functions of the H19 differentially methylated domain. *Human Molecular Genetics*, **13**, 353.
- Vikesaa, J., Hansen, T.V.O., Jønson, L., Borup, R., Wewer, U.M., Christiansen, J. and Nielsen, F.C. (2006) RNA-binding IMPs promote cell adhesion and invadopodia formation. *EMBO Journal*, **25**, 1456.
- Vinciguerra, M., Carrozzino, F., Peyrou, M., Carlone, S., Montesano, R., Benelli, R. and Foti, M. (2009a) Unsaturated fatty acids promote hepatoma proliferation and progression through downregulation of the tumor suppressor PTEN. *Journal of Hepatology*, **50**, 1132.
- Vinciguerra, M., Sgroi, A., Veyrat-Durebex, C., Rubbia-Brandt, L., Buhler, L.H. and Foti, M. (2009b) Unsaturated fatty acids inhibit the expression of tumor suppressor phosphatase and tensin homolog (PTEN) via microRNA-21 up-regulation in hepatocytes. *Hepatology*, **49**, 1176.
- Vinciguerra, M., Veyrat-Durebex, C., Moukil, M.A., Rubbia-Brandt, L., Rohner-Jeanrenaud, F. and Foti, M. (2008) PTEN Down-Regulation by Unsaturated Fatty Acids Triggers Hepatic Steatosis via an NF- κ B/p65/mTOR-Dependent Mechanism. *Gastroenterology*, **134**, 268.
- Vivanco, I. and Sawyers, C.L. (2002) The phosphatidylinositol 3-kinase-AKT pathway in human cancer. *Nature Reviews Cancer*, **2**, 489.
- Vu, T.H. and Hoffman, A.R. (1994) Promoter-specific imprinting of the human insulin-like growth factor-II gene. *Nature*, **371**, 714.
- Wang, T., Fan, L., Watanabe, Y., McNeill, P.D., Moulton, G.G., Bangur, C., Fanger, G.R., Okada, M., Inoue, Y., Persing, D.H. and Reed, S.G. (2003) L523S, an RNA-binding protein as a potential therapeutic target for lung cancer. *Br J Cancer*, **88**, 887.
- Weber, M., Milligan, L., Delalbre, A., Antoine, E., Brunel, C., Cathala, G. and Forné, T. (2001) Extensive tissue-specific variation of allelic methylation in the Igf2 gene during mouse fetal development: relation to expression and imprinting. *Mechanisms of Development*, **101**, 133.

- Weinstein-Oppenheimer, C.R., Henríquez-Roldán, C.F., Davis, J.M., Navolanic, P.M., Saleh, O.A., Steelman, L.S., Franklin, R.A., Robinson, P.J., McMahon, M. and McCubrey, J.A. (2001) Role of the raf signal transduction cascade in the in vitro resistance to the anticancer drug doxorubicin. *Clinical Cancer Research*, **7**, 2898.
- Wellbrock, C., Karasarides, M. and Marais, R. (2004) The RAF proteins take centre stage. *Nature Reviews Molecular Cell Biology*, **5**, 875.
- Weng, L.P., Brown, J.L. and Eng, C. (2001) PTEN coordinates G1 arrest by down-regulating cyclin D1 via its protein phosphatase activity and up-regulating p27 via its lipid phosphatase activity in a breast cancer model. *Human Molecular Genetics*, **10**, 599.
- Whittaker, S., Marais, R. and Zhu, A.X. The role of signaling pathways in the development and treatment of hepatocellular carcinoma. *Oncogene*, **29**, 4989.
- Wilusz, C.J. and Wilusz, J. (2004) Bringing the role of mRNA decay in the control of gene expression into focus. *Trends in Genetics*, **20**, 491.
- Winston, L.A. and Hunter, T. (1995) JAK2, Ras, and Raf are required for activation of extracellular signal-regulated kinase/mitogen-activated protein kinase by growth hormone. *Journal of Biological Chemistry*, **270**, 30838.
- Wood, C.B., Habib, N.A. and Apostolov, K. (1985) Reduction in the stearic to oleic acid ratio in human malignant liver neoplasms. *European Journal of Surgical Oncology*, **11**, 347.
- Wu, J., Qin, Y., Li, B., He, W.-z. and Sun, Z.-l. (2008) Hypomethylated and hypermethylated profiles of H19DMR are associated with the aberrant imprinting of IGF2 and H19 in human hepatocellular carcinoma. *Genomics*, **91**, 443.
- Xu, W., Fan, H., He, X., Zhang, J. and Xie, W. (2006) LOI of IGF2 is associated with esophageal cancer and linked to methylation status of IGF2 DMR. *Journal of Experimental and Clinical Cancer Research*, **25**, 543.
- Yahagi, N., Shimano, H., Hasty, A.H., Matsuzaka, T., Ide, T., Yoshikawa, T., Amemiya-Kudo, M., Tomita, S., Okazaki, H., Tamura, Y., Iizuka, Y., Ohashi, K., Osuga, J.I., Harada, K., Gotoda, T., Nagai, R., Ishibashi, S. and Yamada, N. (2002) Absence of sterol regulatory element-binding protein-1 (SREBP-1) ameliorates fatty livers but not obesity or insulin resistance in Lep(ob)/Lep(ob) mice. *Journal of Biological Chemistry*, **277**, 19353.
- Yamamoto, M., Yoshizaki, K., Kishimoto, T. and Ito, H. (2000) IL-6 is required for the development of Th1 cell-mediated murine colitis. *Journal of Immunology*, **164**, 4878.
- Yamashita, T., Honda, M., Takatori, H., Nishino, R., Minato, H., Takamura, H., Ohta, T. and Kaneko, S. (2009) Activation of lipogenic pathway correlates with cell proliferation and poor prognosis in hepatocellular carcinoma. *Journal of Hepatology*, **50**, 100.
- Yan, F., Wang, X.M., Pan, C. and Ma, Q.M. (2009) Down-regulation of extracellular signal-regulated kinase 1/2 activity in P-glycoprotein-mediated multidrug resistant hepatocellular carcinoma cells. *World Journal of Gastroenterology*, **15**, 1443.
- Yao, Y.J., Ping, X.L., Zhang, H., Chen, F.F., Lee, P.K., Ahsan, H., Chen, C.J., Lee, P.H., Peacocke, M., Santella, R.M. and Tsou, H.C. (1999) PTEN/MMAC1 mutations in hepatocellular carcinomas. *Oncogene*, **18**, 3181.
- Yi, H.K., Kim, S.Y., Hwang, P.H., Kim, C.Y., Yang, D.H., Oh, Y. and Lee, D.Y. (2005) Impact of PTEN on the expression of insulin-like growth factors (IGFs) and

- IGF-binding proteins in human gastric adenocarcinoma cells. *Biochemical and Biophysical Research Communications*, **330**, 760.
- Yoshida, T., Hisamoto, T., Akiba, J., Koga, H., Nakamura, K., Tokunaga, Y., Hanada, S., Kumemura, H., Maeyama, M., Harada, M., Ogata, H., Yano, H., Kojiro, M., Ueno, T., Yoshimura, A. and Sata, M. (2006) Spreds, inhibitors of the Ras/ERK signal transduction, are dysregulated in human hepatocellular carcinoma and linked to the malignant phenotype of tumors. *Oncogene*, **25**, 6056.
- Yoshimizu, T., Miroglio, A., Ripoche, M.A., Gabory, A., Vernucci, M., Riccio, A., Colnot, S., Godard, C., Terris, B., Jammes, H. and Dandolo, L. (2008) The H19 locus acts in vivo as a tumor suppressor. *Proceedings of the National Academy of Sciences of the United States of America*, **105**, 12417.
- Yvonne P. Dragan, Sargent, L.M., Babcock, K., Kinunen, N., Pitot, H.C. (2004) Alterations in specific gene expression and focal neoplastic growth during spontaneous hepatocarcinogenesis in albumin-SV40 T antigen transgenic rats. *Molecular Carcinogenesis*, **40**, 150-159.
- Zeng, P., Wagoner, H.A., Pescovitz, O.H. and Steinmetz, R. (2005) RNA interference (RNAi) for extracellular signal-regulated kinase 1 (ERK1) alone is sufficient to suppress cell viability in ovarian cancer cells. *Cancer Biology and Therapy*, **4**, 961.
- Zhang, J.-Y., Chan, E.K.L., Peng, X.-X. and Tan, E.M. (1999) A Novel Cytoplasmic Protein with RNA-binding Motifs Is an Autoantigen in Human Hepatocellular Carcinoma. *J. Exp. Med.*, **189**, 1101-1110.
- Zhang, J. and Chan, E.K.L. (2002) Autoantibodies to IGF-II mRNA binding protein p62 and overexpression of p62 in human hepatocellular carcinoma. *Autoimmunity Reviews*, **1**, 146.
- Zhang, J.Y., Chan, E.K.L., Peng, X.X., Lu, M., Wang, X., Mueller, F. and Tan, E.M. (2001) Autoimmune responses to mRNA binding proteins p62 and Koc in diverse malignancies. *Clinical Immunology*, **100**, 149.
- Zhang, L., Himi, T., Morita, I. and Murota, S.I. (2000) Hepatocyte growth factor protects cultured rat cerebellar granule neurons from apoptosis via the phosphatidylinositol-3 kinase/Akt pathway. *Journal of Neuroscience Research*, **59**, 489.
- Zhang, W., Wu, N., Li, Z., Wang, L., Jin, J. and Zha, X.L. (2006) PPAR γ activator rosiglitazone inhibits cell migration via upregulation of PTEN in human hepatocarcinoma cell line BEL-7404. *Cancer Biology and Therapy*, **5**, 1008.
- Zhang, Y. and Tycko, B. (1992) Monoallelic expression of the human H19 gene. *Nature Genetics*, **1**, 40.
- Zhao, L.J., Wang, L., Ren, H., Cao, J., Li, L., Ke, J.S. and Qi, Z.T. (2005) Hepatitis C virus E2 protein promotes human hepatoma cell proliferation through the MAPK/ERK signaling pathway via cellular receptors. *Experimental Cell Research*, **305**, 23.
- Zhou, Y., Rong, L., Zhang, J., Aloysius, C., Pan, Q. and Liang, C. (2009) Insulin-like growth factor II mRNA binding protein 1 modulates Rev-dependent human immunodeficiency virus type 1 RNA expression. *Virology*, **393**, 210.

Publications

Original publications

Tybl E, Shi FD, **Kessler SM**, Tierling S, Walter J, Bohle RM, Wieland S, Zhang J, Tan EM, Kiemer AK. Overexpression of the IGF2-mRNA binding protein p62 in transgenic mice induces a steatotic phenotype. *Journal of Hepatology*, In Press

Kessler SM, Pokorny J, Zimmer V, Lammert F, Bohle RM, Kiemer AK. The insulin-like growth factor II (IGF2) mRNA binding protein p62 in hepatocellular carcinoma: anti-apoptotic action is independent of IGF2 signalling. *In preparation*.

Abstracts to short talks / poster presentations

Schmelter M, **Kessler SM**, Wartenberg M, Sauer H. Cardiovascular differentiation of mouse embryonic stem cells by mechanical strain. Short talk at the 51th annual meeting of the Deutsche Physiologische Gesellschaft, Hannover, Germany. *Acta Physiologica* 2007; 189:S653.

Kessler SM, Tybl E, Weber S, Jüngling B, Lammert F, Kiemer AK. The Insulin-like growth factor II (Igf2) mRNA binding protein p62 regulates Igf2 mRNA expression and protects from apoptosis. Short talk at the 51th annual meeting of the Deutsche Gesellschaft für Experimentelle und Klinische Pharmakologie und Toxikologie, Mainz, Germany. *Naunyn-Schmiedeberg's Archives of Pharmacology* 2010; 381:S1.

Kessler SM, Pokorny J, Risch R, Zimmer V, Diesel B, Lammert F, Bohle RM, Kiemer AK. The non-translated *H19* RNA acts as a tumor suppressor in human hepatocellular carcinoma. Poster presentation at the Keystone meeting "Non-coding RNAs and cancer", Banff, Alberta, Canada. *Conference proceedings*, 2011.

Kessler SM, Pokorny J, Zimmer V, Tybl E, Lammert F, Bohle RM, Kiemer AK. The insulin-like growth factor II (IGF2) mRNA binding protein p62 in hepatocellular carcinoma: anti-apoptotic action is independent of IGF2 signalling. Abstract accepted for a poster presentation at The International Liver Congress 2011 by EASL (46th annual meeting), Berlin, Germany, 2011. Supported by an EASL Young Investigator's Bursary offered by BMS, Gilead, MSD and Roche.

Acknowledgements

Prof. Dr. Alexandra K. Kiemer danke ich ganz herzlich für die Möglichkeit, in ihrer Arbeitsgruppe promovieren zu dürfen. Ihr großes Interesse an diesem Thema, ihre Diskussionsbereitschaft und ihre hilfreichen Anregungen haben diese Arbeit entscheidend vorangebracht. Ich bedanke mich für ihr entgegengebrachtes Vertrauen, ihre Geduld und ihre beständige Motivation.

Prof. Dr. Rolf W. Hartmann danke ich für die freundliche Übernahme des Zweitgutachtens.

Herrn Prof. Rainer M. Bohle und Frau Juliane Pokorny möchte ich für die sorgfältige Zusammenstellung der humanen HCC-Proben danken. Den Mitarbeitern des Instituts für Pathologie danke ich für die methodische Unterstützung.

Herrn Prof. Dr. Frank Lammert und seinen Mitarbeitern Herrn Dr. Vincent Zimmer und Frau Dr. Susanne Weber danke ich für die Beratung bezüglich der verschiedenen Mausmodelle sowie der Zusammenstellung der klinischen Patientendaten.

Aus der Arbeitsgruppe von Herrn Prof. Dr. Rolf Müller möchte ich mich besonders bei Herrn Dominik Pistorius für die Durchführung der Fettsäurebestimmung bedanken.

Des Weiteren danke ich aus der Arbeitsgruppe von Herrn Prof. Dr. Jörn Walter Herrn Dr. Sascha Tierling für die Hilfe bei der Durchführung der SNUPE-Analysen. Mein besonderer Dank gilt Frau Eva Dilly für ihre geduldige und stets mit großer Unterstützung verbundene Einführung in die Mauszucht.

Frau Dr. Diesel danke ich für ihre Hilfestellung bei Problemen und Fragen aller Art.

Allen Mitarbeitern der Arbeitsgruppe danke ich für die kollegiale Zusammenarbeit. Einen besonders herzlichen Dank möchte ich Kerstin Hirschfelder und Jessica Hoppstädter für die freundschaftliche Zusammenarbeit, die stets offenen Ohren und die intensiven sowie produktiven Diskussionen aussprechen. Weiterhin möchte ich Rebecca Risch, Yvette Simon und Stephan Laggai sehr für die große Unterstützung gerade in der jüngeren Vergangenheit dieser Arbeit danken. Ferner danke ich Nadège Ripoché, Lisa Eifler, Sabine Meiser, Jenni Schmidt und Astrid Decker für sehr schöne, heitere Momente.

Acknowledgements

Meiner Familie danke ich für die langjährige Unterstützung und ihre ständige Bereitschaft, mir mit Rat und Tat zur Seite zu stehen.

Zu guter Letzt danke ich von ganzem Herzen meiner Verlobten Christine Krausch für ihre wunderbare Unterstützung und die vielen motivierenden Worte, stets zum rechten Zeitpunkt.